Can Indices of Landscape Function Analysis (LFA) be Derived from Ground-Based Spectroscopy?

A case study from gold mines on the Highveld of South Africa

David G. Furniss

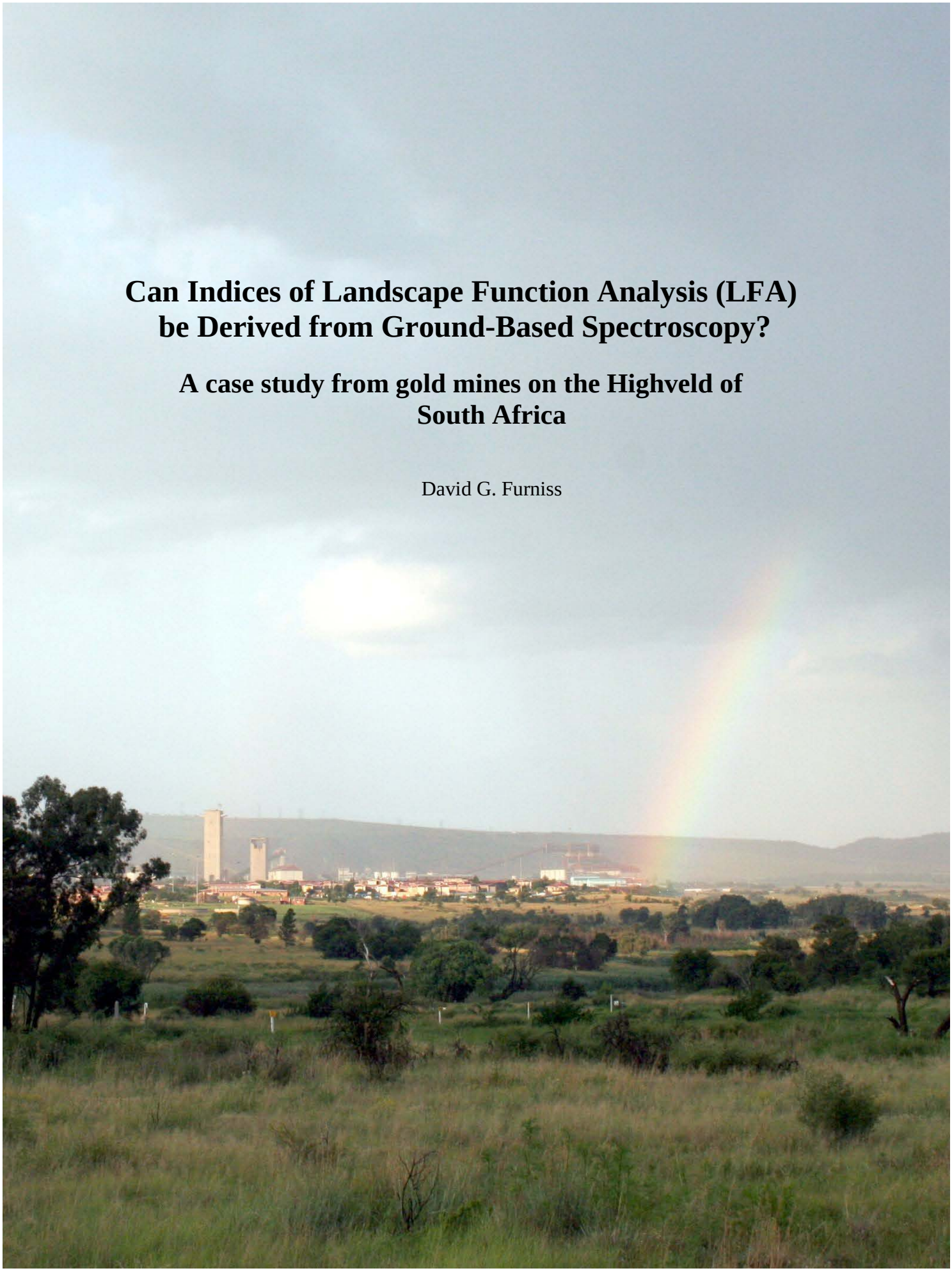

Can Indices of Landscape Function Analysis (LFA) be Derived from Ground-Based Spectroscopy?
A case study from gold mines on the Highveld of South Africa

David G. Furniss
Student No.: 0711251J

Research report submitted in partial fulfilment of the requirements for the degree of Master of Science by course work.
School of Animal, Plant and Environmental Science
University of the Witwatersrand, Johannesburg, South Africa
December 2008

Supervisors:

Isabel Weiersbye / Prof Ed Witkowski: School of Animal, Plant and Environmental Sciences, University of the Witwatersrand, Johannesburg, South Africa.
David Tongway: CSIRO Sustainable Ecosystems & Australian National University, Australia
Dr Robi Stark: Elbit Systems Electro-Optics (Elop), Israel.

DECLARATION

I declare that this research report is my own, unaided work. It is being submitted in partial fulfilment of the requirements for the Degree of Master of Science by coursework in the University of the Witwatersrand, Johannesburg. It has not been submitted before for any degree or examination in any other University.

Signed: 

On 09 day of February 2009

This study was conceived and designed by I.M. Weiersbye with input from E.T.F. Witkowski, D.J. Tongway and D.G. Furniss. The literature review was conducted by D.G. Furniss. The LFA data was collected by D.G. Furniss with field assistance from H. Nel, E. Grond, B. Oageng and M.F. Edi. The hyperspectral data was collected by R. Stark, N. Margalit, I.M. Weiersbye and D.G Furniss. All photographic data was collected by D.G. Furniss. D.G. Furniss performed all LFA and hyperspectral data input, selected all VI's, did all statistical analyses, modelling, interpretation, and wrote this research report.

ABSTRACT

The Minerals and Petroleum Resources Act (MRPDA) No 28 of 2002 of South Africa states that the holder of a mining permit remains liable for environmental consequences until a closure certificate has been issued, but does not stipulate the environmental standards required to obtain such a certificate. Monitoring of surface mining environments requires a consistent, repeatable and efficient method of monitoring that can be applicable to heterogeneous landscapes on large properties. To this end, this study forms a component towards the development and local testing of an internationally accepted, monitoring toolkit to monitor mine rehabilitation. Landscape Function Analysis (LFA) is a technique to rapidly determine broad biogeochemical processes occurring at the soil surface in heterogeneous landscapes. However, LFA is time consuming. Hyperspectral remote sensing (HSRS) is an alternative technique for monitoring large landscapes and is sensitive to both plant response to stress and soil minerals. The aim of this study is to derive LFA indices from HSRS (i.e. surface reflectance) data acquired with a hand-held spectrometer in order to predict landscape condition on deep-level gold mining surface environments in the Highveld region. The first objective was to test the potential of Partial Least Squares Regression (PLSR) modelling to predict LFA indices from the spectral data. The second objective was to test the potential for using Vegetation Indices (VI), calculated from hyperspectral data, to predict LFA indices. Twenty-three VIs, covering plant pigments (i.e. chlorophyll, carotenoids and anthocyanins), plant structural components (cellulose and lignin) and plant water content, were tested.

The study was carried out in winter (dry season) as this is the season when disturbance is most visible, and both seasonal (deciduous) vegetation growth and annual species are absent. The study was carried out at two gold and uranium mining operations in the Highveld grassland biome: West Wits Operations near Carletonville (Gauteng Province) and Vaal River Operations near Klerksdorp (North West Province). At Vaal River, data was collected from high and low disturbance sites replicated three times, in each of four of the dominant vegetation types: wet grasslands, non-rocky grasslands, rocky grasslands and woody shrub sites representing increasing structural complexity. At West Wits Operations (n = 6 sampling plots), only non-rocky grasslands were sampled. Twenty five circular quadrats of 50 cm diameter were evenly distributed on five gradsects within each plot (Total quadrats = 750). Paired data acquired from each quadrat were reflectance data (44 cm field of view), LFA data (50 cm circular quadrat), and a photograph for later allocation of the remaining LFA data. Time constraints collecting LFA data reduced the total number of quadrats sampled in the field from 750 quadrats to 150 quadrats. Difficulties in accurately pairing the LFA and HSRS data further reduced the number of quadrats I used for statistical analyses to 105.

The results of ranking the three LFA indices showed that stability was above the threshold value for sustainability, while infiltration was below threshold and nutrient cycling was close to threshold for all vegetation types and disturbance levels combined. These results suggest that soils were crusted and promoting run-off, and that disturbance was mainly impacting the vegetation component, rather than the soil component of the landscape. A comparison of non-rocky grasslands between the two mining regions showed that West Wits had higher LFA indices for infiltration and nutrient cycling (t-test, $P \leq 0.01$, DF = 36.8 and 26.4 respectively) than Vaal River. All three LFA indices: stability, infiltration and nutrient cycling, differed between vegetation types (One-way ANOVA, $P < 0.05$, DF = 3, 101) with wet grasslands having consistently higher LFA indices than the other three vegetation types. Disturbance levels, combining vegetation types and mining region, also differed (t-tests, $P < 0.01$, DF = 81.8, 102.3 and 100.08 for stability, infiltration and nutrient cycling respectively), with high disturbance quadrats having lower LFA indices than low disturbance quadrats. When comparing LFA indices between disturbance levels within each vegetation type, low disturbance sites generally still had higher LFA indices than high disturbance sites ($P < 0.05$). These findings support the initial selection of distinct vegetation types and disturbance levels, with exceptions to this pattern believed to be a result of low replication (n = 5) for these vegetation types.

The twenty-three VIs were not useful for predicting LFA indices from HSRS data under my experimental conditions. All the VIs had generally low indices as expected (in the case of chlorophyll and plant water-based VIs) for winter senesced Highveld grasses. All linear regressions between LFA indices and VIs had very weak coefficients of determination ($r^2 <$ 26%). The lignin index (NDLI) had the strongest coefficient of determination for both the stability (r^2 = 25%, $P < 0.01$) and the nutrient cycling indices (r^2 = 25%, $P < 0.01$). The infiltration index had the strongest coefficient of determination with the standard normalised difference vegetation index (NDVI) (r^2 = 16%, $P < 0.01$). VIs had generally very low indices due to the winter senesced state of the Highveld vegetation. PLSR modelling produced much stronger regression coefficients of determination than did the VIs. The best PLSR model was a 15-component model to predict nutrient cycling (r^2 = 54%, $P < 0.01$). A 13-component model predicting stability had an r^2 = 38 % ($P < 0.01$), while a 17-component model was derived for infiltration (r^2 = 32%, $P < 0.01$). In all three cases, these models were able to account for more than 90% of the spectral variability within the first two components. However, more than 16 components were required to account for 90% of the variability in the LFA measurements. It may be possible to reduce the number of components required for the PLSR modelling of the latter with a more standardised approach to the LFA data collection, i.e. having one observer who acquires all the LFA data in the field, and increased replication.

ACKNOWLEDGEMENTS

This study was funded by AngloGold Ashanti Ltd and THRIP (National Research Foundation and the Department of Trade and Industry of South Africa). Thank you to my Supervisors, especially Isabel Weiersbye for providing the opportunity, emotional support, resources and funds for this research. I am immensely grateful. To me, this means far more than just a certificate, publication, degree or some science. Thank you to David Tongway who showed a true teacher's touch in imparting his years of experience and his techniques of Landscape Function Analysis with insight and gentleness, not to mention a Herculean effort in the field. Thank you to Dr Robi Stark and Nir Margalit of El-Op for their patience in imparting some of the mysteries of light and spectroscopy to an often highly stressed student, and their hard work in the field collecting spectral measurements.

Thank you to Prof Kevin Balkwill who, when I had given up, said no, knock again. Thank you to my research committee: Prof Graham Alexander and Prof Dave Mycock for their skill and knowledge in chairing my research meetings. To Prof Ed Witkowski, for his insightful input, open door policy, and what must have been a painful reading of my first draft. To Dr Barend Erasmus, for always having a moment to chat if I had a question. Thank you to the staff and students of AP&ES and especially Dr Jason Marshal for showing me "as.matrix".

Thank you to the many staff members from AngloGold Ashanti who toiled in the field collecting data and supplying pertinent advice and suggestions: Henk Nel, Etiene Grond and Malcolm Sutton. Thank you to Mark Cooper and Benjamin Oageng, Isabel's assistants, and her students, Joseph Chauke and Lindokuhle Hlongwane who helped in the field and kept me smiling on campus.

A special thank you to Laura Patterson in Boulder, Colorado, for emergency references, moral support and much much more. Another special thank you to Vincent Snow for improving my grasp of some aspects of English grammar, but most of all, for his patience with a student struggling to pay his rent. Thank you to my parents. To my dad, Basil Furniss, thank you for all the support over the years and the special things you have shown me. And to my mother, Frayne Furniss Mathijs, thank you for being such an inspiration and stalwart of support, patience and diplomacy in too many ways to mention, every step of this journey.

CONTENTS **Page**

LIST OF FIGURES **Page**

LIST OF TABLES **Page**

GLOSSARY

AMD	Acid Mine Drainage
"Anglo" NDVI	Standard NDVI with a 750 nm NIR wavelength
ANOVA	Analysis of Variance
ARI1	Anthocyanin Reflectance Index 1
ARI2	Anthocyanin Reflectance Index 2
ASD	Analytical Spectral Devices
CAI	Cellulose Absorption Index
CARA	Conservation of Agricultural Resources Act No 43 of 1983
CRI1	Carotenoid Reflectance Index 1
CRI2	Carotenoid Reflectance Index 2
ECA	Environment Conservation Act
ECEC	Effective cation exchange capacity
FOV	Field-of-View
GNDVI	Green Normalised Difference Vegetation Index
GPS	Global Positioning System
HS	Hyperspectral
HSRS	Hyperspectral Remote-sensing
LAI	Leaf Area Index
LFA	Landscape Function Analysis
LOO	Leave-One-Out cross-validation
MAP	Mean annual precipitation
$mNDVI_{705}$	modified red edge Normalised Difference Vegetation Index
MPRDA	Mineral and Petroleum Resources Development Act No 28 of 2002
MSI	Moisture Stress Index
MSDI	Moving Standard Deviation Index
mSR_{705}	modified red edge Simple Ratio Index
NDII	Normalised Difference Infrared Index
NDII5	Normalised Difference Infrared Index 5
NDII7	Normalised Difference Infrared Index 7
NDLI	Normalised Difference Lignin Index
NDVI	Normalised Difference Vegetation Index

$NDVI_{705}$	Red edge Normalized Difference Vegetation Index
NDVI800	Normalised Difference Vegetation Index
NDWI	Normalized Difference Water Index
NEMA	National Environmental Management Act No 107 of 1998
NIR	Near-InfraRed
NWA	National Water Act No 36 of 1998
p	Hemispherical spectral reflectivity
PAR	Photosynthetically Active Radiation
pls	Partial Least Squares package for R software
PLSR	Partial Least Squares Regression
PRI	Plant Reflectance Index
PS II	Photo System II
PSRI	Plant Senescent Reflectance Index
r	correlation coefficient
r^2	coefficient of determination
RMSEP	Root Mean Square Error of Prediction
RVI	Ratio Vegetation Index
RWC	Relative Water Content
SAVI	Soil Adjusted Vegetation Index
SIPI	Structure Insensitive Pigment Index
SMA	Spectral Mixture Analysis
SSCI	Soil Surface Condition Indices
SSI	Soil Surface Indicators
SWIR	Short Wave InfraRed
VI	Vegetation Index
VOG2	Vogelmann Red Edge Index 2
VOG3	Vogelmann Red Edge Index 3
WBI	Water Based Index

1. Introduction

1.1 General Background

Deep level gold mines in South Africa, although underground based activities, produce numerous surface environmental impacts including land degradation and loss of productivity (Sutton *et al.*, 2006; Sutton and Weiersbye, 2007). These surface activities include transport, storage or dumping of waste rock and tailings, the building and usage of roads, railway and pipe lines, and the leasing of surface grasslands for grazing. Land degradation can also be caused by contamination of surface waters, ground waters and soil through acid mine drainage (AMD) (Akcil and Koldas, 2006) or dust pollution (Weiersbye *et al.*, 2006a). AMD decreases the pH of soil and water and thereby releases heavy metals into the environment at concentrations exceeding natural background values (Akcil and Koldas, 2006). Weiersbye and Witkowski (2003, 2007) showed that there was reduced regeneration, with more abnormalities in seedlings, reduced rates of viability and germination percentages, for seeds collected from gold mine polluted soils than those from non-polluted sites. Furthermore, the embryos of such seeds had lower concentrations of N and P than those from trees on unpolluted sites, and higher concentrations of S, Mn, Fe, Co, Ni, Cu and Zn.

The motivation for this research stems from the requirements for mine closure in the Mineral and Petroleum Resources Development Act (MPRDA) No 28 of 2002. More specifically section 43 (1) of the MPRDA states that the holder of a "mining permit remains responsible for any environmental liability, pollution or ecological degradation, and the management thereof, until the Minister has issued a closure certificate to the holder concerned." The Act does not stipulate the standards required for the issuing of a closure certificate, although the Constitution of South Africa, Act 108 of 1996; the Conservation of Agricultural Resources Act (CARA) No 43 of 1983, the Environment Conservation Act (ECA) No 73 of 1989, the National Environmental Management Act (NEMA) No 107 of 1998 and consequent legislation (Biodiversity Act 10 of 2004) and the National Water Act (NWA) No 36 of 1998, all stipulate various standards with respect to environmental and human health, which are also applicable to mining lands during operations and post closure. An objective and

repeatable means of assessing progress towards rehabilitation and closure criteria is therefore essential in order for mines to obtain closure certificates in South Africa. To this end, my research will contribute to the development and local testing of an internationally accepted monitoring toolkit with which to routinely assess progress on mine rehabilitation objectives. This involves developing models to derive indices of Landscape Function Analysis (LFA); i.e. stability, infiltration and nutrient cycling (Tongway and Hindley, 2004) from spectral reflectance of representative landscape surfaces on Highveld gold mines. Developing models to efficiently and accurately predict landscape condition on deep-level gold mining surface environments will eventually allow the mapping (not part of this research report) with remotely sensed, aerial imaging spectroscopy data of the entire surface of these environments. Thus maps of remotely sensed LFA indices can potentially be used for management purposes of these surface mining environments (Ong *et al.*, 2004; 2008).

This introductory chapter (Chapter 1) discusses the rationale for my research together with the literature pertinent to the techniques employed and states the aims and objectives for my research. Chapter 2 describes my study areas and the methods and materials employed. Chapter 3 presents my results and chapter 4 my discussion of these results. The final, concluding chapter summarizes my findings and defines the way forward.

1.2 **The Rationale for this Research**

Landscape Function Analysis (LFA) is a technique to rapidly determine broad biogeochemical processes occurring in heterogeneous landscapes (Tongway and Hindley, 2004). The basic assumption in LFA is that landscape structure, both biotic and abiotic, controls resource allocation in both space and time. Therefore environments that lose resources ("leaky") become more degraded and show this degradation as an increase in patchiness and a reduction in resource cycling. Resource loss may occur through removal from the landscape (soil erosion, run-off or leaching) or reduced inputs (decreased infiltration or reduced litter deposition or nutrient cycling) or reduced storage capacity (reduced vegetation or topsoil). Central to LFA is the measurement of biogeochemical processes at the soil-vegetation interface through the use of Soil Surface Indicators (SSI). There are eleven SSIs and

these are resolved into three Soil Surface Condition Indices (SSCI) (Figure 1). These three SSCIs are surrogates for measuring disturbance or degradation. The three SSCIs are stability, infiltration and nutrient cycling (Tongway and Hindley, 2004). Stability is defined as the ability of a soil to withstand and recover from erosive forces. Infiltration is a measure of the partitioning of precipitation into soil water and runoff. Nutrient cycling indicates how efficiently organic matter is cycled back into the soil. Together these indices provide information about the resilience of a landscape.

But LFA has constraints as a management technique. It is a subjective method in the sense that it relies to some extent on the practitioners' skills and experience. It is less time-consuming than many empirical techniques but still involves many man-hours to collect field data. And LFA requires replication both spatially and temporally while requiring sites to be accessible. For management of surface mining environments, a monitoring toolkit is required that is consistent across heterogeneous landscapes on large properties. This monitoring needs to be time and energy efficient and repeatable.

Disturbance and pollution resulting from deep-level gold and uranium mining activities impact negatively on the surface environment in terms of hydrology and salinity (Akcil and Koldas, 2006), and consequently on soils and vegetation (Witkowski and Weiersbye, 1998; Weiersbye and Witkowski, 2003; 2007). On the South African deep-level gold mines, these impacts may be detected through changes in species composition and biomass (Weiersbye *et al.*, 2006b), soil surface condition or plant stress (Weiersbye and Witkowski, 2007). Plant stress affects the quality and concentration of foliar pigments, which are in turn detectable using spectrometry techniques (Carter, 1993) – absorbance, transmission, and reflectance, which is the basis of hyperspectral remote sensing (HSRS). Bare soil (iron oxides) (Huete and Escadafal, 1991; Ben-Dor *et al.*, 2006) and mineral contaminants (`salts') (Basnyat *et al.*, 2000; Sutton *et al.*, 2006; Weiersbye *et al.* 2006a) are also detectable using HSRS. Therefore landscape condition can be determined from HSRS-detectable changes in biomass, plant physiological state and soil surface indicators.

Remote sensing has a number of advantages over other forms of data collection. First, the time taken to collect the data is minimal. For example Pickup *et al.* (1998)

described physically measuring a grazing gradient taking seven man-days even though the landscape was not complex. In contrast, HSRS data can be rapidly collected from a single flight or from satellite sources. Second, remote sensing can collect data over large mining regions that are difficult to inspect on the ground, with a high spatial and spectral resolution (Sutton *et al.*, 2006; Weiersbye *et al.*, 2006a). Finally, remote sensing is generally not subject to human forms of bias during data collection (Ong *et al.*, 2004) although it may be subject to bias during interpretation (Price, 1994; 1998). Generating suitable models for deriving indices of LFA (stability, infiltration, nutrient-cycling) from HSRS data will allow mapping of environmental health over large areas at low cost, and assist in prioritising areas for more detailed, ground-based, study and in planning future land-use. My study focuses on the development of these models from ground-sensed spectral data.

1.3 Measuring Degradation and the Functional Status of the Environment

Both the nature and extent of environmental degradation is difficult to quantify (Pickup *et al.*, 1998) and there is some disagreement about what factors are important in measuring the condition of rangelands (Jordaan *et al.*, 1997). Land degradation often results in a lack of vegetation cover over time, but a lack of vegetation cover *per se* may not be a result of degradation but a response to variability in rainfall (Pickup *et al.*, 1998). Pickup *et al.* (1998) therefore chose to measure degradation as a function of the systems loss of resilience. Resilience was defined as the ability of a landscape to recover to its original pattern of vegetation growth after change has occurred. Loss of resilience was deemed to be a function of soil erosion, a reduction in infiltration and moisture-holding capacity, loss of seed banks and an increase in undesirable species which limit the ability of desirable species to establish and grow (Pickup *et al.*, 1998). Snyman and du Preez (2005) showed that degradation of semi-arid grasslands in South Africa was accompanied by increased soil compaction and soil temperature, a decrease in soil-water content and infiltration, a decrease in the rate of litter and root turnover, and reduced organic carbon and nitrogen.

Two approaches to quantifying environmental degradation have developed: nominal approaches which do not directly measure soil properties but are based on categorical variables; and empirical approaches which directly measure continuous variables such as soil carbon and nitrogen, landscape heterogeneity, erosion, infiltration and water holding capacities of soils (Holm *et al.*, 2002). In this study, Landscape Function Analysis (LFA), a categorical system based on indices derived from landscape organisation and soil surface characteristics (Tongway and Hindley, 2004), was used as a surrogate to measure degradation.

1.4 Landscape Function Analysis (LFA)

LFA (Tongway and Hindley, 2004) is a categorical technique developed from traditional empirical techniques for measuring change in rangelands. It has been refined for monitoring rehabilitation and reclamation processes in mining environments. LFA is a monitoring procedure that uses field assessed, soil surface indicators to characterise the biogeochemical functioning of landscapes at the hillslope and patch scale (Tongway and Hindley, 2004). It is based on measuring whether a landscape is losing function through "leaking" resources or is retaining or gaining function by controlling the loss and capture of resources from the landscape. Measurements over time at the same sites can show whether a landscape is storing or losing resources and therefore (from a mining land perspective) whether management approaches are on successful rehabilitation / restoration trajectories or not.

The underlying assumption in LFA is that landscapes develop non-random heterogeneity (which could be termed 'functional' heterogeneity) and that this heterogeneity provides important information on the surface and near-surface processes that allocate and re-allocate vital resources in space and time (Tongway, 2004). LFA is based on three key questions:

1. What are the landscape components? (Inventory)
2. How do they fit together? (Pattern)
3. How do they "work" together? (Process and function)

The assumption is that the pattern of a landscape structures the processes, which define the functions occurring in a landscape. As a result, every natural landscape type should have a characteristic spatial organization, termed patchiness, that

minimizes the loss of resources and maximizes their recycling within that landscape unit (Tongway, 2004).

Ludwig and Tongway (1995) hypothesised that patchiness in arid to semi-arid landscapes develops to optimize the capture and storage of limited resources such as water and nutrients. This hypothesis was developed out of Noy-Meir's (1973) theory that many arid lands are source-sink or runoff-run-on systems. Ludwig *et al.* (1999) modelled a semi-arid savanna in Australia and found that areas of intact patches had significantly higher soil nitrogen, organic carbon, infiltration rates, and plant productivity when compared to disturbed patches or inter-patches. At the landscape level, Sparrow *et al.* (2003) found that on disturbed areas, vegetation biomass was halved compared to non-disturbed areas. This suggested that resources were being lost from more disturbed areas or being made unavailable to plants. In arid and semi-arid ecosystems, patches are a direct result of the limitation of resource availibilty (Noy-Meir, 1973, Tongway *et al.*, 2003) but as disturbance processes such as injury from defoliation or trampling continue, the ability of vegetation to maintain patch structure and function is reduced. This reduces the ability of these patches to capture or retain mobile resources such as organic matter and water. These resources then leak from the landscape. This causes patches to decrease in size and bare inter-patch spaces to increase in size (Friedel *et al.*, 2003; Tongway *et al.*, 2003). By defining the patchiness of a landscape and then measuring biogeochemical processes occurring in and around these patches, it can be shown whether a landscape is degrading, retaining or improving its resource allocation.

Tongway and Hindley (2004) developed the soil surface condition indices (SSCI) derived from the soil surface indicators (SSI) to characterise these biogeochemical processes around patches. The LFA practitioner measures the SSIs in the field using visually assessed or tactile measurements of biogeochemical processes operating on or within the soil surface (Tongway and Hindley, 2004). Soil stability is defined as the ability of a soil to withstand erosive forces and recover (Tongway and Hindley, 2004). It is calculated (as a percentage) from the SSI measures of rain splash protection or soil cover, perennial vegetation basal cover, litter cover, cryptogam cover, presence of deposited materials, erosion type and severity, a soil slake test, surface resistance, and crust brokenness (Figure 1).

The index of water infiltration and/or runoff is a measure of the partitioning of rainfall into soil water or water runoff and possibly removing other resources as it runs off (Tongway and Hindley, 2004). This is calculated from the SSI measures for perennial vegetation cover, surface roughness, soil slake test, litter cover and properties, surface resistance to disturbance, and soil texture (Figure 1). The index of nutrient cycling status is defined as how efficiently organic matter is integrated back into the soil (Tongway and Hindley, 2004). The calculation includes the SSI measures of perennial vegetation basal cover, litter cover properties, cryptogam cover, and surface roughness characteristics (Figure 1).

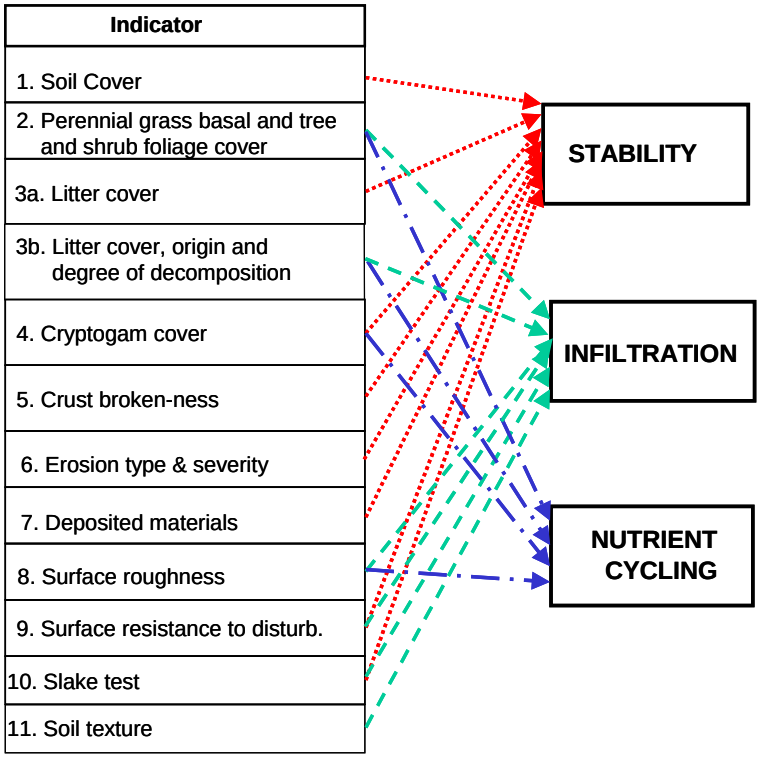

Figure 1 The allocation of the eleven soil surface indices (SSI) into the three soil condition indices (SSCI): stability, infiltration and nutrient cycling (Tongway and Hindley, 2004).

These eleven SSI's have been developed to score across the full range of an indicator from zero effect to maximal effect, and are based on a wide body of literature. Balliette *et al.* (1986) found that infiltration rates under sagebrush canopies in northern New Mexico rangelands were 35% higher than inter-patch areas. They believed these higher infiltration rates resulted from high litter yield, increased basal cover and higher soil organic carbon under canopies. They found that sediment

production was related to soil texture, canopy cover, and total vegetation production. Zhang *et al.* (2003) found that detachment rates of soil were higher in disturbed soils than undisturbed soils when subject to surface water flow. They found that slope angle also played a role in detachment rates but this depended on flow rate. Removal of vegetation leads to increased runoff and potential soil evaporation rates resulting in decreased soil water content while runoff yield, peak flow and sediment load increased with the severity of grazing (Sharma, 1998).

Biology plays an important role in both the stabilization and the degradation of soil aggregates. At macroscales, roots and hyphae bond soil particles together, while at microscales, mucilages from roots, hyphae, bacteria, and soil fauna such as earthworms stabilize soil microaggregates and the linings of biopores (Oades, 1993). Soil aggregates are not only degraded by the presence and/or absence of soil microbes but also tillage of the soil and large animal and vehicle traffic (Oades, 1993). Edgerton *et al.* (1995) showed that there was a linear relationship between increasing soil aggregate stability and soil microbial biomass.

Soil physical crusts have significant impacts on infiltration and nutrient cycling. Valentin and Bresson (1992) classified three main types of non-biological crust based on whether they were structurally based, erosion-based or deposition-based. Structural crusts are based on a rearrangement of soil particles. Casenave and Valentin (1992) showed that infiltration capacity depends upon surface characteristics such as surface crusts, vegetation cover, faunal activity, surface roughness, vesicular porosity, and soil texture. Biological crusts or cryptogamic crusts may decrease infiltration but increase stored soil moisture and nutrients. Belnap and Gillete (1998) in North America, and Eldridge and Leys (2003) in Australia showed that cryptogamic soil crusts had important stabilising influences when subjected to wind erosion compared to sites where these bio-crusts had been disturbed. Evans and Belnap (1999) showed that these disturbed sites had reduced soil nitrogen compared to sites with intact cryptogam crusts. As in the soil texture triangle, the clay content of soils controls the expansive properties of soils and therefore sands have minimal changes in structural organisation, while clays can potentially change the most, with loams somewhere between the two (Oades, 1993). van Gestel *et al.*, (1991) found that the properties of microaggregation and cation exchange capacity had significant

impacts on the retention of nutrients during periods of wetting and drying. Dutartre *et al.* (1993) found that crusting due to rainfall in tropical sandy soils was related to low clay and organic matter content. They further showed that as organic carbon content of soils increased, microaggregates were more stable to wetting and drying processes. Holm *et al.* (2002), working in Australia, found that the soil surface condition indices as proposed by Tongway and Hindley (2004) were positively related to empirical indicators of soil fertility but less closely correlated to proportional areas of vegetated patches. They believed the relationship between SSCI's and empirical measures of soil condition might be community specific. McIntyre and Tongway (2005) found that as patches were increasingly closely grazed, stability, infiltration and nutrient cycling indices declined but stability was markedly resistant to change unlike the other two indices.

Rezaei *et al*. (2006), working in Iran, found that vegetation type had significant influences on the infiltration and nutrient cycling indices. They showed that the stability index was significantly correlated with foliage cover. Furthermore, these researchers found that nutrient cycling, stability and landscape organization indices provided the best predictors of rangeland total yield production but not of herbaceous plant production. They showed that the nutrient cycling index best explained the variation in soil productivity and consequently can be used as a surrogate for soil capability and monitoring. But, Rezaei *et al.* (2006) argued that a high infiltration index did not mean that the soil could store the infiltrated water and so this index was not necessarily well correlated with soil productivity. Similarly a high stability index does not mean high soil productivity but high resistance to erosion. But if high stability occurs with high nutrient cycling and landscape organization indices, this generally reflects extensive vegetation cover and high soil productivity (Rezaei *et al.*, 2006). The above discussion suggests that the LFA methodology and in particular the SSIs and SSCIs provide a suitable surrogate measure of environmental degradation. However, it should be noted that SSI's and SSCI's are surrogates for, and not direct measurements of stability, infiltration and nutrient cycling (McIntyre and Tongway, 2005).

1.5 **Remote Sensing**

Remote sensing in the broadest sense is the use of electromagnetic radiation to gather information about an object without making physical contact with the object (Rees, 2001). Hyperspectral remote sensing (HSRS), or reflectance imaging spectroscopy, involves sampling many different wavelengths across the electromagnetic spectrum with passive sensors which require an external source of light, such as the sun, to generate reflectance. The radiance or reflectance values collected by a sensor are stored as a pixel. The target which produces the radiance or reflectance captured by a sensor is termed a rexel (Rees, 2001). The pixel only stores the intensity of the reflectance for different wavelengths and no other information. The value of this intensity has no units as it is the ratio of the reflectance obtained from some reference standard and the reflectance obtained from the object of interest or rexel. An image may be composed of a single pixel or a number of pixels. In my study the spectral image is a single pixel acquired from a circular quadrat corresponding in size to the circular field of view (FOV) of the HSRS sensor.

Passive sensors can only determine the amount of radiation received from the target. They provide no more information about the target other than the radiation emitted or reflected from that surface (Rees, 2001). As a result the reflectance measured by the sensor needs to be interpreted in some way. One way to interpret HS information involves the selection of specific bands based on biochemical or physiochemical properties in vegetation or soils, and their transformation by the use of a specific algorithm. A band is a single wavelength or range of wavelengths. A Vegetation Index (VI) is one of the simplest transformations and most commonly involves the red (600 to 700 nm) and Near-InfraRed bands (NIR; generally from 800 to 1000 nm) (Rees, 2001). HSRS has been used for many environmental metrics, including detection or inference of pasture biomass (Boutton and Tieszen, 1983; Kogan *et al.*, 2004), C4/C3 grassland distributions (Davidson and Csillag, 2001), lianas in forest canopies (Kalacska *et al.*, 2007), plant stress (Carter, 1993), monitoring infiltration rates in semi-arid soils (Ben-Dor *et al.*, 2004), predicting LFA indices (Ong *et.al.*, 2004, 2008), soil rubification processes on sand dunes (Ben-Dor *et al.*, 2006) and urban planning (Feingersh *et al.*, 2007), to mention a few.

1.6 **Hyperspectral Vegetation Indices**

The most basic VI is the Ratio Vegetation Index (RVI) (Jordan, 1969) which is simply the ratio between a near infrared band and a red band:

$$RVI = R_{nir} / R_{red}$$

where: R_{nir} is the radiation in the near infrared band and
R_{red} is the radiation in the red band.

This index was first proposed by Jordan (1969) to measure Leaf Area Index (LAI) in a perennially green canopy forest in Puerto Rico. He used the wavelength of 800 nm for NIR and 675 nm for his red band. Jordan (1969) further showed that the red light reaching the canopy is slightly higher than NIR but the ratio of NIR to red light above the canopy was constant. Red light received by a canopy is absorbed by chlorophyll and this greatly reduces the red light received underneath a canopy or reflected back into the atmosphere. NIR on the other hand is relatively unaffected beneath a canopy. Put differently, a non-linear inverse relationship exists between red radiance and green biomass, while a non-linear direct relationship exists between NIR and green biomass (Tucker, 1979). Jordan (1969) showed that the more leaves present in the canopy, the greater the ratio between NIR and red light on the canopy floor. One constraint with the RVI ratio is that if the red reflectance or radiance is zero, the index diverges to infinity. An index which is much more widely used and solves the problem of the calculated index possibly diverging to infinity is the Normalised Difference Vegetation Index (NDVI) (Table 1). One advantage of this index is that all possible values will lie between +1 and –1 (Rees, 2001). The NDVI was first described by Rouse *et al.* (1973, *loc. cit.* Tucker, 1979). Tucker (1979) evaluated various red, green and NIR wavelengths and found the red wavelengths were significantly better at discriminating the amount of photosynthetically active vegetation than the green wavelengths. He also found no significant difference between various NIR wavelengths across the 750 to 900 nm band.

The NDVI is affected by a number of factors including vegetation characteristics, soil reflectance (Huete, 1988), senescent vegetation and/or leaf litter (van Leeuwen and Huete, 1996; Tucker, 1978; Tucker *et al.*, 1981). van Leeuwen and Huete (1996) showed that leaf litter had significant variability in spectral reflectance but that this was similar to soil reflectance patterns. Huete (1988) examined the effects of soil on the NDVI and found that darker soil substrates under partial canopies resulted in higher NDVI values. Red and yellow soils also have major influences on spectral vegetation indices. In response to the effects of soil background on VIs, the Soil Adjusted Vegetation Index (SAVI) was developed (Huete, 1988) (Table 1). The SAVI resulted in better vegetation discrimination and less soil noise levels but reduced the amplitude in the VI compared to the NDVI. The SAVI was developed by adding a soil adjustment factor (L) to the NDVI calculation. Huete (1988) found that as vegetation density varied so did the optimal adjustment factor. In general the value of L for a specific soil is difficult to determine but a value of 0.5 reduced soil noise considerably across the range of vegetation densities (Huete, 1988). The NDVI and the SAVI both use the absorption spectra of chlorophyll at the 680 nm absorption centre of chlorophyll (Ting, 1982) but other indices have used different chlorophyll absorption centres. Gitelson *et al.* (1996) used the "green" absorption centre around 520 to 630 nm to develop a green or GNDVI (Table 1) where ρ_{nir} = 750 nm and ρ_{green} = 550 nm. They suggested that this index was five times more sensitive than the standard NDVI.

The NDVI and other VIs discussed above are known as broadband indices as they were designed to use the bands available from various satellites. These satellite bands cover a range of wavelengths but as spectral instruments become more sophisticated, narrow band indices have been developed which can use features expressed in much narrower ranges of wavelengths (ENVI 4.2). The following indices are all narrow-band indices using the transition from chlorophyll absorption and near-infrared scattering known as the red-edge which is from 690 – 740 nm (Curran *et al.*, 1995). Gitelson and Merzylak (1994) found that in horse chestnut (*Aesculus hippocastanum* L.) and Norway maple (*Acer platanoides* L.) the standard NDVI saturates at relatively low chlorophyll concentration levels. They developed the Red Edge Normalized Difference Vegetation Index ($NDVI_{705}$) (Table 1) after showing that the wavelength at 705 nm was much more sensitive to high chlorophyll concentrations. Sims and

Gamon (2002) developed the modified red edge Simple Ratio Index (mSR_{705}) and the modified red edge Normalised Difference Vegetation Index ($mNDVI_{705}$) (Table 1) in response to high leaf surface specular reflectance. They found that reflectance of chlorophyll and carotenoids were constant at the 445 nm wavelength until chlorophyll concentration was very low. They therefore used this wavelength with the red edge 705 nm and NIR 750 nm wavelengths in their two VIs to compensate for this high leaf surface reflectance (Sims and Gamon, 2002). Vogelmann *et al.* (1993) also used the red edge studying leaves from sugar maple (*Acer saccharum* Marsh.) trees that had suffered intensive insect damage. They developed a number of indices, of which two, the Vogelmann Red Edge Index 2 (VOG 2) and the Vogelmann Red Edge Index 3 (VOG 3) were used in my study (Table 1).

All the indices discussed above are based on chlorophyll absorption features, however, indices have also been developed which use both chlorophyll and other plant pigments such as carotenoids. The Structure Insensitive Pigment Index (SIPI) (Table 1) was developed by Peñuelas *et al.* (1995) using the 680 nm wavelength for chlorophyll and the 445 nm wavelength for carotenoids. Increases in SIPI are thought to indicate increased canopy stress (ENVI 4.2). Merzlyak *et al.*, (1999) developed the Plant Senescent Reflectance Index (PSRI) (Table 1). This index uses reflectance around 500 nm which is sensitive to chlorophyll *a*, chlorophyll *b* and the carotenoids, and reflectance around 680 nm which is only sensitive to chlorophyll *a* (Merzlyak *et al.*, 1999).

One of the constraints with using chlorophyll to detect vegetation cover during periods of dormancy is that it is one of the first pigments to decompose during senescence. Other pigments, such as the carotenoids, remain in senescing tissue for much longer periods. Furthermore there is an overlap in light absorption between chlorophyll and other pigments. The Plant Reflectance Index (PRI) (Table 1) was developed by Gamon *et al.*, (1992). The PRI focuses on the xanthophyll cycle where the conversion of violaxanthin to zeaxanthin occurs when absorbed photosynthetically active radiation (PAR) exceeds photosynthetic capacity (Gamon *et al.*, 1992). Gamon *et al.*, (1997) later tested this index on 20 species covering annuals, deciduous perennials and evergreen perennials and found it effective for measuring photosynthetic function across these species.

Table 1 Vegetation indices (VIs), algorithms and wavelengths used in this study.

VI Name	VI Acronym	Environmental features	Algorithm	Wavelength (nm)	Reference
Normalised Difference Vegetation Index	NDVI	Chlorophyll and canopy leaf area.	$(\rho_{NIR} - \rho_{RED}) / (\rho_{NIR} + \rho_{RED})$	800 680	Tucker (1979)
"Anglo" NDVI	ANDVI	Chlorophyll and canopy leaf area.	$(\rho_{NIR} - \rho_{RED}) / (\rho_{NIR} + \rho_{RED})$	750 676	Revivo *et al.* (2005)
Green Normalised Difference Vegetation Index	GNDVI	Chlorophyll	$(\rho_{nir} - \rho_{green}) / (\rho_{nir} + \rho_{green})$	550 750	Gitelson *et al.* (1996)
Soil Adjusted Vegetation Index	SAVI	Chlorophyll adjusting for soil background	$1.5(R_{nir} - R_{red}) / (R_{nir} + R_{red} + 0.5)$	670 800	Huete (1988)
Red Edge Normalized Difference Vegetation Index	$NDVI_{705}$	Chlorophyll and canopy leaf area.	$(\rho_{750} - \rho_{705}) / (\rho_{750} + \rho_{705})$	750 705	Gitelson and Merzlyak, (1994)
Modified Red Edge Simple Ratio Index	mSR_{705}	Chlorophyll and canopy leaf area.	$(\rho_{750} - \rho_{445}) / (\rho_{705} - \rho_{455})$	750 705 445	Sims and Gamon (2002)
Modified Red Edge Normalized Difference Vegetation Index	$mNDVI_{705}$	Chlorophyll and canopy leaf area.	$(\rho_{750} - \rho_{705}) / (\rho_{750} + \rho_{705} - 2\rho_{445})$	750 705 445	Sims and Gamon (2002)
Vogelmann Red Edge Index 2	VOG 2	Chlorophyll, canopy leaf area and water content	$(\rho_{734} - \rho_{747}) / (\rho_{715} + \rho_{726})$	715 726 734 747	Vogelmann *et al.* (1993)
Vogelmann Red Edge Index 3	VOG 3	Chlorophyll, canopy leaf area and water content	$(\rho_{734} - \rho_{747}) / (\rho_{715} + \rho_{720})$	715 720 734 747	Vogelmann *et al.* (1993)

Table 1 continued Vegetation indices (VI), their algorithms and wavelengths used in this research.

VI Name	VI Acronym	Environmental features	Algorithm	Wavelength (nm)	Reference
Structure Insensitive Pigment Index	SIPI	Chlorophyll and carotenoids	$(\rho_{800} - \rho_{445}) / (P_{800} - \rho_{680})$	445 680 800	Peñuelas *et al.* (1995)
Plant Senescence Reflectance Index	PSRI	Chlorophyll and carotenoids	$(\rho_{680} - \rho_{500}) / P_{750}$	500 680 750	Merzlyak *et al.* (1999)
Photochemical Reflectance Index	PRI	Carotenoids	$(\rho_{531} - \rho_{570}) / (P_{531} + \rho_{570})$	531 570	Gamon *et al.* (1992)
Carotenoid Reflectance Index 1	CRI 1	Carotenoids	$(1 / \rho_{510}) - (1 / \rho_{550})$	510 550	Gitelson *et al.* (2002)
Carotenoid Reflectance Index 2	CRI 2	Carotenoids	$(1 / \rho_{510}) - (1 / \rho_{700})$	510 700	Gitelson *et al.* (2002)
Anthocyanin Reflectance Index 1	ARI 1	Anthocyanins	$(1 / \rho_{550}) - (1 / \rho_{700})$	550 700	Gitelson *et al.* (2001)
Anthocyanin Reflectance Index 2	ARI 2	Anthocyanins	$\rho_{800} ((1 / \rho_{550}) - (1 / \rho_{700}))$	550 700 800	Gitelson *et al.* (2001)
Cellulose Absorption Index	CAI	Cellulose	$0.5 ((\rho_{2000} - \rho_{2200}) / \rho_{2100})$	2000 2100 2200	Daughtry *et al.* (2004)
Normalized Difference lignin Index	NDLI	Lignin	$(\log (1 / \rho_{1754}) - \log (1 / \rho_{1680})) / (\log (1 / \rho_{1754}) + \log (1 / \rho_{1680}))$	1680 1754	Serrano *et al.* (2002)

Table 1 continued Vegetation indices (VI), their algorithms and wavelengths used in this research.

VI Name	VI Acronym	Environmental features	Algorithm	Wavelength (nm)	Reference
Water Band Index	WBI	Plant water content	ρ_{900} / ρ_{970}	900 970	Peñualas *et al.* (1993)
Normalized Difference Water Index	NDWI	Plant water content	$(\rho_{857} - \rho_{1241}) / (\rho_{857} + \rho_{1241})$	857 1241	Gao (1996)
Normalised Difference Infrared Index	NDII	Plant water content	$(\rho_{819} - \rho_{1649}) / (\rho_{819} + \rho_{1649})$	819 1649	Hardisky *et al.* (1983)
Normalised Difference Infrared Index 5	NDII 5	Plant water content	$(R_{800} - R_{1625}) / (R_{800} + R_{1625})$	800 1625	Numata *et al.* (2007)
Normalised Difference Infrared Index 7	NDII 7	Plant water content	$(R_{800} - R_{2220}) / (R_{800} + R_{2220})$	800 2220	Numata *et al.* (2007)

A different set of carotenoid VIs that detect carotenoid levels in plants while compensating for chlorophyll reflectance effects have been developed by Gitelson *et al.* (2002). These researchers developed two indices for measuring carotenoid concentrations in plants: the CRI1 and CRI2 (Table 1) using the inverse reflectances at 510 and 550 nm or 510 and 700 nm respectively (Gitelson *et al.*, 2002). The reciprocal reflectance at 510 nm was linearly related to the total pigment content of leaves from Norway maple (*Acer platanoides* L.), horse chestnut (*Aesculus hippocastanum* L.) and beech (*Fagus sylvatica* L.). The inverse reflectance at 510 and 700 nm was used to remove the influence of chlorophyll from the reflectance at 510 nm in order to produce an estimation of the carotenoid content of these leaves (Gitelson *et al.*, 2002). High values for this index reflect higher levels of carotenoids relative to chlorophyll (ENVI 2.4). Similarly, Gitelson *et al.*, (2001) developed the anthocyanin reflectance indices ARI1 and ARI2 (Table 1) using leaves from the Norway maple (*Acer platanoides* L.), cotoneaster (*Cotoneaster alaunica* Golonite), dogwood (*Cornus alba* L. (*Swida alba* (L.) Opiz)) and *Pelagonium zonale* L'Herit (ex Soland). These authors identified a peak at 550 nm related to anthocyanin absorption *in vivo* whose magnitude was proportional to anthocyanin content. This wavelength is also related to chlorophyll absorption. Subtraction of the inverse reflectance at 700 nm was used to remove the chlorophyll from the anthocyanin signal in the ARI1 algorithm, and at 700 and 800 nm in the ARI2 algorithm (Gitelson *et al.*, 2001).

Other VIs have been developed that use the reflectance properties of plant tissues and plant materials that are unrelated to plant pigments (Fourty *et al.*, 1996) (Table 1). These include cellulose, lignin and plant water content. The Cellulose Absorption Index (CAI) (Daughtry, 2001, Daughtry *et al.*, 2004) is a VI developed to assess crop residue by focusing on a cellulose-lignin absorption feature near 2100 nm. This index was developed from the observation that cellulose, lignin and nitrogen affected absorption around 1730, 2100 and 2300 nm. The CAI algorithm uses three reflectance bands, one from the centre of cellulose absorption at 2100 nm, and two from the shoulders of the absorption feature at 2000 and 2200 nm to estimate cellulose (Daughtry *et al.*, 2004). The CAI is affected by the Relative Water Content (RWC) of soils and plant residues, and may be difficult to separate from soil spectra at high RWC (Daughtry, 2001). The Normalised Difference Lignin Index (NDLI) (Serrano *et al.*, 2002) was developed to capitalise on the lignin absorption feature at

1754 nm. According to Serrano *et al.*, (2002) the NDLI may produce inaccurate results in senescent vegetation and this could be a constraint with winter data.

Water in its various phases and in a free state can influence remote sensing measurements quite extensively by masking features through overlapping absorption wavelengths or depressing the spectral signature of a desired feature, such as in moist soils, however, it can also be used to quantify plant-water metrics. Peñualas *et al.* (1993) developed the Water Based Index (WBI) which uses the ratio at 950 and 900 nm wavelengths to measure the plant RWC. One water absorption centre is between 950 and 970 nm, while 900 nm is used as a reference reflectance. It was found that in *Gerbera jamesonii*, *Capsicum annuum* and *Phaseolus vulgaris*, this ratio increased as RWC decreased (Peñualas *et al.*, 1993). These authors further found that this ratio was stronger at canopy level than at leaf level, and when LAI was constant and plant cover was 100 % of soil, indicating its usefulness in more humid, tropical ecosystems (Peñualas *et al.*, 1993).

The Normalized Difference Water Index (NDWI) was developed by Gao (1996) and used by Jackson *et al.*, (2004) to map daily vegetation water content of soybean and corn. This index is based on weak absorption by liquid water in the plant body at 1240 nm. Gao (1996) found that dry vegetation produced slightly negative numbers for this index while green vegetation produced positive values. It was further shown that the index gave progressively higher values for bare soil, grassland and crop at the peak of the growing season on the high plains of Colorado (Gao, 1996). Hardisky *et al.* (1983) developed the Normalised Difference Infrared Index (NDII) which Numata *et al.*, 2007) adapted to the closely related NDII 5 and 6. It was shown that the NDII was closely correlated with plant water content and soil salinity in *Spartina alterniflora* Loisel. growing in a salt marsh. In an Amazonian study of overgrazed and degraded rangelands, Numata *et al*. (2007) found that the NDVI resulted in the poorest correlation to winter senesced degraded grassland, while the NDII 5 and 7 gave stronger correlations with biophysical measures of rangeland degradation.

In summary, a number of VIs have been described (Table 1), although this is by no means a complete list. VIs are based on two or more wavelengths of reflectance – one which absorbs light depending on the abundance of the feature responsible for the

light absorption, and a second wavelength which is nearly 100% reflected. These two wavelengths are used to generate an index which acts as a proxy measure for the substance responsible for the light absorption. This substance in turn is a proxy for some environmental factor such as biomass or plant constituents, and thus plant physiological status. Most VIs are based on plant pigments, most commonly chlorophylls, but also carotenoids and anthocyanins, or plant structural materials, or plant water content.

1.7 Environmental Degradation, Remote Sensing and Vegetation Indices

Land degradation can be defined in many ways yet generally means a reduction in biological productivity of a landscape as indicated by changes in vegetation structure and composition, with increased spacing between vegetation, soil erosion, and a loss of resources (Wessels *et al.*, 2004). The measurement of environmental degradation through remote sensing has mainly involved characterizing changes in VIs over time (Wessels *et al.*, 2004; Numata *et al*, 2007). The assumption is that changes in biomass indicate changes in the environment, and if these changes indicate less biomass, than some form of environmental degradation is occurring. But degradation may not show initially as a change in biomass. For example, an initial response to disturbance may be a change in species composition (Yamano *et al.*, 2003), or a reduction in biomass may be a response to climate variability rather than a sign of degradation (Pickup *et al.*, 1998).

The most commonly used vegetation index is the NDVI and various elaborations of this index have been applied in South Africa (Wessels *et al.*, 2004), Syria (Geerken and Ilaiwi, 2004), Australia (Holm *et al.*, 2003), the USA (Goodin and Henebry, 1997), and Botswana (Ringrose and Matheson, 1987). Ringrose and Matheson (1987) found that at vegetation aerial covers of less than 50 %, NDVI did not detect changes in vegetation cover. They suggested that high soil reflectance results in high NIR measurements and confounds the NDVI ratios when vegetation aerial cover is less then 50%. Tanser and Palmer (1999) used a Moving Standard Deviation Index (MSDI) applied to the red band (Landsat TM 3). They then compared the MSDI to NDVI values across fence lines separating degraded and non-degraded areas in four areas in the Eastern Cape, South Africa. In all but one area there were significantly

different results in both MSDI and NDVI. For the exception, MSDI gave significant differences between degraded and non-degraded rangeland, whereas the NDVI showed no significant difference between the two rangeland conditions.

Pickup *et al.* (1998) used the PD54 index to measure degradation in Australian rangelands. The PD54 index essentially plots the radiance in the green bands against the visible red bands, where the upper limit indicates bare soil and the lower limit characterises areas with 100 % vegetation aerial cover (Pickup *et al.*, 1998). Implicit in this index is the observation that environmental degradation is characterised by an increase in bare soil. Yamano *et al.* (2003) attempted to discriminate two grass species, one that tolerated salinity, and another that tolerated increased aridity, from other grass species. Fourth derivative peaks around 670 and 720 nm were used to separate out this species from other grass species common in the study area. Numata *et al.* (2007) used a number of vegetation indices as well as spectral mixture analysis (SMA) (Roberts *et al.*, 1998) to measure degradation in a Brazilian rangeland. The vegetation indices used included the NDVI (Tucker, 1979), SAVI (Huete, 1988), and two infrared indices (NDII5 and NDII7). The NDVI and SAVI are chlorophyll based indices whereas the NDII5 and NDII7 are plant water content based indices. All four vegetation indices were found to have positive correlations with pasture based measures of degradation, but with highest correlation for plant water content and lowest for biomass. This lower correlation of chlorophyll based vegetation indices was interpreted as being associated with a high proportion of non-photosynthetic material (Numata *et al.*, 2007). In my study data was collected in winter as LFA SSI's are not masked by deciduous or annual vegetation, and although chlorophyll may degrade, carotenoids are still present in senesced vegetation.

1.8 **Partial Least Squares Regression Modelling**

Partial Least Squares Regression (PLSR) modelling of full spectrum hyperspectral data to predict LFA indices was successfully applied to data from Goldsworthy decommissioned iron ore mine and the bauxite mines of Huntley and Boddington, all in arid to semi-arid regions of Australia (Ong *et al.*, 2004, 2008). Maps were produced of stability, infiltration and nutrient cycling from airborne HyMap hyperspectral data of the mine surfaces. My study builds on the research of Ong *et al.*

(2004), and forms an independent test of the method on representative vegetation types of increasing complexity in two gold mining environments in South Africa.

The Partial Least Squares method was developed by H.S. Wold in the sixties in the field of econometrics, and applied at a later stage to chemometrical problems (Geladi and Kowalski, 1986, Wold *et al.*, 2001). Geladi and Kowalski (1986) describe PLSR as more robust than classical multiple linear regression and principle component regression analyses in the sense that the model parameters do not change much when new calibration samples are added. PLSR is particularly useful because it can be used to analyze highly collinear, noisy data with numerous X-axis variables (Wold *et al.*, 2001). PLSR is a data compression tool which produces a sequence of models as components or "latent variables" are added to the modelling process (Frank and Friedman, 1993). PLSR is unusual in that it models both the X and Y-variables through maximising the explained X/Y covariance (Martens, 2001), and further has the flexibility of being able to incorporate a number of response or Y-variables into the modelling process (Martens and Næs, 1989).

PLSR is widely used for the reduction of large chemical spectrometry data sets, and has been applied to a growing number of environmental questions in the remote sensing field. Townsend *et al.* (2003) applied PLSR to satellite data in order to map the relative amounts of canopy nitrogen in forests from satellite data, while Hansen and Schjoerring (2003) measured canopy biomass and nitrogen in wheat, and Coops *et al.* (2003) and Huang *et al.* (2004) predicted relative nitrogen contents in Eucalypt foliage. Schmidtlein and Sassin (2004) used PLSR in mapping floristic gradients in grasslands, while Kooistra *et al.* (2004) and Wilson *et al.* (2004) examined the potential of PLSR in mapping plants growing on metal contaminated soil. Recently the technique was used to predict soil salinity (Farifteh *et al.*, 2007), organic carbon content in agricultural soils (Stevens *et al.*. 2008) and soil condition in tropical regions of sub-Saharan Africa (Awiti *et al*., 2008).

1.9 **Aims and Objectives of Research**

The goal of my study is to contribute towards the development of a toolkit to monitor disturbance and rehabilitation processes on gold mining environments towards eventual closure of gold mines. To this end the aim of this study is to derive LFA indices to predict rangeland condition on deep-level gold mining surface environments from hyperspectral data. Two methods of achieving this aim were tested. The first objective was to develop usable Partial Least Squares Regression (PLSR) models from full spectrum hyperspectral data to predict Landscape Function Analysis (LFA) indices (Figure 2). The PLSR models and their predictions provide the potential to accurately map environmental degradation from airborne or satellite resources across the entire surface of gold mines for management and monitoring purposes. The second objective was to test 23 spectral Vegetation Indices (VI) against the Landscape Function Analysis (LFA) indices as possible alternatives to PLSR for predicting LFA indices from hyperspectral data. This has further value in providing possible insight into the environmentally meaningful interpretation of the coefficients and loadings produced during PLSR modelling. The key questions and hypotheses related to these objectives are elaborated on in the methods section discussing the statistical tests used (Section 2.7) and results (Chapter 3).

This report presents the results and discussion in a different order to the objectives presented above. Of the two objectives, I regarded PLSR as more important than the VIs, in the context of this study, and therefore PLSR is defined as objective one. However, in presenting and discussing the results, the natural flow is from LFA through the VIs to PLSR, and the report follows this natural flow.

2. Methods and Materials

2.1 Tasks Required to Achieve Objectives

To achieve the aim and objectives, the following tasks needed to be performed (Figure 2):

1. The collection of paired LFA and HS field data from 50 cm diameter circular quadrats of natural rangeland, covering four vegetation types with two broad disturbance categories (high and low) in two mining regions during winter;
2. Calculating the three LFA indices (SSCIs: stability, infiltration and nutrient cycling) from the eleven field assessed SSIs;
3. Calculating the 23 VIs using the VI algorithms and their respective wavelengths from the hyperspectral data;
4. Correlation analysis between VIs to test the integrity of the VI values calculated from winter senesced vegetation in the absence of empirical values for these VI features;
5. Simple linear regression with the LFA indices as the response and the VIs as the predictor variable;
6. Removing the atmospheric water noise, change in sensor steps, Short Wave Infra-Red (SWIR) and Ultra-Violet (UV) noise from the full spectrum hyperspectral data prior to PLSR modelling;
7. Pairing each quadrat's LFA index with its respective full spectrum hyperspectral measurement, and splitting the paired data into calibration data (n = 79), and validation data (n = 26);
8. Calibrating the PLSR models with the paired HS full spectrum data (n = 79) as the predictor matrix (X values), and the LFA indices as the response variable (Y);
9. Validating the selected best-fit calibration models with new data (n = 26).

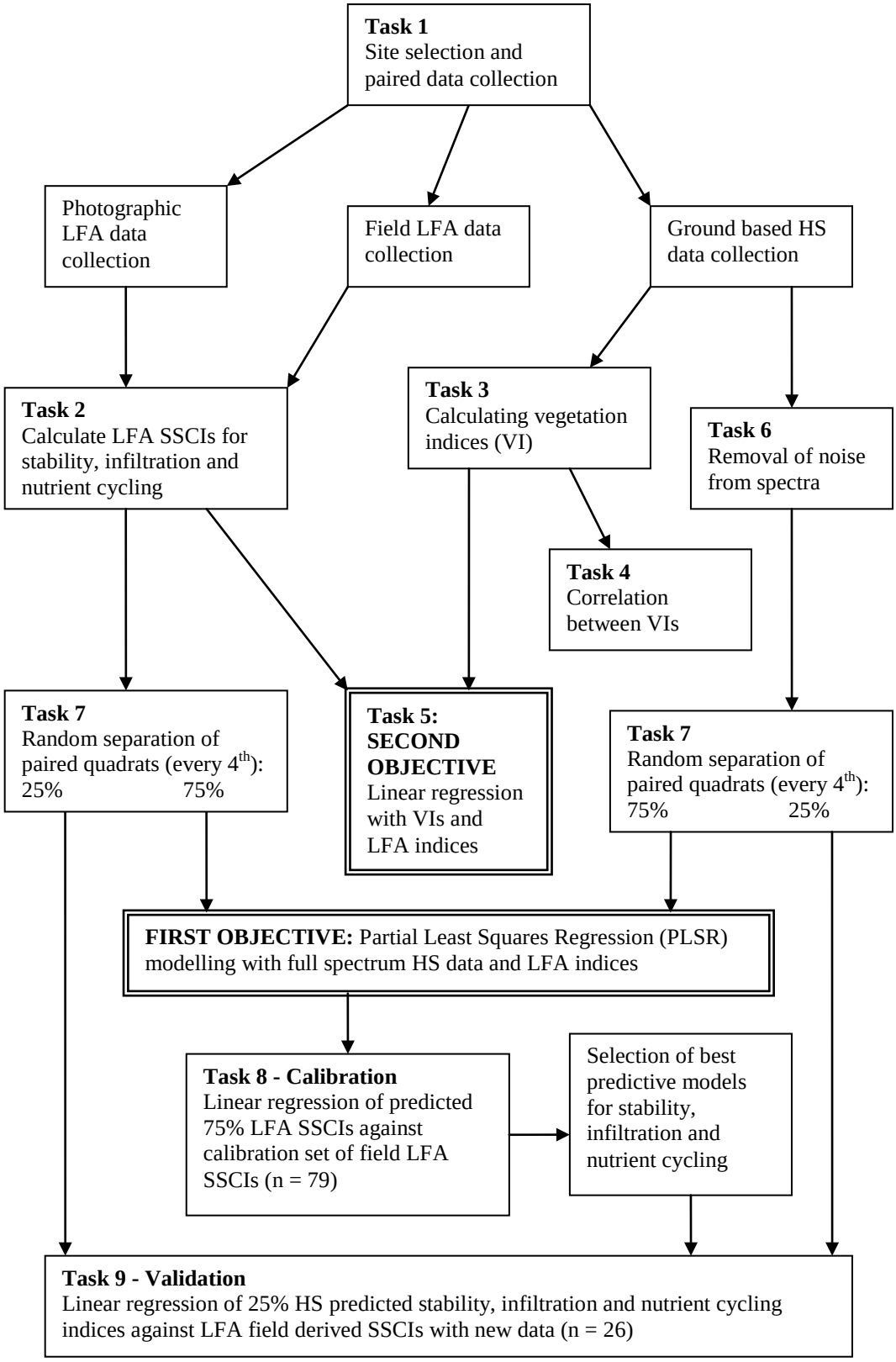

Figure 2 Flow diagram of the data acquisition and processing steps.

2.2 **The Study Sites**

The study was conducted at AngloGold Ashanti's Vaal River gold and uranium mining operations near Klerksdorp, North West Province, and West Wits mining operations near Carletonville, Gauteng Province. The two mining regions are within the summer rainfall zone with seasonal extremes in temperature (Schultz, 1997). The Vaal River mining region, at an altitude of 1300 to 1350 m, receives a mean annual precipitation (MAP) of 560 mm (Mucina and Rutherford, 2006) with a high inter-annual variability of 25 to 30 %. The Vaal River sites are situated on the North bank of the Vaal River on dolomites of the Malmani Subgroup (Chuniespoort Group, Transvaal Supergroup; Mucina and Rutherford, 2006). Soils are predominantly shallow (50 – 150 mm) and rocky, and dominated by Mispah, Glenrosa and Hutton soil forms (Mucina and Rutherford, 2006). Acocks (1988) characterised these sites into three vegetation types: the western variation of Bankenveld (61a), a southern variation of *Cymbopogon-Themeda* veld (48a), and a northern variation of Dry *Cymbopogon-Themeda* veld (50a).

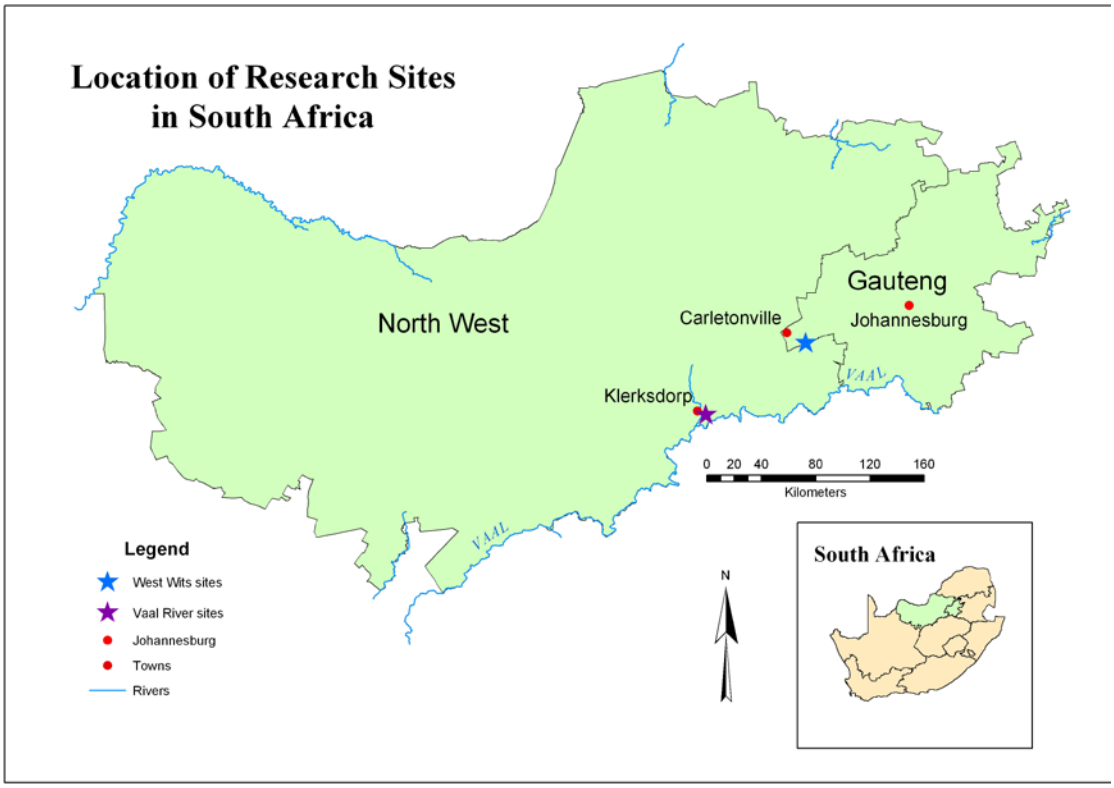

Figure 3 The Republic of South Africa showing the location of the two research sites.

Mucina and Rutherford (2006) called the vegetation Vaal Reefs Dolomite Sinkhole Woodland (Gh 12). Important taxa include small trees such as *Acacia erioloba* E.Mey., *Celtis Africana* Burm.f. and *Rhus lancea* L.f., and graminoids such as *Aristida congesta* Roem & Schult, *Digitaria eriantha* Steudel, *Eragrostis curvula* (Schrad.) Nees and *Themeda triandra* Forsk. amongst others (Mucina and Ritherford, 2006). The mean daily temperature minima and maxima for Vaal River is 0ºC (July) and 25ºC (January) respectively. Frost is common in winter at both mining regions with frost experienced 150 – 175 days of the year (Schultz, 1997), and evaporation rates being high with January A-pan evaporation around 250 – 300 mm and July around 100 – 140 mm (Schulze, 1997).

The West Wits sites, with a MAP of 650 mm (Mucina and Rutherford, 2006), are situated on rocky quartzite and shale in the C6 + 7 subdivisions at 1 600 to 1 650 m with Bankenveld, xeric grassland (klipveld) and *Acacia karroo* savanna (Weiersbye *et al.*, 2006b). Acocks (1988) defined the West Wits sites as Bankenveld (61) possibly a transition between the western and central variations. O'Connor and Bredenkamp (1997) defined these as the central plateau grasslands, being the A2 subdivision, which is dominated by *Panicum coloratum* and *Eragrostis curvula*. Mucina and Rutherford (2006) described the vegetation around the West Wits sites as Gauteng Shale Mountain Bushveld (SVcb 10). This is a short (3 – 6 m tall), semi-open thicket dominated by a variety of woody species and an understorey dominated by a number of grasses.

However, the process of mining has substantially altered the vegetation at both mines with the loss of many phraetophyte (Weiersbye and Witkowski, 2003, 2007) and herbaceous species (Weiersbye *et al*., 2006). Weiersbye *et al.* (2006b) documented a total of 462 taxa colonizing slimes dams and polluted soils alone at three gold mining regions (the two study regions together with a third region at Welkom), although a higher number of taxa could be present on the properties as a whole. Cattle ranching, game (rangelands) and crop (maize and sunflower) agriculture are the predominant regional land uses surrounding the deep-level gold mining regions. Within these gold mining landscapes, wastelands such as degraded and derelict land with little vegetation cover, and swampy lands inundated with seepage from tailings dams are common (Weiersbye *et al.*, 2006b).

2.3 **Site Selection**

Possible sites were initially identified from aerial photographs (Figure 4 and 5). Thereafter a ground inspection by D. Furniss and I. Weiersbye was conducted and actual sites selected to cover the four broad vegetation types at Vaal River. One of these vegetation types was replicated at West Wits. The vegetation types at Vaal River were selected to encompass the entire catena (with the exception of the riparian woodland zone, *Phragmites* reed beds and perennial wetlands) in order of increasing vegetation structure and physiognomic complexity. These vegetation types from simple to complex physiognomy were (i) wet grassland, (ii) dry, non-rocky grasslands, (iii) dry, rocky grasslands, and (iv) perennial evergreen shrubs and trees dominated by *R. lancea* L.f. in a grassland matrix (Table 2). These *R.lancea* plots are a remnant of the Vaal Reefs Dolomite Sinkhole Woodland (Mucina and Rutherford, 2006). At West Wits only one vegetation type, non-rocky, dry grassland was selected. At Vaal River all four vegetation types were selected. The biodiversity of the sites has a different order to the physiognomic complexity (Weiersbye, pers. comm.), with wet grasslands having the lowest diversity and dominated by *Cynodon dactylon* (L.) Pers. and *Schoenoplectus corymbosus* (Roth. Ex Roem. & Schult.) J. Raynal. Non-rocky grassland has a higher biodiversity than wet grassland and is dominated by *E. curvula* and *Hyparrhenia hirta* (L.) Stapf. The woody shrub plots follow non-rocky grasslands in biodiversity, and the rocky grasslands have the highest biodiversity.

The entire gold mining region on the Highveld is characterised by various forms of disturbance ranging from general mining activities, acid mine drainage (AMD) and livestock grazing. Sites within the research area were subjectively selected at two disturbance extremes: low and high, both situated on shallow slopes (< 10°). A low disturbance site was visually determined by having a thick, generally closed canopy vegetation cover, with no evidence of major resource loss and erosion, whereas a high disturbance site was selected by having a very patchy vegetation cover with visible areas of bare ground and evidence of soil erosion and resource loss (e.g. loose surface particles, pedicels and alluvial fans). The causes of disturbance were not characterised as the purpose is not to determine particular disturbance impacts on HS measurements, but rather to determine if HS measurements can discriminate the general range of disturbance impacts on vegetation and soil in mining environments.

The result from site selection was four vegetation types, with non-rocky grassland replicated between the two gold mining regions, each at two different disturbance levels (Table 2). Plots at Vaal River were selected along two transects, from top to bottom of the catena, excluding riparian zones, and attempting to get a good distribution of all vegetation types and disturbance regimes across the mine property (Figure 4). Plots at West Wits were selected from a natural grassland along a shorter transect on a catena between a gold tailings storage dam and a natural stream, again excluding the riparian zone (Figure 5).

All field work was carried out during three field trips. The first fieldtrip occurred on the 9 August 2007 to select suitable sites. The second field trip involved the collection of LFA and HS data: three days from the 13 – 15 August 2007 were spent at Vaal River gold mining region (n = 24 plots) and one day, the 16 August 2007, at West Wits gold mining region (n = 6). A follow-up trip was made to West Wits on the 29 August 2007 and to Vaal River from the 30 August to 1 September 2007 to finalize the Global Positioning System (GPS) coordinates for the corners of each plot and the LFA data.

2.4 **Layout of Plots**

Each plot was laid out and sampled in the same manner (Figures 6, 7, 8, 9 and 10). All the grassland sites were measured as 10 m × 10 m square plots with the corners marked with stainless steel pegs and these points geolocated using a Trimble GPS with an accuracy of approximately one metre. The 10 m x 10 m plot size was selected as airborne HSRS on these mines were acquired at spatial resolution (pixel size) of 3 m. This meant a plot on the ground would be covered by a 4 x 4 pixel in the airborne data. The woody shrub *R. lancea* plots were measured as a 20 m × 20 m square with the corners similarly treated to the grassland plots. The woody shrub plots were increased in size because of the dimensions of the *R. lancea* tree canopy (approximately 2 to 6 m), and to capture any gradient effects between under-canopy and outside-canopy in LFA and HS data. Although the woody plots were bigger than the grassland plots, they were sampled in exactly the same way as grassland plots with the exception of the spacing of circular quadrats within the plots. Within each plot,

five transects were laid out running parallel to the slope gradient (gradsects) and each other (Figure 7 and 8).

Table 2 Selected vegetation types, plot size, disturbance level, and plot numbers sampled for each vegetation type in the two mining regions. Five circular quadrats per plot were sampled, a total of 150 quadrats. * indicates plots removed from the statistical analysis as explained in section 2.5. Plot numbers 3, 11, 12, 13, 15 and 18 at Vaal River were identified but not sampled due to time constraints.

Gold Mining Region	**Vegetation type**	**Size (m)**	**Disturbance**	**Plot Number (total = 30)**
Vaal River	Grassland, wet	10 x 10	Low (n = 3)	VR 9 VR 19 VR 27 *
			High (n = 3)	VR 17 * VR 20 * VR 28
	Grassland, dry non-rocky	10 x 10	Low (n = 3)	VR 1 VR 8 VR 21 *
			High (n = 3)	VR 16 VR 29 * VR 26 *
	Grassland, dry rocky	10 x 10	Low (n = 3)	VR 2 VR 23 VR 24
			High (n = 3)	VR 5 VR 14 VR 25
	Woody shrub cluster	20 x 20	Low (n = 3)	VR 7 VR 10 VR 22
			High (n = 3)	VR 4 VR 6 * VR 30 *
West Wits	Grassland, dry non-rocky	10 x 10	Low (n = 3)	WW 4 WW 5 WW 6 *
			High (n = 3)	WW 1 WW 2 WW 3

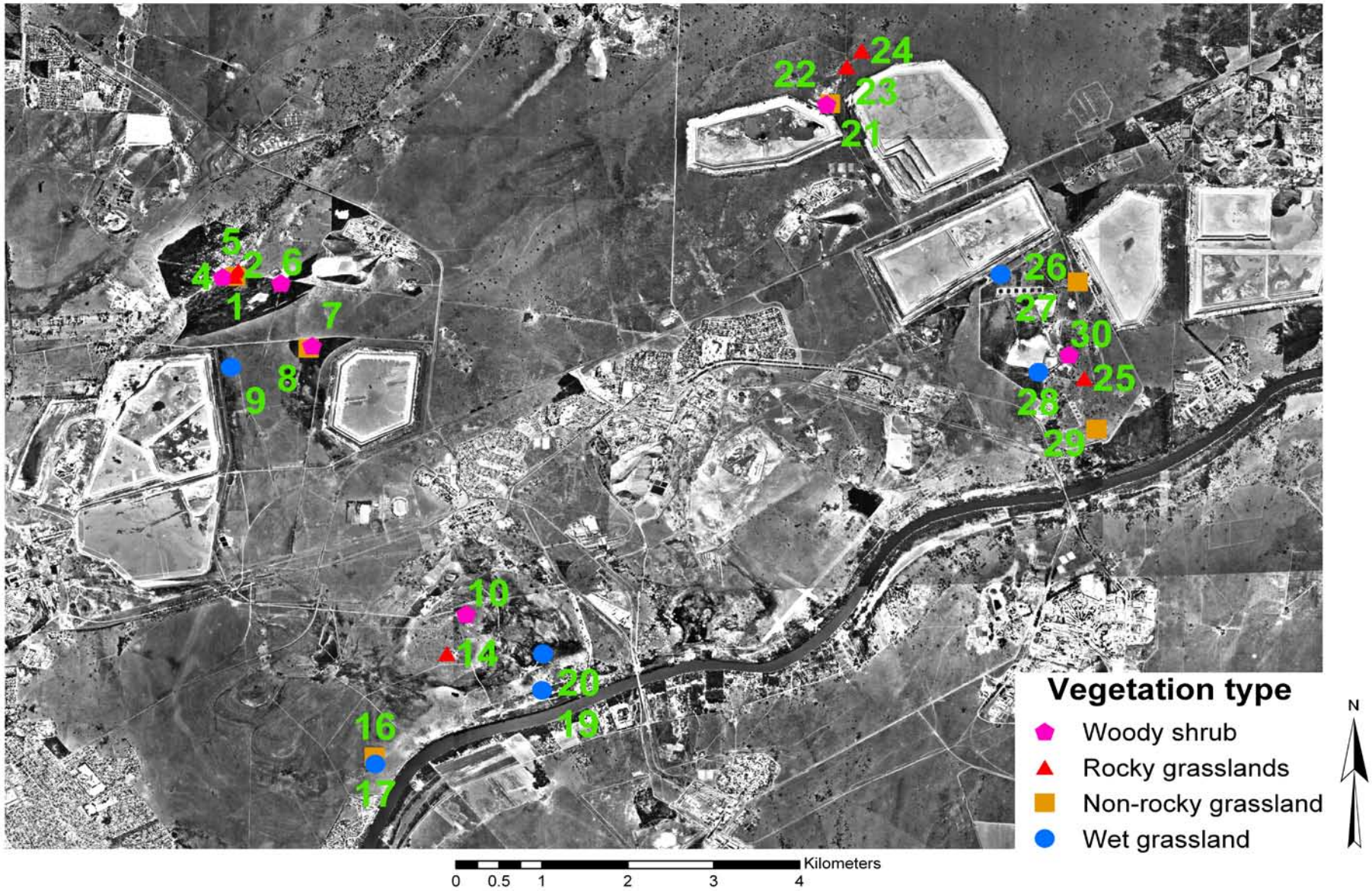

Figure 4 A mosaic of aerial photographs (2006) showing the distribution of plots along two transect lines at Vaal River mining region. Numbers correspond to the plot number (minus the VR) as described in Table 2.

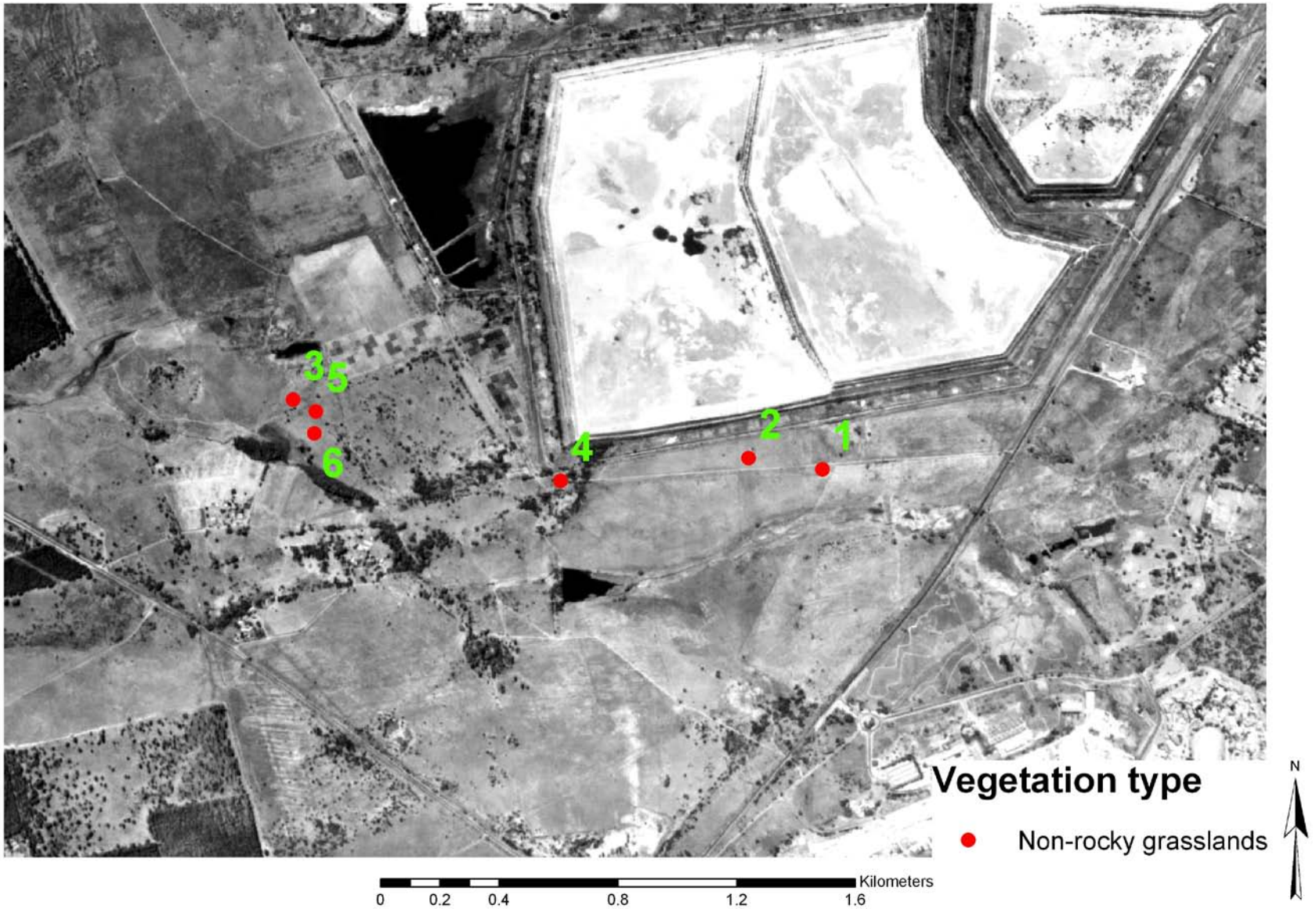

Figure 5 Aerial photograph (2006) showing the distribution of plots at West Wits mining region. Numbers correspond to the plot number (minus the WW) as described in Table 2.

These transects were two metres apart and the first and last (fifth) transect were one meter in from the boundary of the plot. Along each transect, five circular quadrats (Figure 6 and 7) were laid two metres apart, beginning one metre in from the top boundary of the plot and ending one metre in from the bottom boundary of the plot. This meant the transect length from first quadrat to last (fifth) quadrat was 8 m long. These quadrats were constructed from 4 mm spring steel shaped into a circle with a diameter of 50 centimetres. The 50 cm diameter size for the quadrats was chosen as this was slightly larger than the Field-of-View (FOV) for the field spectrometer at handheld height (approximately 1 m).

The spacing differed between the 100 m^2 grassland plots and the 400 m^2 woody plots, but the pattern was identical. In the 100 m^2 plots the steel quadrats were two metres apart, whereas in the 400 m^2 plots the quadrats were four metres apart. In both cases, the first transect began at the top right-hand corner of the plot. The end result was five transects within a plot, each with five quadrats, making a total of 25 circular quadrats spread evenly across the plot. The total for the 30 plots across both gold mining regions was 750 quadrats. Each plot was numbered (Table 2) and each transect within the plot was numbered from 1 – 5. The quadrats in each plot were also numbered from *.1 to *.5 such that the number of any quadrat could be located relative to it's transect and position on transect (i.e., quadrat 1.3 was transect 1, quadrat 3 within a specified plot). Once a plot and its quadrats were laid out, a photograph of each quadrat was taken, followed by spectral readings for all 25 quadrats, and finally LFA data from five quadrats within a plot as described in the next section.

(a)  (b) 

Figure 6 Examples of quadrats. (a) VR 2 at Vaal River, a rocky grassland with low disturbance. (b) WW2 at West Wits, a non-rocky grassland with high disturbance.

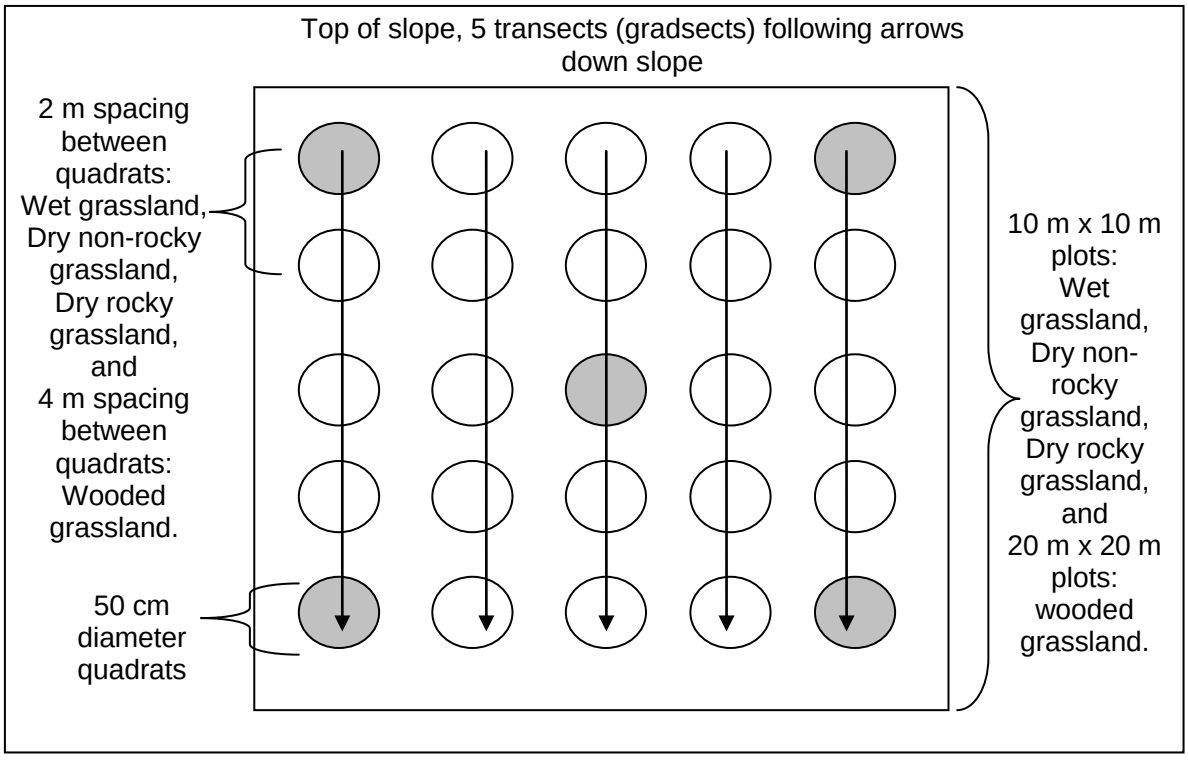

Figure 7 Diagram showing the layout of plots and quadrats. Quadrats coloured grey (n = 5) were used for statistical analysis (Section 2.4).

(a)

(b)

Figure 8 (a) A high disturbance wet grassland plot (10 m x 10 m), VR 17, showing the layout of quadrats in five transects. Each quadrat is marked with a flag. (b) A low disturbance, wet grassland plot, VR 19.

(a) 

(b) 

(c) 

(d) 

Figure 9 Examples of non-rocky grassland plots at both disturbance levels from each of the two mining regions.

(a) Non-rocky grassland, Low disturbance, Vaal River VR 8.
(b) Non-rocky grassland, High disturbance, Vaal River VR 16
(c) Non-rocky grassland, Low disturbance, West Wits WW 4
(d) Non-rocky grassland, High disturbance, West Wits WW 1

(a)

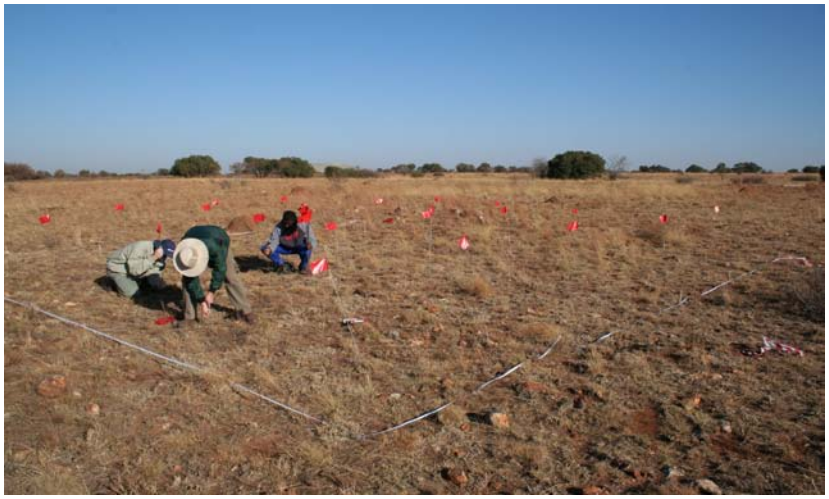

(b)

(c)

(d)

Figure 10 Examples of rocky grassland and woody shrub plots at both disturbance levels from Vaal River mining region.

(a) Rocky grassland, Low disturbance, Vaal River VR 24
(b) Rocky grassland, High disturbance, Vaal River VR 14
(c) Woody shrub, Low disturbance, Vaal River VR 22
(d) Woody shrub, High disturbance, Vaal River VR 7

2.5 **Acquisition of LFA Data**

The purpose of using LFA techniques, and in particular the SSIs and the SSCIs, is to acquire surrogate measures of land surface condition. However, as the aim of this study is not to undertake an LFA assessment of the mine, but to determine the relationship between LFA and HS measurements at the same spatial resolution (where a single HS pixel is equivalent to a single LFA observation), three deviations from the standard assumptions of the LFA technique were made.

The first was that spectral data was sampled across a single 50 cm diameter quadrat whose size was based on the FOV of the field spectrometer (Figure 6). The result was that a quadrat contained small patches and inter-patches within a single pixel, i.e., the resultant HS data is a mixed pixel, within which bare soil, rock, biogenic crust, debris and vegetation (i.e. patch and inter-patches) vary in direct proportion to each other. In LFA, a patch is a landscape unit defined by a boundary in which the deposition of material occurs (Tongway and Hindley, 2004). Inter-patches are defined as areas in which removal, in some form or other, of material is occurring. In homogenous vegetation types with continuous swards or large inter-patch areas the patch or inter-patch size is much larger than the quadrat (rexel) or HS pixel. But in many plots in this study in a semi-arid environment, patch and inter-patch size was defined by a tuft of grass or the space between tufts respectively. This results in many quadrats containing both patches and inter-patches, in varying proportions depending on the vegetation type and disturbance. The eleven SSIs are measured as patch indicators, and since most quadrats tended to be mixtures of patches, this could increase the high variance in the final three calculated SSCIs. However, the study required discrimination between four vegetation types of varying condition, and not between individual patches and inter-patches within each vegetation type.

The second deviation from the standard LFA approach occurred due to the limitation of the HS sensor to define LFA sampling units (i.e. 3 x 3 m pixel size in airborne and a 44 cm diameter FOV for the ground-based HS sensor when held at a height of 1 m). When LFA is used for monitoring purposes as is standard, the importance of an SSCI value is determined as a weighted mean based on respective patch and inter-patch proportions along a gradsect. However, in this study such weighted means could not

be calculated, first, because the length of patches and inter-patches along a transect was not measured, as it was considered irrelevant to the study objectives, and second, because the sampling unit was based on HS sensor FOV limitations, and not patch and inter-patch sizes. In a plot which was essentially a continuous sward, this deviation is of little significance, but especially in some high disturbance plots or plots with high heterogeneity this deviation may have been of higher significance and introduced bias into the final LFA SSCI values.

The third deviation from the standard LFA technique arose as a result of time constraints. The HSRS equipment and team were only available for four days of fieldwork. This put constraints on the gathering of SSI data which is far more labour intensive and therefore time consuming than the gathering of HS data. Furthermore, the objective is to have paired readings for each unit of HS and LFA data. To meet this objective the LFA process was therefore adapted so that it could be paired with the HS reading for each quadrat. The amendment took the form of collecting a high resolution photograph of each quadrat for later allocation of the eleven SSI's. But some SSI's cannot or are difficult to allocate accurately from photographs and were therefore measured directly in the field (Table 3). But again, with time being limited, these were not measured for every quadrat in a plot. Rather five quadrats – viz. the four corner quadrats (quadrats 1.1, 1.5, 5.1 and 5.5) for each plot together with a central quadrat (most commonly 3.3) were photographed and sampled on the ground as per table 3 for these indices. This pattern was chosen as it was thought it covered any pattern that might exist in a plot (Figure 7).

Photographs were taken of the plot in its setting (Figure 8. 9 and 10) so that background details and local situation around the plot was characterised and documented. Then each quadrat was photographed in sequence. The photograph was taken such that the circular quadrat almost filled the field of view (Figure 6). Each photograph was taken as close to the zenith as possible taking into account that photographs were taken through the midday period. Later the photograph for each quadrat was examined and the remaining six SSIs allocated (Table 3).

Table 3 LFA SSI's measured from photographs or directly in the field.

SSI	Source of measurements
Soil cover	Photograph
Basal cover	Photograph
Litter cover, origin and degree of decomposition	Field
Cryptogam cover	Field
Crust brokenness	Photograph
Erosion type and severity	Photograph
Deposited materials	Photograph
Surface roughness	Photograph
Surface resistance to disturbance	Field
Slake test	Field
Soil texture	Field

Finally these eleven SSI's were used to calculate the three SSCI's using three algorithms developed by Tongway and Hindley (2004). When acquiring the data for 9 plots, errors were made in the field measurements – i.e. some photographs were omitted or the quadrats within the plots were found to have been measured inconsistently, or as in the case with the last plot (VR30) HS measurements could not be recorded because the sun had dropped too close to the horizon. This meant that accurate pairing of HS and LFA data could not be accomplished for these 9 plots and therefore they were omitted from the statistical analysis (reducing the available number of plots to 21 plots). The 5 quadrats from each plot sampled for LFA values were used resulting in a total of 105 quadrats available for statistical analysis (Table 2).

2.6 **Hyperspectral Data Collection**

Hyperspectral data was collected using an Analytical Spectral Device (ASD) spectrometer, the FieldSpec-Pro (Analytical Spectral Devices Inc., Boulder, Colorado, USA) with a range of 350 nm to 2500 nm and a sampling interval of 1.4 nm from 350 – 1000 nm and 2 nm from 1000 – 2500 nm. The spectral resolution (full width half maximum) was 3 nm at 700 nm, and 10 nm at 1400 nm to 2100 nm. HS data was collected between 9 am and 3 pm only, and when the quanta of radiant energy was suitable. The decision not to measure was made when "noise" amplitude became too high in the Short Wave Infra-Red (SWIR) region of the electromagnetic spectrum around 2.5 μm. Furthermore, the LFA photographs were taken immediately before the spectral readings to ensure that ambient light conditions and vegetation shadows were the same for both data sets. The LFA field measurements were made within a few hours of the spectral readings. Measurements were made using a bare fibre optic sensor with the spectrometer mounted in a backpack on the operators back. Rundquist *et al.* (2004) showed that spectra acquired using a handheld sensor can vary up to 25% compared to a mounted sensor and therefore we used a central tripod mounted with the sensor and a plumb line to position the sensor at the quadrat azimuth. The FOV for the sensor was approximately 25°, held at 1 m above ground level, which acquired a ground level footprint of approximately 44 cm in diameter.

Before and during the acquisition of spectral readings in a plot, the spectrometer was calibrated to the incoming solar radiation using a calibrated Spectralon® 100% reference panel. This calibration process was repeated according to the operators judgement, or whenever "noise" amplitude in the measurements increased, or intensity levels between successive readings differed. The 25 quadrats within the plot were then measured (Figure 6, 7) with a standard protocol used on every plot, beginning at the top right hand corner of the plot and moving down than up successive transects. The operator held the sensor at the azimuth above the quadrat and the steel hoop was removed prior to sampling the quadrat so that the metal did not contaminate the readings. After HS sampling the hoop was replaced so that the LFA team could sample the same place. Each quadrat was sampled 80 times in one sequence and then the average of the 80 readings was saved as the reading for that quadrat. The measured reflectances are a ratio between the reference standard and the target. No

atmospheric post-processing of the spectra was required as all spectral measurements were calibrated at ground level with the reference panel. For the calculation of VIs, the wavelengths and algorithms as described in Table 1 were used to calculate the respective VI. For PLSR modelling, the spectra were prepared as described in section 2.7. Analysis of the spectra for mineralogical information was beyond the scope of my study.

2.7 **Statistical Analysis**

All statistics were performed using Microsoft Excel 2003 and R open source software (R Development Core Team, 2007). In all statistical testing, significant differences were regarded as probability values less than 1 % (**) or 5 % (*) and all t-tests used corrected degrees of freedom. A number of key questions and hypotheses were posed:

- My first key question was to determine if the selected quadrats, when combined, were generally above or below the threshold for self-sustainability? This was tested by ranking the LFA SSCIs from lowest to highest and the distribution compared to the calculated theoretical threshold allowing one to draw conclusions about the level of degradation and the self-sustainability of the biogeochemical processes at the soil surface (Tongway and Hindley, 2004). The threshold is calculated as the central value in the range reflecting the inflection point between the two curves generated by the ranking of the obtained LFA index values. This threshold is not an absolute value as it is dependent on the quality of range end-points in reflecting the extremes available in the environment under study;
- I hypothesised that there was no difference in stability, infiltration or nutrient cycling between quadrats in the two mining regions, and tested this with a Welch Two Sample t-test by comparing the non-rocky grassland quadrats from each mining region, with disturbance levels combined;
- Similarly, I hypothesised that there would be no difference in LFA indices between disturbance levels, when combining vegetation and mines for each disturbance level, and tested this with a Welch Two Sample t-test;

- To test my hypothesis of no difference between vegetation types, a one-way ANOVA was applied to the LFA indices for the four vegetation types, after combining disturbance levels and mining regions within each vegetation type;
- My final hypothesis, for the LFA data, was that stability, infiltration and nutrient cycling indices would have no difference between low disturbance sites compared to high disturbance sites within each vegetation type. For this analysis I regarded non-rocky grasslands from Vaal River and West Wits regions as separate entities. This hypothesis was tested with a number of Welch Two Sample t-tests.

The VI values were subjected to the same basic hypotheses and statistical approach described above for the LFA indices, without ranking the results, as threshold values for a VI are irrelevant.

- A further key question was to test the accuracy of the VIs in measuring the plant characteristic they were designed for (i.e. chlorophyll or plant water content), in the absence of empirical data about these plant characteristics, when using spectral reflectance of winter senesced vegetation. To this end, correlation analysis was performed between the VIs to test for relationships between the VIs. The underlying assumption being that VIs measuring a similar plant characteristic but using widely separated wavelengths should give highly correlated results.
- To test the hypothesis that VIs can predict LFA indices, simple linear regression (Galpin, 2007) was applied between the LFA indices as response variables, and the VIs as the predictor variables. In all analyses, outliers were identified as extreme values inconsistent with the general trend in the data, and tests repeated with outliers removed but this did not improve statistical results, so all results in this report are shown with no quadrats removed from any analysis.

2.8 **Partial Least Squares Regression Modelling**

PLSR is a data compression method using matrix algebra techniques for extracting "latent variables" or components from two data sets through maximising the explained X/Y covariance (Frank and Friedman, 1993; Martens, 2001). PLSR modelling was performed with R open source software (R Development Core Team, 2007) and the pls package (Mevik and Wehrens, 2007, Wehrens and Mevik, 2007). The LFA indices and spectral data were paired. Thereafter, the pairs were randomly separated into two datasets by allocating each fourth spectrum into validation data (n = 26), with the remaining data (n = 79) used to calibrate suitable PLSR models. The validation data was used as new data to test the predictive accuracy of the models selected from the calibration phase. The LFA data was used as calculated with no transformations or scaling. The spectral data first had the wavelengths affected by sensor steps or atmospheric water interference removed (Ong *et al.*, 2004, 2008; Figure 11) and were then centred by the pls algorithm (Mevik and Wehrens, 2007), but not scaled as all the spectral measurements have the same units (Geladi and Kowalski, 1986). The Root Mean Square Error of Prediction (RMSEP) was calculated using Leave-One-Out (LOO) Cross-Validation (CV) (Mevik and Wehrens, 2007, Mevik and Cederkvist, 2004). The RMSEP was used to select the best fitting models while avoiding over-fitting. Over-fitting is when a model with many parameters gives a strong fit to the data, often by modelling both the features and the "noise" in the data. However, such models with many parameters, some of which are modelling data "noise", have poor predictive abilities with new data. Such best fitting models are identified by having the lowest or lowest local RMSEP. Interpretation of the main environmental features influencing the models was performed by examining the plots of the loading factors for components constituting the model parameters (Mevik and Wehrens, 2007).

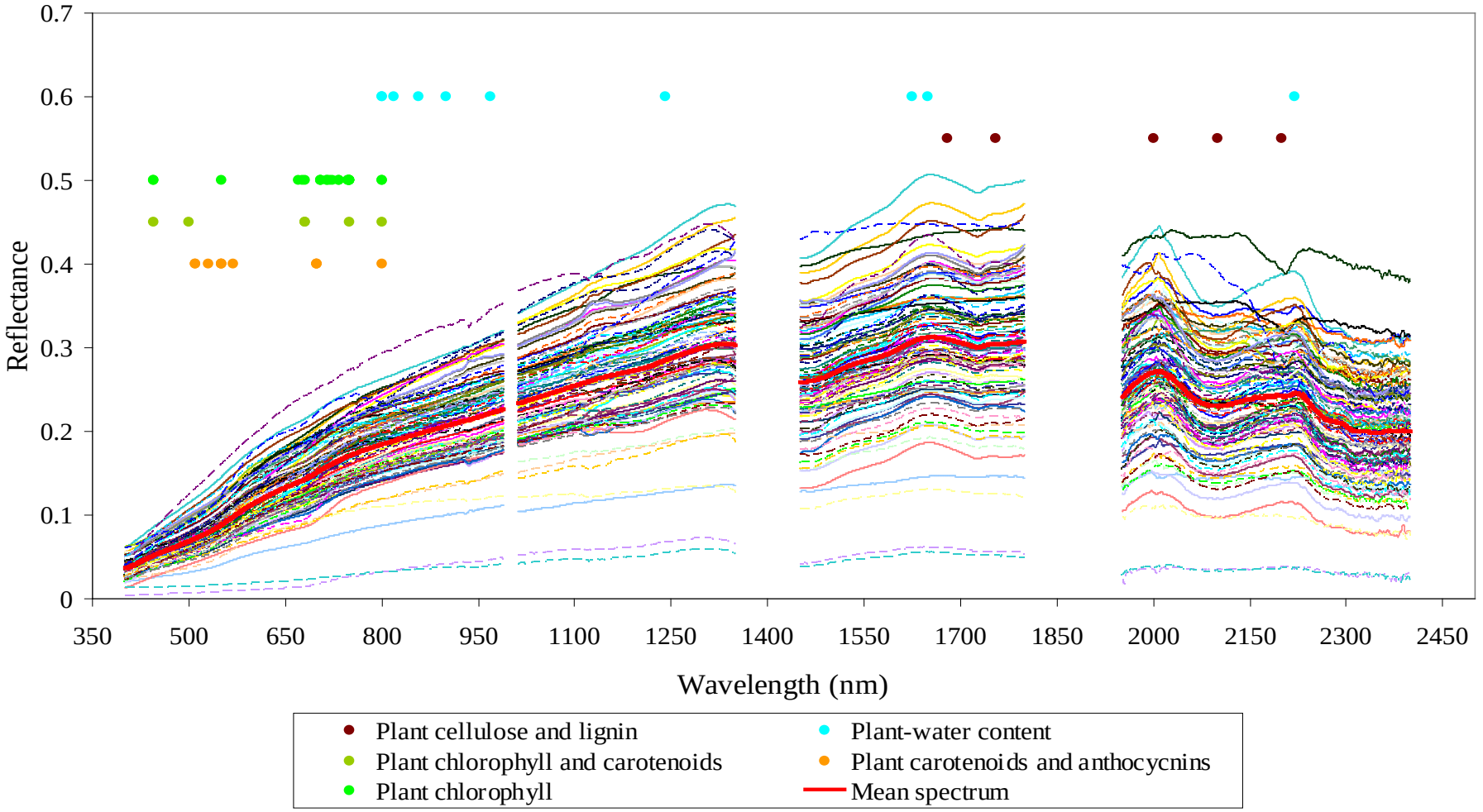

Figure 11 The full spectrum for each quadrat (n = 105) showing the position of the selected bands for different categories of Vegetation Index (VI). The spectra themselves show the prepared spectra for PLSR modelling with removal of the initial UV / visible region (350 – 399 nm), the step between sensors (990 – 1010 nm), atmospheric water noise (1350 – 1450, 1800 – 1950 nm) and sensor/ source noise in the SWIR (2400 – 2500 nm).

3. Results

3.1 LFA Results

3.1.1 Relationship of the LFA Values to the Threshold Value

Key question: Are the LFA values for quadrats above or below the threshold value for self-sustainability.

To answer this question, the LFA values for stability, infiltration and nutrient cycling, were ranked, then plotted from low to high values (Figure 12). The threshold value for each index is calculated by finding the central value in the range and is indicated by an arrow in Figure 12. The threshold value is an estimator of where there may be a change from self-sustainability in biogeophysical processes around the soil surface to non-sustainability (losing resources) within a quadrat (Tongway and Hindley, 2004).

The values obtained for stability are markedly higher then those for the other two indices where infiltration is slightly higher than nutrient cycling. Eighty percent of quadrats lay above the stability threshold value of 52.92% (Table 4; Figure 12). Of the 20% below threshold, 29% of high disturbance quadrats and 13% of low disturbance quadrats were below threshold. The high end of the stability range (70.83%) was dominated by low disturbance quadrats while the low end (35%) was dominated by high disturbance quadrats.

The ranked infiltration values produced a lower distribution of values compared to stability (Figure 12). The range was from 50.14 to 15.31% with a threshold for infiltration of 32.74% (Table 4). Contrary to the pattern for stability, only 38% of quadrats fell above the threshold value of 32.74% for infiltration. Of the 62% of quadrats below threshold, 71% of high disturbance quadrats and 55% of low disturbance quadrats fell below threshold.

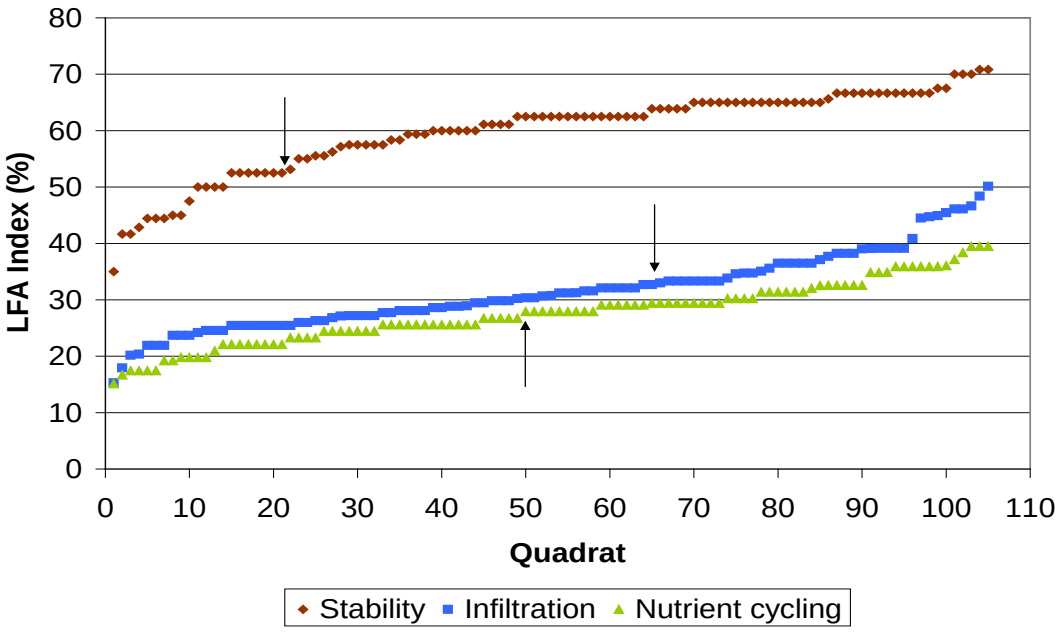

Figure 12 Ranked distributions of LFA SSCI values: stability, infiltration and nutrient cycling for all Vaal River and West Wits quadrats (n = 105). The arrows indicate the threshold value for that index.

Table 4 Results from ranking LFA SSCIs for stability, infiltration and nutrient cycling for all quadrats from Vaal River and West Wits mining regions combined (n = 105).

	Stability (%)	**Infiltration (%)**	**Nutrient cycling (%)**
Range	70.8 – 35.0	50.1 – 15.3	39.5 – 15.1
Threshold value	52.9	32.7	27.3
% above threshold	80	38	53
% high disturbance above threshold	71	29	33
% low disturbance above threshold	87	45	68
% below threshold	20	62	47
% high disturbance below threshold	29	71	67
% low disturbance below threshold	13	55	32

Nutrient cycling produced the lowest distribution of LFA values, being generally slightly lower than infiltration values (Figure 12). The threshold value for nutrient cycling (27.30%) was much closer to a central value in its distribution than that for either stability or infiltration. Forty-seven percent of quadrats fell below the nutrient cycling threshold. This 47% below threshold for nutrient cycling values represented 67% of high disturbance quadrats and 32% of low disturbance quadrats.

3.1.2 **Comparison of LFA Results Between Quadrats from Different Mining Regions**

- My hypothesis was that there was no difference in stability, infiltration or nutrient cycling between quadrats from the two mining regions.

T-tests comparing non-rocky grasslands between mines (Table 5, Figure 13) showed no difference for the stability index. Infiltration differed ($P < 0.01$, $DF = 36.79$) with West Wits having higher values ($30.88 \pm 0.99\%$) than Vaal River ($27.17 \pm 0.90\%$). Nutrient cycling differed ($P < 0.01$, $DF = 26.4$) with West Wits having higher mean values ($27.24 \pm 0.63\%$) than Vaal River ($24.26 \pm 0.94\%$). I therefore accept the hypothesis of no difference for the stability index and rejected the hypothesis for the infiltration and nutrient cycling indices.

3.1.3 **Comparison of LFA Results Between Vegetation Types**

- My hypothesis was that there was no difference in stability, infiltration or nutrient cycling between vegetation types.

A one-way ANOVA (Table 6) showed that the stability index differed between the four vegetation types ($P < 0.01$, $DF = 3, 101$). The infiltration ($P < 0.05$, $DF = 3,101$) and nutrient cycling indices ($P < 0.05$, $DF = 3,101$) also differed between vegetation types. I therefore reject the hypothesis of no difference between LFA values for the four vegetation types, and accept the alternative hypothesis that all three LFA indices, stability, infiltration and nutrient cycling, differed between the four vegetation types when combining disturbance levels.

Wet grassland produced the highest values for all three indices (stability = 63.97 ± 0.79%, infiltration = 34.53 ± 1.25% and nutrient cycling = 31.53 ± 1.08%) (Figure 14) and had the narrowest range for the three LFA indices (Appendix 1). Analysis of the raw SSI values (not shown) showed that wet grasslands had high rain splash protection, high litter cover and low presence of physical crusts with low values for deposition and erosion, compared to the other vegetation types.

For the other three vegetation types, there was a switch in the ranking order of the means when comparing stability with infiltration and nutrient cycling (Figure 14). Non-rocky grassland had the higher stability (62.58 ± 0.82%) followed by rocky grassland (58.57 ± 1.52%), with woody shrub having the lowest stability index (53.27 ± 1.66 %) (Figure 14). The high stability for non-rocky grasslands results from high SSI values for rain splash protection and cryptogams (not shown). Infiltration and nutrient cycling had the reverse trend with woody shrub higher (33.83 ± 1.75% and 28.02 ± 1.48% respectively), followed by rocky grassland (31.43 ± 1.56% and 27.33 ± 1.19% respectively).

Non-rocky grassland had the lowest infiltration and nutrient cycling (29.49 ± 0.75% and 26.12 ± 0.57% respectively). This reversal of trend was principally due to higher litter and soil roughness values for woody shrub quadrats and low soil roughness and litter for non-rocky grasslands (not shown). The variable and sometimes small sample sizes ($n \geq 5$) may have contributed to these observations.

3.1.4 **Comparison of LFA Results Between Disturbance Levels**

- My hypothesis was that there would be no difference between LFA indices from high or low disturbance levels.

Stability, infiltration and nutrient cycling indices differed between high and low disturbance quadrats when combining mining regions and vegetation types (Table 7), therefore in all three LFA indices, I reject the hypothesis of no difference. In all three cases: stability, infiltration and nutrient cycling, low disturbance quadrats were higher (61.82 ± 0.82 %, 33.24 ± 0.92 % and 29.30 ± 0.70 % respectively) with a broader range of LFA values (Appendix 1) than high disturbance quadrats (57.25 ± 1.19 %, 29.32 ± 0.86 % and 25.34 ± 0.72 % respectively) (Figure 15).

Table 5 Welch Two Sample t-tests comparing LFA values for non-rocky grasslands between Vaal River (n = 15) and West Wits (n = 25) mining regions combining disturbance levels. * is significant at the 5 % level, and ** is significant at the 1 % level.

LFA	t-value	Corrected Degrees of Freedom	Probability
Stability	-1.51	26.63	0.14
Infiltration	-2.78	36.79	0.009 **
Nutrient Cycling	-2.62	26.43	0.01 **

Table 6 One-way ANOVA table of LFA Indices for the four vegetation types (n = 105) when pooling mining regions and disturbance levels. * is significant at the 5 % level, and ** is significant at the 1 % level.

LFA index	Degrees of Freedom	F value	Probability
Stability	3, 101	11.68	< 0.0001 **
Infiltration	3, 101	2.92	0.03 *
Nutrient Cycling	3, 101	3.86	0.011 *

Table 7 Welch Two Sample t-tests comparing LFA values between disturbance levels for all vegetation types and mining regions combined. Low disturbance n = 60, high disturbance n = 45. * is significant at the 5 % level, and ** is significant at the 1 % level.

LFA	t-value	Corrected Degrees of Freedom	Probability
Stability	3.17	81.78	0.003 **
Infiltration	3.10	102.32	0.003 **
Nutrient Cycling	3.94	100.08	0.0002 **

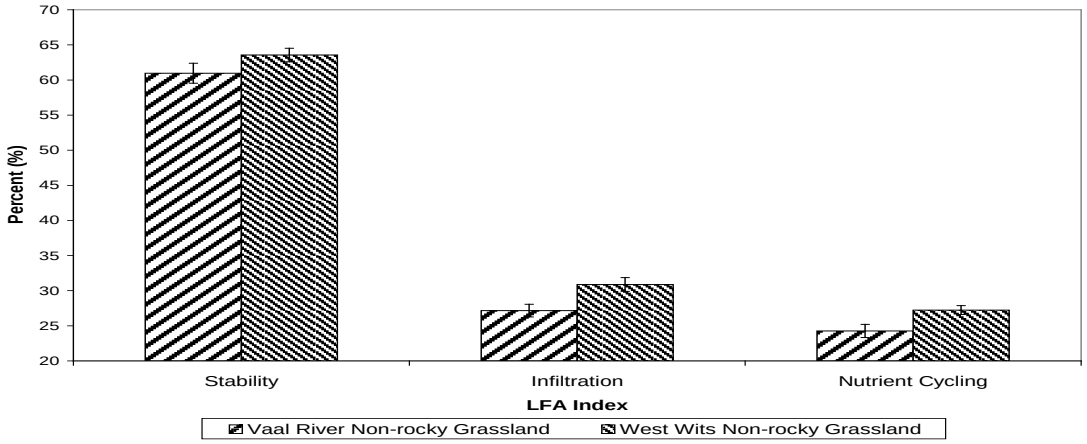

Figure 13 Comparison of LFA indices (means and standard errors) for non-rocky grassland between Vaal River and West Wits mining regions combining disturbance levels.

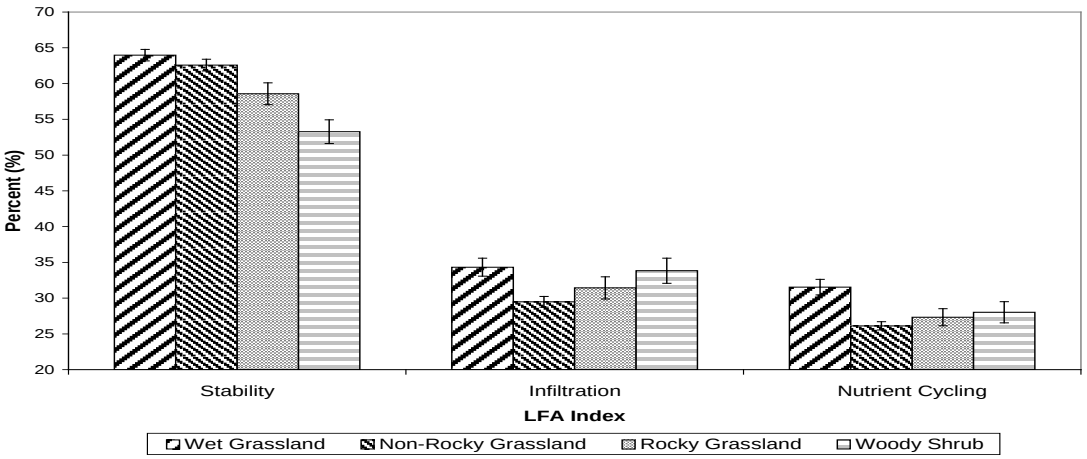

Figure 14 Comparison of LFA indices (means and standard errors) between the four vegetation types combining mining regions and disturbance levels.

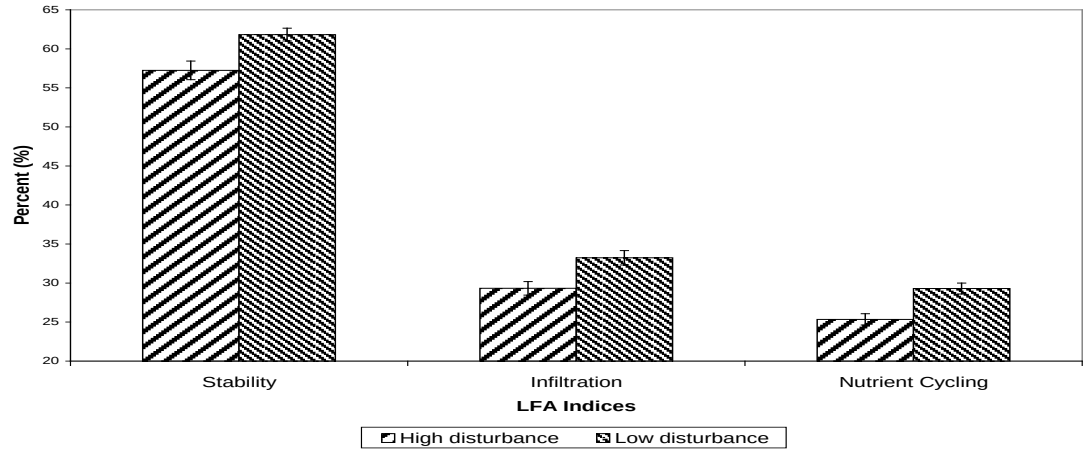

Figure 15 Comparison of LFA indices (means and standard errors) between high and low disturbance quadrats, combining mining regions and vegetation types.

3.1.5 **Differences in Stability Between Disturbance Levels for the Different Vegetation Types**

- My hypothesis was that there was no difference for stability indices between low and high disturbance quadrats from the same vegetation type.

Low disturbance quadrats had higher stability indices than high disturbance quadrats across all vegetation types, with the exception of wet grasslands and non-rocky grasslands at Vaal River (Table 8a, Figure 16a). These differences were significant for non-rocky grassland from West Wits ($P < 0.01$, $DF = 22.97$), and for Vaal River rocky grassland ($P < 0.01$, $DF = 16.92$) and woody shrub quadrats ($P < 0.01$, $DF = 11.24$). Therefore the hypothesis of no difference in stability indices between disturbance levels is accepted for wet grasslands and non-rocky grasslands at Vaal river, but rejected for non-rocky grasslands at West Wits and rocky grasslands and woody shrub quadrats at Vaal River. Low disturbance non-rocky grassland quadrats from West Wits had the highest stability values ($66.73 \pm 0.94\%$). The exception, Vaal River non-rocky grassland reversed the trend with higher stability indices ($62.50 \pm 1.37\%$) for high disturbance compared to low disturbance ($60.19 \pm 2.02\%$) but this was not significant. The data range for low disturbance had higher values than that for high disturbance (Appendix 1) suggesting that this exception may be an artefact of a small sample size ($n = 5$) from one plot.

3.1.6 **Differences in Infiltration Between Disturbance Levels for the Different Vegetation Types**

- My hypothesis was that there was no difference for infiltration indices between low and high disturbance quadrats from the same vegetation type.

Infiltration indices had a similar pattern compared to the stability indices (Table 8b, Figure 16b), with the exception of wet grasslands at Vaal River. Both wet grasslands ($P < 0.01$, $DF = 11.2$) and non-rocky grasslands ($P < 0.05$, $DF = 7.07$) at Vaal River had higher infiltration indices for high disturbance than low disturbance quadrats. In contrast, West Wits non-rocky grassland (non-significant) and Vaal River rocky grasslands ($P < 0.01$, $DF = 25.18$) and woody shrub ($P < 0.01$, $DF = 17.26$) quadrats had the reverse pattern, with low disturbance having higher infiltration indices and

high disturbance having low infiltration values (Figure 16b). Therefore I reject the hypothesis of no difference between disturbance levels for wet grassland, non-rocky grassland, rocky grassland and woody shrub quadrats from Vaal River, but accept the hypothesis for non-rocky grasslands from West Wits. Similar to the results for stability indices, the vegetation types with higher infiltration indices in high disturbance quadrats (wet grassland and non-rocky grassland from Vaal River) had narrow data ranges (Appendix 1) with few replicates (n = 5) from a single plot. This low degree of replication from single plots may have contributed to the direction and significant differences between disturbance levels in these two vegetation types.

3.1.7 **Differences in Nutrient Cycling Between Disturbance Levels for the Different Vegetation Types**

- My hypothesis was that there was no difference between nutrient cycling indices from high and low disturbance quadrats from the same vegetation type.

The pattern for nutrient cycling indices was similar to the infiltration indices but with slight changes where the differences occurred (Table 8c, Figure 16c). Low disturbance plots in non-rocky grassland from West Wits ($P < 0.01$, $DF = 18.12$), and rocky grassland ($P < 0.01$, $DF = 27.99$) and woody shrub ($P < 0.05$, $DF = 9.27$) from Vaal River plots had higher nutrient cycling than high disturbance plots. I therefore reject the hypothesis of no difference between disturbance levels for the nutrient cycling index in non-rocky grasslands from West Wits, and rocky grasslands and woody shrub quadrats from Vaal River. However, I accept the hypothesis of no difference between disturbance levels for nutrient cycling in wet grasslands and non-rocky grasslands from Vaal River. Nutrient cycling indices for wet grassland and non-rocky grassland from Vaal River tended to be higher (non-significant) in high disturbance quadrats than in low disturbance quadrats. These two exceptions are possibly an artefact of small sample size (n = 5) from a single high disturbance plot in each vegetation type. The highest mean nutrient cycling index (31.73 ± 1.27 %) was from high disturbance wet grassland (Figure 16c), although low disturbance rocky grassland produced some higher individual quadrat values (Appendix 1) for the nutrient cycling index. Conversely high disturbance woody shrub had the lowest mean nutrient cycling indices (22.33 ± 2.06 %) (Figure 16c).

Table 8 Welch Two Sample t-tests comparing (a) stability, (b) infiltration and (c) nutrient cycling from high and low disturbance vegetation types. * is significant at the 5 % level, and ** is significant at the 1 % level.

(a)

Vegetation	High Disturbance n	Low Disturbance n	t- value	Corrected Degrees of Freedom	Probability
Wet grassland Vaal River	5	10	2.16	10.30	0.06
Non-rocky grassland both mines	20	20	1.51	26.63	0.14
Non-rocky grassland Vaal River	5	10	-0.95	12.99	0.36
Non-rocky grassland West Wits	15	10	3.42	22.97	0.002 **
Rocky grassland Vaal River	15	15	4.54	16.92	0.0002 **
Woody shrub Vaal River	5	15	3.27	11.24	0.007 **

(b)

Vegetation	High Disturbance n	Low Disturbance n	t- value	Corrected Degrees of Freedom	Probability
Wet grassland Vaal River	5	10	-3.15	11.20	0.009**
Non-rocky grassland both mines	20	20	-0.20	37.99	0.84
Non-rocky grassland Vaal River	5	10	-2.88	7.07	0.02*
Non-rocky grassland West Wits	15	10	2.06	22.99	0.051
Rocky grassland Vaal River	15	15	3.08	25.18	0.004**
Woody shrub Vaal River	5	15	5.31	17.26	0.00005**

(c)

Vegetation	High Disturbance n	Low Disturbance n	t- value	Corrected Degrees of Freedom	Probability
Wet Grassland Vaal River	5	10	-0.15	12.45	0.89
Non-rocky grassland both mines	20	20	2.62	26.43	0.014*
Non-rocky grassland Vaal River	5	10	-1.31	7.06	0.23
Non-rocky grassland West Wits	15	10	4.89	18.12	0.0001**
Rocky grassland Vaal River	15	15	3.55	27.99	0.001**
Woody shrub Vaal River	5	15	2.91	9.27	0.016*

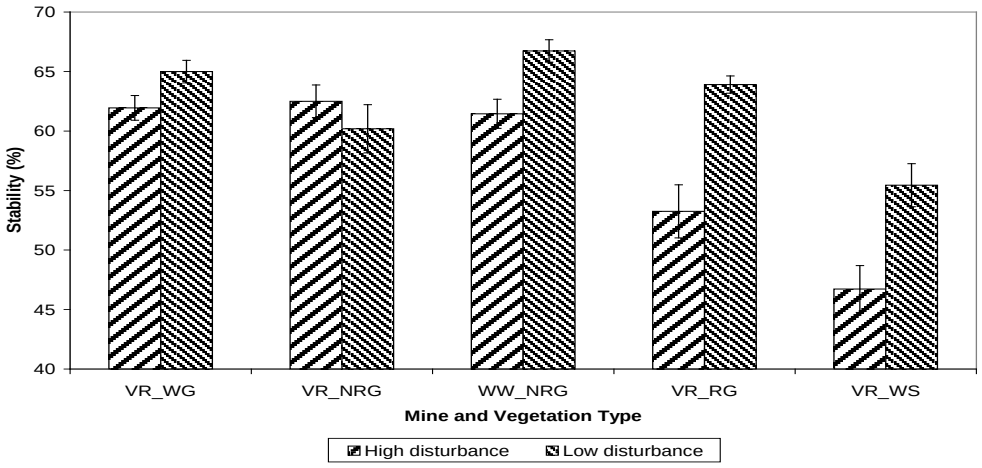

(a)

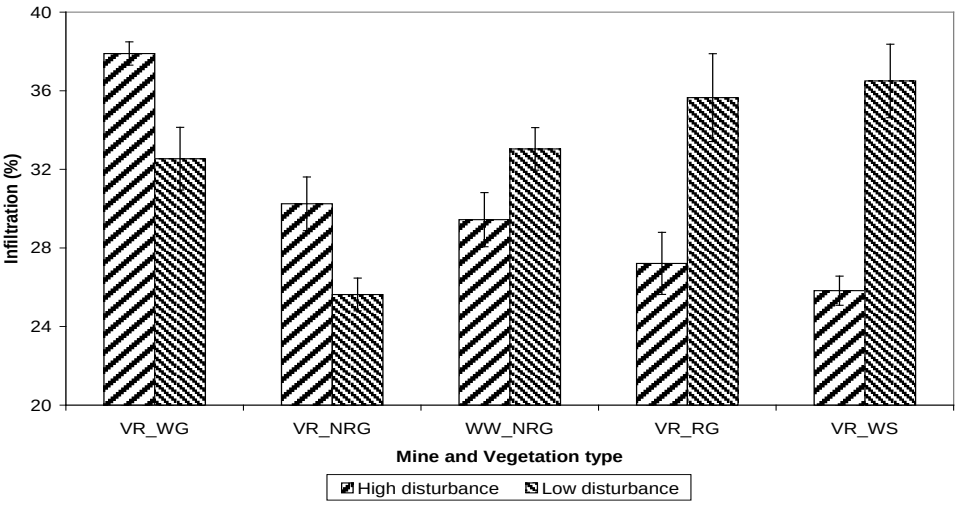

(b)

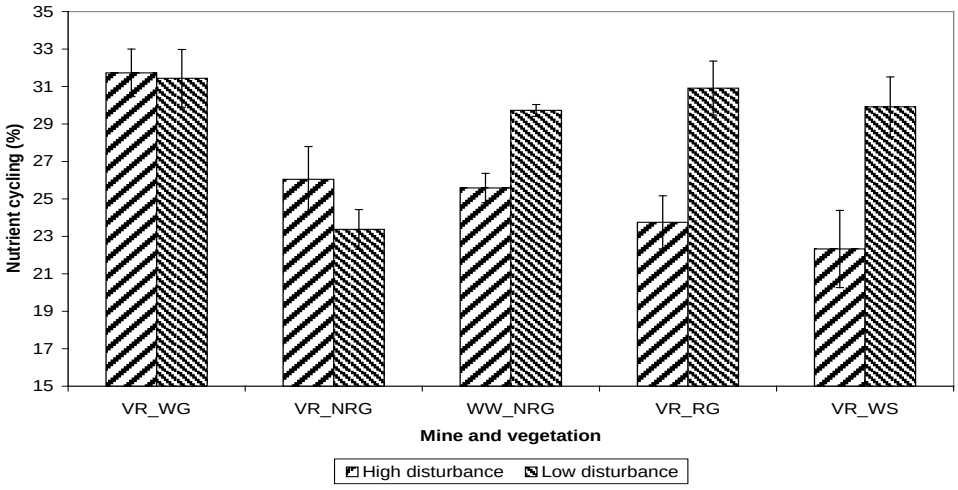

(c)

Figure 16 Comparing indices of (a) stability, (b) infiltration and (c) nutrient cycling (mean and standard error) for high and low disturbance quadrats in different vegetation types. VR = Vaal River, WW = West Wits, WG = Wet Grassland, NRG = Non-Rocky Grassland, RG = Rocky Grassland, and WS = Woody Shrub.

3.2 Results for the Vegetation Indices

3.2.1 Ranges Obtained for VIs

The ranges for the various chlorophyll based vegetation indices for my winter (dry season) survey were within the ranges given in the ENVI 4.2 chapter dealing with vegetation indices for green vegetation (Table 9). However, they tended towards the lower end of the scale. The VOG2 and VOG3 indices produced slightly negative values (-0.05 to -0.005) for my winter senesced vegetation, contrasting with those given in ENVI 2.4 which are from 0 to 20 for green vegetation (commonly between 4 and 8). Of the mixed chlorophyll and carotenoid indices, the SIPI results for this study were within the lower end of the range described in ENVI 4.2. The PSRI for our winter senesced vegetation had values above the range shown for green vegetation in ENVI 4.2.

Carotenoid indices produced some extreme values (Table 9). The PRI was within the range postulated by ENVI 4.2. CRI1 had a single quadrat, VR7_5-5 from a low disturbance woody shrub plot which was an extremely high value. Examination of a photograph of this quadrat showed mixed shade and sunlight on a thick litter layer with minimal soil showing. The shadowing may have dampened the amplitude of the spectral reading. This quadrat was an outlier for many VIs, with exceptions to this being the SAVI, PSRI, PRI, NDLI and some plant-water indices: NDII, NDII5 and NDII7 indices. This quadrat produced one of two very low overall reflectance spectra (Figure 11). The other quadrat which produced a very low overall spectrum was VR10_4-3, another woody shrub quadrat of low disturbance. This quadrat produced extreme values for the PRI, PSRI and SAVI indices.

Table 9 Vegetation Indices, their range, means and standard errors obtained for this study compared to common ranges obtained for green vegetation (ENVI 4.2).

VI	Range (ENVI 4.2)	Common range for green vegetation (ENVI 4.2)	Range obtained in this research	Mean	SE
Chlorophyll based VIs:					
NDVI	-1 to 1	0.2 to 0.8	0.05 – 0.38	0.13	0.004
$NDVI_{750}$	-1 to 1	Not available	0.047 – 0.308	0.09	0.003
GNDVI	-1 to 1	Not available	0.219 – 0.528	0.32	0.005
SAVI	-1 to 1	Not available	0.026 – 0.153	0.08	0.002
$NDVI_{705}$	-1 to 1	0.2 to 0.9	0.024 – 0.175	0.06	0.002
mSR_{705}	0 to 30	2 to 8	1.08 – 1.56	1.18	0.007
$mNDVI_{705}$	-1 to 1	0.2 to 0.7	0.039 – 0.219	0.08	0.003
VOG 2	0 to 20	4 to 8	-0.046 – -0.005	-0.015	0.0005
VOG 3	0 to 20	4 to 8	-0.047 – -0.005	-0.015	0.0005
Mixed chlorophyll and carotenoid based VIs:					
SIPI	0 to 2	0.8 to 1.8	0.329 – 0.594	0.408	0.004
PSRI	-1 to 1	-0.1 to 0.2	0.274 – 0.54	0.428	0.005
Carotenoid based VIs:					
PRI	-1 to 1	-0.2 to 0.2	-0.17 – -0.048	-0.106	0.002
CRI 1	0 to 15	1 to 12	1.38 – 35.103	3.03	0.32
CRI 2	0 to 15	1 to 11	3.626 – 101.67	8.654	0.93
Anthocyanin based VIs:					
ARI 1	0 to 0.2	0.001 to 0.1	2.246 – 66.565	5.622	0.62
ARI 2	0 to 0.2	0.001 to 0.1	0.508 – 2.101	0.896	0.02
Plant structural VIs:					
CAI	-3 to 4	-2 to 4	-0.059 – 0.194	0.06	0.003
NDLI	0 to 1	0.005 to 0.05	-0.005 – 0.024	0.008	0.0006
Plant-water based VIs:					
WBI	Not available	0.8 to 1.2	0.886 – 0.964	0.928	0.001
NDWI	-1 to 1	-0.1 to 0.4	-0.282 – -0.056	-0.181	0.003
NDII	-1 to 1	0.02 to 0.6	-0.331 – -0.08	-0.244	0.005
NDII 5	-1 to 1	Not available	-0.335 – -0.079	-0.247	0.005
NDII 7	-1 to 1	Not available	-0.305 – 0.094	-0.134	0.008

The anthocyanin indices (Table 9), ARI1 and ARI2 had ranges for my winter senesced vegetation that are well above the ranges for green vegetation outlined in ENVI 4.2. Both the cellulose (CAI) and lignin (NDLI) indices are within the range postulated by ENVI 4.2 (Table 9) but the NDLI had some quadrats producing negative values whereas the ENVI 4.2 range is given as positive. Of the plant-water based indices (Table 9), the WBI was within the range from ENVI 4.2 but towards the lower end of this range. The NDWI and the NDII and its derivatives were all negative and below the ranges described in ENVI 4.2 for green vegetation.

3.2.2 **Comparison of the VIs Between Mining Regions**

- My hypothesis was that there was no difference between VIs for non-rocky grasslands from the two mining regions.

The chlorophyll indices gave mixed results with differences for the NDVI ($P < 0.05$, DF = 36.33), "Anglo" NDVI ($P < 0.01$, DF = 36.84), GNDVI ($P < 0.05$, DF = 33.72), SAVI ($P < 0.01$, DF = 37.04) and Red Edge NDVI ($P < 0.01$, DF = 32.95), but not for the other chlorophyll based indices. However, for all chlorophyll based VIs, with the exception of the VOG2 and VOG3, West Wits mining region had higher mean values than did Vaal River mining region (Table 10).

Amongst the mixed chlorophyll and carotenoid indices, the SIPI had differences between mines ($P < 0.01$, DF = 31.83) but the PSRI did not. The SIPI followed the trend described for the chlorophyll indices, with West Wits mining region having a higher mean value (0.413 ± 0.005) than Vaal River mining region (0.390 ± 0.006). None of the carotenoid or anthocyanin based indices had differences between mining regions. However, differences occurred between mining regions for both plant structure based indices, the CAI ($P < 0.01$, DF = 30.63) and the NDLI ($P < 0.01$, DF = 27.83), with West Wits (0.063 ± 0.003 and 0.012 ± 0.001 respectively) having higher mean indices than Vaal River mining region (0.042 ± 0.004 and 0.004 ± 0.001 respectively) (Table 10).

The plant water content VIs showed differences for the NDWI ($P < 0.05$, DF = 32.9), NDII ($P < 0.01$, DF = 34.21), NDII5 ($P < 0.01$, DF = 34.83) and NDII7 ($P < 0.01$, DF = 0.01) but not the WBI (Table 10). For all five plant water content VIs, indices

for West Wits had higher means than those for Vaal River mining region (Table 10). Values for all plant water content VIs except the WBI were negative. Therefore I reject the hypothesis of no difference between mining regions for the NDVI, "Anglo" NDVI, GNDVI, SAVI, Red Edge NDVI, SIPI, CAI, NDLI, NDWI, NDII, NDII5 and NDII7.

3.2.3 **Comparison of the VIs Between Vegetation Types**

- My hypothesis was that there was no difference in VIs between the four vegetation types when combining mining region and disturbance levels.

The results were mixed (Table 11) with only the SAVI, mSR705 and mNDVI705 differing ($P < 0.05$, DF = 3, 101) between vegetation types for the chlorophyll indices. Within the two mixed chlorophyll and carotenoid indices, the PSRI had highly significant differences ($P < 0.01$, DF = 3, 101) between vegetation types. Similarly, amongst the carotenoid and anthocyanin indices, only the PRI ($P < 0.01$, DF = 3, 101) and the ARI2 ($P < 0.05$, DF = 3, 101) differed between vegetation types. Of the plant structural indices, the cellulose index (CAI) ($P < 0.05$, DF = 3, 101) and the lignin index (NDLI) differed ($P < 0.01$, DF = 3, 101) between vegetation types. One plant-water based index differed between vegetation types, i.e. NDII7 ($P < 0.05$, DF = 3, 101). The hypothesis of no difference is rejected for the SAVI, mSR705, mNDVI705, PSRI, PRI, ARI2, CAI, NDLI and NDII7.

Table 10 Welch Two Sample t-tests comparing vegetation indices between mining regions for non-rocky grasslands, when combining disturbance levels. Data are means ± standard errors and significant differences are indicated in bold. * is significant at the 5 % level, and ** is significant at the 1 % level.

VI	T-value	DF	Probability	Vaal River (n = 15)	West Wits (n = 25)
Chlorophyll based VIs:					
NDVI	**-2.3725**	**36.33**	**0.02** *	**0.116 ± 0.004**	**0.130 ± 0.004**
$NDVI_{750}$	**-2.8249**	**36.84**	**0.008** **	**0.084 ± 0.003**	**0.097 ± 0.003**
GNDVI	**-2.0368**	**33.72**	**0.05** *	**0.299 ± 0.009**	**0.327 ± 0.009**
SAVI	**-4.0347**	**37.04**	**0.0003** **	**0.071 ± 0.002**	**0.085 ± 0.003**
$NDVI_{705}$	**-2.6921**	**32.95**	**0.01** **	**0.047 ± 0.002**	**0.054 ± 0.002**
mSR_{705}	-1.667	27.55	0.11	1.156 ± 0.007	1.170 ± 0.005
$mNDVI_{705}$	-1.6677	26.89	0.11	0.072 ± 0.002	0.078 ± 0.002
VOG2	1.9386	29.00	0.06	-0.013 ± 0.0006	-0.015 ± 0.0005
VOG3	1.9495	29.11	0.06	-0.013 ± 0.0006	-0.015 ± 0.0005
Mixed chlorophyll and carotenoid based VIs:					
SIPI	**-2.9699**	**31.83**	**0.006** *	**0.390 ± 0.006**	**0.413 ± 0.005**
PSRI	-0.6567	19.27	0.52	0.428 ± 0.013	0.437 ± 0.006
Carotenoid based VIs:					
PRI	0.1977	21.06	0.85	-0.102 ± 0.007	-0.104 ± 0.003
CRI1	0.139	23.87	0.89	2.657 ± 0.246	2.618 ± 0.146
CRI2	-0.1122	26.68	0.91	7.492 ± 0.661	7.582 ± 0.451
Anthocyanin based VIs:					
ARI1	-0.2483	28.83	0.81	4.835 ± 0.417	4.964 ± 0.313
ARI2	-1.9748	36.22	0.06	0.805 ± 0.041	0.924 ± 0.044
Plant structural based VIs:					
CAI	**-3.8722**	**30.63**	**0.0005** **	**0.042 ± 0.004**	**0.063 ± 0.003**
NDLI	**-5.1631**	**27.83**	**< 0.0001** **	**0.004 ± 0.001**	**0.012 ± 0.001**
Plant-water based VIs:					
WBI	-0.9887	37.15	0.33	0.929 ± 0.002	0.932 ± 0.002
NDWI	**-2.3177**	**32.90**	**0.03** *	**-0.182 ± 0.006**	**-0.164 ± 0.005**
NDII	**-5.2091**	**34.21**	**< 0.0001** **	**-0.272 ± 0.008**	**-0.211 ± 0.008**
NDII5	**-5.321**	**34.83**	**< 0.0001** **	**-0.275 ± 0.008**	**-0.213 ± 0.008**
NDII7	**-7.4813**	**32.85**	**< 0.0001** **	**-0.212 ± 0.013**	**-0.078 ± 0.012**

Table 11 One-way ANOVA of vegetation indices (VI) between the four vegetation types for both disturbance levels combined. Wet Grassland, n = 15; non-rocky grassland, n = 40; rocky grassland, n = 30; woody shrub, n = 20. Degrees of freedom = 3, 101. Significant differences are indicated in bold. * is significant at the 5 % level, and ** is significant at the 1 % level.

VI	F-value	Probability
Chlorophyll based VIs:		
NDVI800	1.65	0.18
NDVI750	1.66	0.18
GNDVI	2.48	0.07
SAVI	**3.56**	**0.02** *
NDVI705	2.65	0.05
mSR705	**3.58**	**0.02** *
mNDVI705	**3.46**	**0.02** *
VOG2	1.53	0.21
VOG3	1.56	0.21
Mixed chlorophyll and carotenoid based VIs:		
SIPI	0.46	0.71
PSRI	**9.03**	**< 0.0001** **
Carotenoid based VIs:		
PRI	**9.59**	**< 0.0001** **
CRI1	1.98	0.12
CRI2	2.29	0.08
Anthocyanin based VIs:		
ARI1	2.45	0.07
ARI2	**3.22**	**0.03** *
Plant structural based VIs:		
CAI	**2.78**	**0.04** *
NDLI	**8.11**	**< 0.0001** **
Plant-water based VIs:		
WBI	1.75	0.16
NDWI	2.08	0.11
NDII	0.96	0.42
NDII5	1.08	0.36
NDII7	**3.51**	**0.02** *

3.2.4 **Comparison of the VIs Between Disturbance Levels**

- My hypothesis was that there would be no difference for VIs between disturbance levels when combining mining regions and vegetation types.

All nine chlorophyll based indices differed between disturbance levels for all vegetation types and mining regions combined (Table 12). Amongst the mixed chlorophyll and carotenoid indices, the SIPI differed between disturbance levels ($P < 0.01$, $DF = 102.9$). For the carotenoid indices, the CRI2 had significant differences ($P < 0.05$, $DF = 62.89$) between disturbance levels. Both anthocyanin indices, ARI1 and ARI2, produced differences between low and high disturbance quadrats ($P < 0.05$, $DF = 62.64$, $P < 0.01$, $DF = 102.85$ respectively). The plant structure based indices measuring cellulose (CAI) and lignin (NDLI) had no differences between high and low disturbance and nor did any plant-water based indices. I therefore reject the hypothesis of no difference between disturbance levels for all chlorophyll based indices. Furthermore, I reject the hypothesis of no difference for the mixed chlorophyll and carotenoid based SIPI, the carotenoid only CRI2, and both anthocyanin based indices, the ARI1 and ARI2.

3.2.5 **VI Response to Disturbance in Wet Grasslands at Vaal River**

- My hypothesis was that there was no difference for VIs between high and low disturbance in wet grasslands.

Amongst all the VIs, only the lignin index (NDLI) (Table 13, $P < 0.05$, $DF = 11.19$) differed in wet grasslands, where high disturbance (0.011 ± 0.0007) had lower values than low disturbance quadrats (0.015 ± 0.002). All other indices produced non-significant differences for disturbance levels in wet grasslands. I therefore reject the hypothesis of no difference between high and low disturbance in wet grasslands for the lignin (NDLI) index. However, I accept the hypothesis of no difference between disturbance levels in wet grasslands for all other VIs.

Table 12 Welch Two Sample t-tests for VIs between high and low disturbance combining mining regions and all four vegetation types. Data are means ± standard errors and significant differences are indicated in bold. * is significant at the 5 % level, and ** is significant at the 1 % level.

VI	t-value	Corrected Degrees of Freedom	Probability	Low Disturbance (n = 60)	High Disturbance (n = 45)
Chlorophyll based VIs:					
NDVI800	**3.84**	**98.49**	**0.0002** **	**0.144 ± 0.006**	**0.116 ± 0.004**
NDVI750	**3.62**	**91.76**	**0.0005** **	**0.108 ± 0.005**	**0.087 ± 0.003**
GNDVI	**3.82**	**99.90**	**0.0002** **	**0.337 ± 0.006**	**0.302 ± 0.007**
SAVI	**2.35**	**102.15**	**0.02** *	**0.085 ± 0.003**	**0.076 ± 0.002**
NDVI705	**3.52**	**91.12**	**0.0007** **	**0.062 ± 0.003**	**0.049 ± 0.002**
mSR705	**3.22**	**87.48**	**0.002** **	**1.198 ± 0.011**	**1.159 ± 0.006**
mNDVI705	**3.28**	**91.45**	**0.001** **	**0.089 ± 0.004**	**0.073 ± 0.002**
VOG2	**-3.92**	**97.27**	**0.0002** **	**-0.016 ± 0.0007**	**-0.013 ± 0.0005**
VOG3	**-3.91**	**96.67**	**0.0002** **	**-0.016 ± 0.0008**	**-0.013 ± 0.0005**
Mixed chlorophyll and carotenoid based VIs:					
SIPI	**3.95**	**102.91**	**0.0001** **	**0.419 ± 0.005**	**0.393 ± 0.004**
PSRI	-0.10	102.97	0.91	0.428 ± 0.007	0.429 ± 0.006
Carotenoid based VIs:					
PRI	-0.27	91.49	0.79	-0.107 ± 0.003	-0.105 ± 0.004
CRI1	1.89	63.56	0.06	3.48 ± 0.55	2.43 ± 0.10
CRI2	**2.08**	**62.89**	**0.04** *	**10.10 ± 1.60**	**6.72 ± 0.29**
Anthocyanin based VIs:					
ARI1	**2.17**	**62.64**	**0.03** *	**6.62 ± 1.06**	**4.29 ± 0.19**
ARI2	**3.44**	**102.85**	**0.0008** **	**0.96 ± 0.03**	**0.81 ± 0.03**
Plant structural based VIs:					
CAI	-0.89	95.46	0.37	0.057 ± 0.004	0.063 ± 0.005
NDLI	1.65	102.69	0.10	0.009 ± 0.0009	0.007 ± 0.0008
Plant-water based VIs:					
WBI	-1.77	102.30	0.08	0.927 ± 0.002	0.930 ± 0.001
NDWI	0.84	102.33	0.40	-0.179 ± 0.005	-0.184 ± 0.005
NDII	1.20	96.46	0.23	-0.238 ± 0.007	-0.251 ± 0.008
NDII5	1.06	97.12	0.29	-0.242 ± 0.007	-0.253 ± 0.008
NDII7	0.89	97.81	0.37	-0.128 ± 0.011	-0.143 ± 0.012

Table 13 Welch Two Sample t-tests for vegetation indices (VI) between high and low disturbance in wet grassland quadrats at Vaal River. Data are means ± standard errors and significant differences are indicated in bold. * is significant at the 5 % level, and ** is significant at the 1 % level.

VI	t-value	Corrected Degrees of Freedom	Probability	Low Disturbance (n = 10)	High Disturbance (n = 5)
Chlorophyll based VIs:					
NDVI800	0.99	12.41	0.34	0.160 ± 0.020	0.133 ± 0.017
NDVI750	1.07	12.3	0.30	0.121 ± 0.017	0.096 ± 0.015
GNDVI	0.67	12.78	0.51	0.303 ± 0.016	0.290 ± 0.012
SAVI	0.29	12.99	0.78	0.092 ± 0.011	0.088 ± 0.007
NDVI705	1.27	12.22	0.23	0.075 ± 0.011	0.056 ± 0.010
mSR705	1.20	12.13	0.25	1.246 ± 0.039	1.185 ± 0.034
mNDVI705	1.16	11.86	0.27	0.107 ± 0.015	0.084 ± 0.014
VOG2	-1.93	12.86	0.08	-0.019 ± 0.002	-0.014 ± 0.002
VOG3	-1.92	12.87	0.08	-0.019 ± 0.002	-0.014 ± 0.002
Mixed chlorophyll and carotenoid based VIs:					
SIPI	1.25	12.92	0.23	0.424 ± 0.015	0.400 ± 0.011
PSRI	-0.97	11.94	0.35	0.377 ± 0.013	0.395 ± 0.012
Carotenoid based VIs:					
PRI	-0.97	12.93	0.35	-0.087 ± 0.002	-0.084 ± 0.002
CRI1	2.02	11.93	0.07	2.83 ± 0.30	2.01 ± 0.27
CRI2	1.58	10.93	0.14	7.50 ± 0.74	5.83 ± 0.75
Anthocyanin based VIs:					
ARI1	1.29	10.22	0.23	4.67 ± 0.44	3.83 ± 0.49
ARI2	0.29	12.99	0.77	0.76 ± 0.05	0.75 ± 0.03
Plant structural based VIs:					
CAI	-0.41	12.95	0.69	0.078 ± 0.010	0.083 ± 0.006
NDLI	**2.25**	**11.19**	**0.05** *	**0.015 ± 0.002**	**0.011 ± 0.0007**
Plant-water based VIs:					
WBI	0.64	12.24	0.53	0.926 ± 0.004	0.923 ± 0.002
NDWI	0.001	12.03	0.99	-0.190 ± 0.011	-0.190 ± 0.005
NDII	0.67	11.21	0.52	-0.236 ± 0.021	-0.251 ± 0.008
NDII5	0.83	11.17	0.42	-0.238 ± 0.021	-0.256 ± 0.008
NDII7	1.32	12.77	0.21	-0.066 ± 0.031	-0.114 ± 0.018

3.2.6 **VI Response to Disturbance in Non-Rocky Grassland at Vaal River**

- My hypothesis was that there was no difference for VIs between high and low disturbance in non-rocky grasslands from Vaal River.

Of the chlorophyll based indices (Table 14), only the GNDVI differed ($P < 0.01$, DF = 9.71) between disturbance levels in non-rocky grasslands at Vaal River. Both mixed chlorophyll and carotenoid indices (SIPI and PSRI) differed ($P < 0.01$, DF = 8.09 and 11.63 respectively) between high and low disturbance. Similarly, the pure carotenoid and anthocyanin indices (PRI, CRI1, CRI2, ARI1 and ARI2) differed ($P < 0.01$, DF = 12.06; $P < 0.05$, DF = 10.4; $P < 0.05$, DF = 9.87, $P < 0.05$, DF = 9.7; $P < 0.01$, DF = 12.58 respectively). Neither the cellulose index (CAI) nor the lignin index (NDLI) had any differences between disturbance levels. The plant-water based indices, the NDII, NDII5 and NDII7 produced significant differences ($P < 0.01$; DF = 9.11, DF = 8.64, DF = 9.75 respectively) between high and low disturbance in non-rocky grasslands from Vaal River, but the WBI and NDWI showed no differences. I therefore reject the hypothesis of no difference between disturbance levels for the GNDVI, SIPI, PSRI, PRI, CRI1, CRI2, ARI1, ARI2, NDII, NDII5 and NDII7 indices.

3.2.7 **VI Response to Disturbance in Non-Rocky Grassland at West Wits**

- My hypothesis was that there was no difference for VIs between high and low disturbance in non-rocky grasslands from West Wits.

Of the chlorophyll based indices, the GNDVI at West Wits, like at Vaal River, was different between disturbance levels ($P < 0.01$, DF = 15.89). However, unlike Vaal River, the standard NDVI ($P < 0.05$, DF = 21.84) and the red edge VOG2 and VOG3 ($P < 0.05$, DF = 22.98) differed between disturbance levels in non-rocky grasslands at West Wits (Table 15). Both the mixed chlorophyll and carotenoid indices (SIPI and PSRI) differed between disturbance levels ($P < 0.01$, DF = 22.07; $P < 0.05$, DF = 11.92 respectively) in non-rocky grasslands from West Wits. The carotenoid index, the CRI2 was different ($P < 0.05$, DF = 15.46). Both anthocyanin indices (ARI1 and ARI2) differed ($P < 0.01$; DF = 15.45 and 14.66 respectively) between high and low disturbance.

Table 14 Welch Two Sample t-tests for vegetation indices (VI) from high and low disturbance in non-rocky grassland quadrats at Vaal River. Data are means ± standard errors and significant differences are indicated in bold. * is significant at the 5 % level, and ** is significant at the 1 % level.

VI	t-value	Corrected Degrees of Freedom	Probability	Low Disturbance (n = 10)	High Disturbance (n = 5)
Chlorophyll based VIs:					
NDVI800	0.60	12.69	0.56	0.118 ± 0.006	0.114 0.003
NDVI750	1.53	12.29	0.15	0.087 ± 0.004	0.079 0.002
GNDVI	**10.34**	**9.71**	**< 0.0001** **	**0.324 ± 0.005**	**0.251 0.005**
SAVI	1.84	12.53	0.09	0.074 ± 0.003	0.067 0,002
NDVI705	0.64	12.31	0.53	0.048 ± 0.003	0.046 0.001
mSR705	-1.31	12.02	0.22	1.151 ± 0.010	1.166 0.005
mNDVI705	-1.33	11.97	0.21	0.070 ± 0.004	0.076 0.002
VOG2	0.46	12.81	0.65	-0.013 ± 0.0009	-0.014 0.0005
VOG3	0.45	12.80	0.66	-0.013 ± 0.0009	-0.014 0.0005
Mixed chlorophyll and carotenoid based VIs:					
SIPI	**7.34**	**8.09**	**< 0.0001** **	**0.404 ± 0.003**	**0.361 0.005**
PSRI	**6.30**	**11.63**	**< 0.0001** **	**0.455 ± 0.012**	**0.374 0.005**
Carotenoid based VIs:					
PRI	**-4.56**	**12.06**	**0.0006** **	**-0.114 ± 0.007**	**-0.079 0.003**
CRI1	**2.41**	**10.40**	**0.04** *	**2.94 ± 0.34**	**2.10 0.10**
CRI2	**2.55**	**9.87**	**0.03** *	**8.27 ± 0.90**	**5.93 0.20**
Anthocyanin based VIs:					
ARI1	**2.61**	**9.70**	**0.03** *	**5.34 ± 0.57**	**3.83 0.11**
ARI2	**10.12**	**12.58**	**< 0.0001** **	**0.906 ± 0.023**	**0.604 0.019**
Plant structural based VIs:					
CAI	2.25	7.22	0.06	0.048 ± 0.004	0.029 0.007
NDLI	1.89	12.93	0.08	0.0049 ± 0.0018	0.0009 0.0011
Plant-water based VIs:					
WBI	1.80	11.78	0.10	0.931 ± 0.002	0.926 0.002
NDWI	2.09	10.23	0.06	-0.175 ± 0.007	-0.196 0.007
NDII	**3.57**	**9.11**	**0.006** **	**-0.257 ± 0.008**	**-0.303 0.010**
NDII5	**3.74**	**8.64**	**0.005** **	**-0.260 ± 0.008**	**-0.307 0.010**
NDII7	**3.58**	**9.75**	**0.005** **	**-0.188 ± 0.013**	**-0.260 0.015**

Table 15 Welch Two Sample t-tests for vegetation indices (VI) from high and low disturbance in non-rocky grassland quadrats at West Wits. Data are means ± standard errors and significant differences are indicated in bold. * is significant at the 5 % level, and ** is significant at the 1 % level.

VI	t-value	Corrected Degrees of Freedom	Probability	Low Disturbance (n = 10)	High Disturbance (n = 15)
Chlorophyll based VIs:					
NDVI800	**2.62**	**21.84**	**0.02** *	**0.141 ± 0.004**	**0.123 ± 0.006**
NDVI750	1.73	22.06	0.10	0.103 ± 0.003	0.093 ± 0.005
GNDVI	**3.56**	**15.89**	**0.003** **	**0.361 ± 0.013**	**0.304 ± 0.008**
SAVI	2.02	17.40	0.06	0.091 ± 0.004	0.081 ± 0.003
NDVI705	1.54	22.35	0.14	0.057 ± 0.002	0.052 ± 0.003
mSR705	0.94	20.68	0.36	1.175 ± 0.004	1.167 ± 0.008
mNDVI705	0.99	20.78	0.34	0.080 ± 0.002	0.077 ± 0.003
VOG2	**-2.40**	**22.98**	**0.02** *	**-0.016 ± 0.0005**	**-0.014 ± 0.0006**
VOG3	**-2.39**	**22.98**	**0.03** *	**-0.016 ± 0.0005**	**-0.014 ± 0.0006**
Mixed chlorophyll and carotenoid based VIs:					
SIPI	**2.74**	**22.07**	**0.01** *	**0.428 ± 0.006**	**0.403 ± 0.006**
PSRI	**2.50**	**11.92**	**0.03** *	**0.454 ± 0.01**	**0.426 ± 0.004**
Carotenoid based VIs:					
PRI	-0.79	11.26	0.45	-0.107 ± 0.007	-0.101 ± 0.003
CRI1	1.43	15.99	0.17	2.88 ± 0.26	2.44 ± 0.16
CRI2	**2.52**	**15.46**	**0.02** *	**8.90 ± 0.75**	**6.70 ± 0.45**
Anthocyanin based VIs:					
ARI1	**3.08**	**15.45**	**0.007** **	**6.02 ± 0.49**	**4.26 ± 0.30**
ARI2	**3.83**	**14.66**	**0.002** **	**1.09 ± 0.07**	**0.81 ± 0.04**
Plant structural based VIs:					
CAI	**2.38**	**17.78**	**0.03** *	**0.072 ± 0.005**	**0.057 ± 0.004**
NDLI	0.97	13.85	0.35	0.013 ± 0.002	0.011 ± 0.001
Plant-water based VIs:					
WBI	**-5.83**	**22.22**	**< 0.0001** **	**0.924 ± 0.001**	**0.937 ± 0.002**
NDWI	**-2.19**	**19.15**	**0.04** *	**-0.177 ± 0.007**	**-0.156 ± 0.007**
NDII	-1.93	20.68	0.07	-0.229 ± 0.011	-0.200 ± 0.010
NDII5	**-2.10**	**21.13**	**0.05** *	**-0.232 ± 0.011**	**-0.200 ± 0.010**
NDII7	-1.14	21.61	0.27	-0.094 ± 0.017	-0.067 ± 0.016

Of the plant-water based indices, the WBI, NDWI and NDII5 were different ($P < 0.01$, $DF = 22.22$; $P < 0.05$, $DF = 19.15$; $P < 0.05$, $DF = 21.13$) between high and low disturbance in non-rocky grasslands at West Wits (Table 15). I therefore reject the hypothesis of no difference between disturbance levels in non-rocky grasslands at West Wits for the NDVI, GNDVI, VOG2, VOG3, SIPI, PSRI, CRI2, ARI1, ARI2, CAI, WBI, NDWI and NDII5.

3.2.8 **VI Response to Disturbance in Rocky Grassland at Vaal River**

- My hypothesis was that there was no difference in VIs between high and low disturbance quadrats in rocky grasslands from Vaal River.

All chlorophyll based indices were different between disturbance levels in rocky grasslands from Vaal River (Table 16) with the exception of the VOG2 and VOG3 indices. Of the mixed chlorophyll and carotenoid indices, the SIPI differed between disturbance levels ($P < 0.05$, $DF = 27.52$). Only the ARI2 was different ($P = 0.05$, $DF = 22.74$) amongst the carotenoid and anthocyanin indices. Of the plant-water based indices, the NDWI ($P < 0.05$, $DF = 27.99$), NDII ($P < 0.01$, $DF = 27.82$), NDII5 ($P < 0.01$, $DF = 27.28$) and NDII7 ($P < 0.01$, $DF = 19.59$) differed between high and low disturbance in rocky grasslands at Vaal River. I there reject the hypothesis of no difference between disturbance levels for the NDVI800, NDVI750, GNDVI, SAVI, NDVI705, mSR705, mNDVI705, VOG2, VOG3, SIPI, ARI2, NDWI, NDII, NDII5 and NDII7 (Table 16).

3.2.9 **VI Response to Disturbance in Woody Shrub Grasslands at Vaal River**

- My hypothesis was that there was no difference for VIs between high and low disturbance in woody shrub quadrats at Vaal River.

All chlorophyll based indices except the GNDVI differed between high and low disturbance in woody shrub plots at Vaal River (Table 17). Of the mixed chlorophyll and carotenoid indices, the SIPI differed between disturbance levels in woody shrub plots ($P < 0.05$, $DF = 17.87$) as did the cellulose index (CAI: $P < 0.05$, $DF = 17.35$) amongst the plant structure indices. Amongst the results for the plant-water based indices, only the NDII ($P < 0.05$, $DF = 17.35$) had differences between high and low

Table 16 Welch Two Sample t-tests for vegetation indices (VI) from high and low disturbance in rocky grassland quadrats at Vaal River. Data are means ± standard errors and significant differences are indicated in bold. * is significant at the 5 % level, and ** is significant at the 1 % level.

VI	t-value	Corrected Degrees of Freedom	Probability	Low Disturbance (n = 15)	High Disturbance (n = 15)
Chlorophyll based VIs:					
NDVI800	**2.32**	**26.09**	**0.03** *	**0.142 ± 0.009**	**0.114 ± 0.007**
NDVI750	**2.71**	**23.44**	**0.01** **	**0.109 ± 0.007**	**0.085 ± 0.005**
GNDVI	**2.43**	**22.45**	**0.02** *	**0.358 ± 0.008**	**0.320 ± 0.014**
SAVI	**2.38**	**26.08**	**0.02** *	**0.095 ± 0.006**	**0.077 ± 0.005**
NDVI705	**2.37**	**23.96**	**0.03** *	**0.061 ± 0.004**	**0.048 ± 0.003**
mSR705	**2.28**	**22.52**	**0.03** *	**1.188 ± 0.013**	**1.152 ± 0.008**
mNDVI705	**2.27**	**23.17**	**0.03** *	**0.085 ± 0.006**	**0.071 ± 0.003**
VOG2	**-2.03**	**27.37**	**0.05** *	**-0.015 ± 0.001**	**-0.013 ± 0.001**
VOG3	**-2.04**	**27.34**	**0.05** *	**-0.015 ± 0.001**	**-0.013 ± 0.001**
Mixed chlorophyll and carotenoid based VIs:					
SIPI	**2.17**	**27.52**	**0.04** *	**0.424 ± 0.008**	**0.398 ± 0.009**
PSRI	-0.19	27.04	0.85	0.451 ± 0.009	0.454 ± 0.011
Carotenoid based VIs:					
PRI	0.20	24.74	0.84	-0.120 ± 0.004	-0.122 ± 0.007
CRI1	0.42	21.05	0.68	2.81 ± 0.13	2.70 ± 0.24
CRI2	0.99	21.15	0.34	8.06 ± 0.34	7.33 ± 0.65
Anthocyanin based VIs:					
ARI1	1.30	21.95	0.21	5.25 ± 0.23	4.63 ± 0.41
ARI2	**2.03**	**22.74**	**0.05**	**1.05 ± 0.04**	**0.90 ± 0.63**
Plant structural based VIs:					
CAI	-0.19	24.90	0.85	0.055 ± 0.008	0.057 ± 0.005
NDLI	1.43	27.03	0.16	0.007 ± 0.001	0.004 ± 0.001
Plant-water based VIs:					
WBI	1.55	27.92	0.13	0.930 ± 0.002	0.925 ± 0.002
NDWI	**2.58**	**27.99**	**0.02** *	**-0.172 ± 0.006**	**-0.195 ± 0.006**
NDII	**2.73**	**27.82**	**0.01** **	**-0.228 ± 0.011**	**-0.269 ± 0.010**
NDII5	**2.75**	**27.28**	**0.01** **	**-0.231 ± 0.012**	**-0.273 ± 0.010**
NDII7	**2.92**	**19.59**	**0.008** **	**-0.138 ± 0.016**	**-0.191 ± 0.007**

Table 17 Welch Two Sample t-tests for vegetation indices (VI) from high and low disturbance in woody shrub quadrats at Vaal River. Data are means ± standard errors and significant differences are indicated in bold. * is significant at the 5 % level, and ** is significant at the 1 % level.

VI	t-value	Corrected Degrees of Freedom	Probability	Low Disturbance (n = 15)	High Disturbance (n = 5)
Chlorophyll based VIs:					
NDVI800	**3.33**	**15.59**	**0.004** **	**0.157 ± 0.017**	**0.085 ± 0.013**
NDVI750	**2.76**	**17.97**	**0.01** **	**0.117 ± 0.014**	**0.073 ± 0.007**
GNDVI	1.01	9.39	0.34	0.331 ± 0.018	0.302 ± 0.023
SAVI	**2.30**	**12.81**	**0.04** *	**0.075 ± 0.006**	**0.057 ± 0.018**
NDVI705	**3.14**	**17.98**	**0.006** **	**0.066 ± 0.008**	**0.038 ± 0.004**
mSR705	**3.19**	**17.97**	**0.005** **	**1.223 ± 0.028**	**1.123 ± 0.014**
mNDVI705	**3.39**	**17.71**	**0.003** **	**0.098 ± 0.010**	**0.058 ± 0.006**
VOG2	**-3.76**	**17.04**	**0.002** **	**-0.018 ± 0.002**	**-0.008 ± 0.001**
VOG3	**-3.73**	**17.24**	**0.002** **	**-0.018 ± 0.002**	**-0.008 ± 0.001**
Mixed chlorophyll based VIs:					
SIPI	**2.72**	**17.87**	**0.01** **	**0.417 ± 0.015**	**0.369 ± 0.009**
PSRI	-1.77	9.72	0.11	0.403 ± 0.017	0.451 ± 0.021
Carotenoid based VIs:					
PRI	0.95	5.79	0.38	-0.101 ± 0.007	-0.116 ± 0.015
CRI1	1.40	14.28	0.18	5.36 ± 2.14	2.35 ± 0.22
CRI2	1.47	14.39	0.16	15.90 ± 6.25	6.66 ± 0.74
Anthocyanin based VIs:					
ARI1	1.50	14.48	0.16	10.54 ± 4.12	4.31 ± 0.55
ARI2	1.07	14.83	0.30	0.945 ± 0.098	0.808 ± 0.083
Plant structural based VIs:					
CAI	**-2.88**	**5.58**	**0.03** *	**0.042 ± 0.010**	**0.111 ± 0.022**
NDLI	0.51	9.77	0.62	0.007 ± 0.002	0.006 ± 0.002
Plant-water based VIs:					
WBI	-2.01	10.73	0.07	0.922 ± 0.005	0.936 ± 0.005
NDWI	1.90	15.43	0.08	-0.1814 ± 0.016	-0.220 ± 0.013
NDII	**2.22**	**17.35**	**0.04** *	**-0.2441 ± 0.020**	**-0.296 ± 0.013**
NDII5	1.88	17.62	0.08	-0.2497 ± 0.020	-0.295 ± 0.013
NDII7	-0.12	10.24	0.91	-0.1414 ± 0.029	-0.136 ± 0.034

Table 18 Summary of results (Tables 13 – 17) when comparing VIs for high and low disturbance within the vegetation types. The table shows where significant differences occurred at the 5% level (*) or 1 % level (**).

VI	Wet Grassland Vaal River	Non-rocky Grassland Vaal River	Non-rocky Grassland West Wits	Rocky Grassland	Woody Shrub
Chlorophyll based VIs:					
NDVI800			*	*	**
NDVI750				**	**
GNDVI		**	**	*	
SAVI				*	*
NDVI705				*	**
mSR705				*	**
mNDVI705				*	**
VOG2			*	*	**
VOG3			*	*	**
Mixed chlorophyll and carotenoid based VIs:					
SIPI		**	*	*	**
PSRI		**	*		
Carotenoid based VIs:					
PRI		**			
CRI1		*			
CRI2		*	*		
Anthocyanin based VIs:					
ARI1		*	**		
ARI2		**	**		
Plant structural based VIs:					
CAI			*		*
NDLI	*				
Plant-water based VIs:					
WBI			**		
NDWI			*	*	
NDII		**		**	*
NDII5		**	*	**	
NDII7		**		**	

disturbance in woody shrub plots at Vaal River (Table 17). I therefore reject the hypothesis of no difference between VIs from high and low disturbance wood shrub quadrats for the NDVI800, NDVI750, SAVI, NDVI705, mSR705, mNDVI705, VOG2, VOG3, SIPI, CAI and NDII.

Table 18 summarises the results of the t-tests comparing VI indices for different disturbance levels in each vegetation type as described in sections 3.2.5 to 3.2.9 and Tables 13 to 17.

3.3 **Correlations Between VIs**

A key question was to test the accuracy of the VIs in measuring the plant characteristic they were designed to measure (i.e. chlorophyll or plant water content) when using spectral reflectance of winter senesced vegetation in the absence of empirical data about these plant characteristics.

To this end correlation analysis was applied between the VIs. The chlorophyll based vegetation indices generally produced very strong correlations (r > 0.90) between them (Table 19) and form a single group with the exception of the GNDVI (r = 0.62) and SAVI (r = 0.55). Of the two mixed chlorophyll and carotenoid based indices, the SIPI and PSRI had no correlation with each other (r = 0.03) (Table 19). The SIPI had stronger correlations with the chlorophyll based VIs (r > 0.65) and with the anthocyanin ARI2 (r = 0.81). The SIPI had a weaker correlation with the other anthocyanin index, the ARI1 and with the two carotenoid based indices (CRI1 and 2) (r > 0.50). The PSRI had a strong but negative correlation with the PRI (r = -0.85), but with no other VIs except the chlorophyll based red edge mSR705 and mNDVI705 where a fair, but negative correlation occurred (r = -0.618 and -0.622 respectively).

Table 19 Correlation coefficients (*r*) between Vegetation Indices (VIs). Correlation coefficients in bold have $r \geq 0.80$.

Index	NDVI800	NDVI750	GNDVI	SAVI	NDVI750	mSR705	mNDVI705	VOG2	VOG3	SIPI	PSRI
Chlorophyll VIs:											
NDVI800	**1**	**0.98**	0.62	0.56	**0.98**	**0.94**	**0.94**	**-0.97**	**-0.97**	**0.85**	-0.45
NDVI750	**0.98**	**1**	0.64	0.52	**0.99**	**0.95**	**0.95**	**-0.94**	**-0.95**	**0.84**	-0.43
GNDVI	0.62	0.64	**1**	0.47	0.59	0.45	0.45	-0.58	-0.58	**0.86**	0.40
SAVI	0.55	0.52	0.47	**1**	0.52	0.42	0.45	-0.45	-0.45	0.66	-0.05
NDVI705	**0.98**	**0.99**	0.59	0.52	**1**	**0.97**	**0.97**	**-0.96**	**-0.96**	**0.82**	-0.48
mSR705	**0.94**	**0.95**	0.45	0.42	**0.97**	**1**	**1**	**-0.94**	**-0.94**	0.67	-0.62
mNDVI705	**0.94**	**0.95**	0.45	0.45	**0.97**	**1**	**1**	**-0.94**	**-0.94**	0.68	-0.62
VOG2	**-0.97**	**-0.94**	-0.58	-0.45	**-0.96**	**-0.94**	**-0.94**	**1**	**1**	**-0.80**	0.47
VOG3	**-0.97**	**-0.95**	-0.58	-0.45	**-0.96**	**-0.94**	**-0.94**	**1**	**1**	**-0.80**	0.47
Mixed chlorophyll and carotenoid VIs:											
SIPI	**0.85**	**0.84**	**0.86**	0.66	**0.82**	0.67	0.68	**-0.80**	**-0.80**	**1**	0.03
PSRI	-0.45	-0.43	0.40	-0.05	-0.48	-0.62	-0.62	0.46	0.47	0.03	**1**
Carotenoid VIs:											
PRI	0.14	0.06	-0.61	-0.03	0.12	0.24	0.26	-0.17	-0.17	-0.25	**-0.85**
CRI1	0.66	0.68	0.52	-0.14	0.65	0.61	0.58	-0.69	-0.69	0.57	-0.19
CRI2	0.66	0.67	0.51	-0.16	0.68	0.62	0.59	-0.69	-0.70	0.54	-0.21
Anthocyanin VIs:											
ARI1	0.65	0.66	0.50	-0.17	0.63	0.62	0.59	-0.69	-0.70	0.53	-0.22
ARI2	0.57	0.58	**0.98**	0.36	0.51	0.37	0.36	-0.53	-0.53	**0.81**	0.44
Plant structural VIs:											
CAI	-0.38	-0.38	-0.23	0.08	-0.37	-0.40	-0.40	0.43	0.43	-0.22	0.19
NDLI	0.42	0.39	-0.02	0.48	0.42	0.40	0.41	-0.40	-0.40	0.35	-0.47
Plant-water VIs:											
WBI	-0.54	-0.45	-0.41	-0.23	-0.45	-0.44	-0.44	0.53	0.53	-0.45	0.12
NDWI	-0.15	-0.14	-0.09	0.05	-0.14	-0.18	-0.16	0.14	0.14	-0.03	0.09
NDII	0.11	0.15	0.13	0.20	0.16	0.10	0.11	-0.12	-0.12	0.23	0.02
NDII5	0.07	0.11	0.09	0.18	0.12	0.06	0.08	-0.08	-0.08	0.19	0.02
NDII7	0.27	0.33	0.06	0.24	0.34	0.31	0.31	-0.28	-0.28	0.29	-0.28

Table 19 continued Correlation coefficients (*r*) between Vegetation Indices (VIs). Correlation coefficients in bold have $r \geq 0.80$.

Index	PRI	CRI1	CRI2	ARI1	ARI2	CAI	NDLI	WBI	NDWI	NDII	NDII5	NDII7
Chlorophyll VIs:												
NDVI800	0.14	0.66	0.66	0.65	0.57	-0.38	0.42	-0.54	-0.15	0.12	0.07	0.27
NDVI750	0.06	0.68	0.67	0.66	0.58	-0.38	0.39	-0.45	-0.14	0.15	0.11	0.33
GNDVI	-0.61	0.52	0.51	0.50	**0.98**	-0.23	-0.02	-0.41	-0.09	0.13	0.09	0.06
SAVI	-0.03	-0.14	-0.16	-0.17	0.36	0.08	0.48	-0.23	0.05	0.20	0.18	0.24
NDVI705	0.12	0.65	0.64	0.63	0.51	-0.37	0.42	-0.45	-0.14	0.16	0.12	0.34
mSR705	0.24	0.61	0.62	0.62	0.37	-0.40	0.40	-0.44	-0.18	0.10	0.06	0.31
mNDVI705	0.26	0.58	0.59	0.59	0.36	-0.40	0.41	-0.44	-0.16	0.11	0.08	0.31
VOG2	-0.17	-0.69	-0.69	-0.70	-0.53	0.43	-0.40	0.53	0.14	-0.12	-0.08	-0.28
VOG3	-0.17	-0.69	-0.70	-0.70	-0.53	0.43	-0.40	0.53	0.14	-0.12	-0.08	-0.28
Mixed chlorophyll and carotenoid VIs:												
SIPI	-0.25	0.57	0.54	0.53	**0.81**	-0.22	0.35	-0.45	-0.03	0.23	0.19	0.29
PSRI	**-0.85**	-0.19	-0.21	-0.22	0.44	0.19	-0.47	0.12	0.09	0.02	0.02	-0.28
Carotenoid VIs:												
PRI	**1**	-0.09	-0.05	-0.03	-0.61	0.09	0.55	-0.04	-0.06	-0.09	-0.08	0.25
CRI1	-0.09	**1**	**0.99**	**0.99**	0.60	-0.47	0.01	-0.43	-0.25	-0.04	-0.08	0.07
CRI2	-0.05	**0.99**	**1**	**1.00**	0.59	-0.47	0.02	-0.45	-0.26	-0.06	-0.09	0.07
Anthocyanin VIs:												
ARI1	-0.03	**0.99**	**1.00**	**1**	0.58	-0.46	0.02	-0.46	-0.27	-0.07	-0.10	0.07
ARI2	-0.61	0.60	0.60	0.58	**1**	-0.23	-0.08	-0.43	-0.12	0.07	0.03	-0.01
Plant structural VIs:												
CAI	0.09	-0.45	-0.47	-0.46	-0.23	**1**	0.28	0.09	-0.21	-0.21	-0.18	0.17
NDLI	0.55	0.01	0.02	0.02	-0.08	0.28	**1**	0.001	0.12	0.34	0.34	**0.75**
Plant-water VIs:												
WBI	-0.04	-0.43	-0.45	-0.46	-0.43	0.09	0.001	**1**	0.61	0.56	0.60	0.39
NDWI	-0.06	-0.25	-0.26	-0.27	-0.12	-0.21	0.12	0.61	**1**	**0.89**	**0.89**	0.49
NDII	-0.09	-0.04	-0.06	-0.07	0.07	-0.21	0.34	0.56	**0.89**	**1**	**1.00**	**0.75**
NDII5	-0.08	-0.08	-0.09	-0.10	0.03	-0.18	0.34	0.60	**0.89**	**1.00**	**1**	**0.77**
NDII7	0.25	0.07	0.07	0.07	-0.01	0.17	0.75	0.39	0.49	**0.75**	**0.77**	**1**

Of the pure carotenoid indices (Table 19), the PRI was poorly correlated with the CRI1 and CRI2 but the CRI1 and 2 are strongly correlated. The PRI had a negative correlation with the GNDVI (r = -0.611) and the ARI2 (r = -0.612). No other index produced strong correlations with the PRI. The CRI1 and CRI2 produced a strong correlation with the ARI1 (r = 0.99) but was weakly correlated with any chlorophyll or mixed chlorophyll and carotenoid based index. The ARI2 was weakly correlated with the ARI1 (r = 0.581) but produced strong correlations with the GNDVI (r = 0.98) and the SIPI (r = 0.81) but not with any other pigment based index.

The two plant structural indices measuring cellulose (CAI) and lignin (NDLI) had a weak correlation (r = 0.28) with each other. Furthermore the CAI had only weak correlations with any other VI (Table 19). The NDLI showed no strong correlation with any VI except the plant-water based VI, the NDII7 (r = 0.75).

Correlations between the plant-water based indices grouped the NDWI, NDII and NDII5 together (r > 0.80, Table 19). The WBI is weakly correlated with this group (r < 0.62) and with some chlorophyll based indices (r < 0.55) but has no strong correlations with any index. The NDII had a strong correlation (r = 1.00) with the NDII5 which is as expected as the bands for these two indices are very close together and spectra tend to have high collinearity (Martens and Næs, 1989). The NDII and NDII7 use unrelated wavelengths from the SWIR spectra but still had a strong correlation (r = 0.75). The plant-water based indices had weak correlation coefficients with all non-plant-water based VIs with one notable exception - the NDLI (lignin) and the NDII7 (plant-water) had a correlation coefficient of 0.75.

3.4 **Simple Linear Regression Between LFA Indices and VIs**

- My hypothesis is that VIs can predict the LFA indices of stability, infiltration and nutrient cycling under my experimental conditions of dry season, winter senesced, Highveld vegetation.

Regressions of the VIs as the predictor variable against the LFA stability index gave weak coefficients of determination for all VIs (Table 20). The strongest coefficient of determination was for the lignin index (NDLI) (r^2 = 0.24, P < 0.01) (Figure 17a). This was followed by the PRI (r^2 = 0.15, P < 0.01), a carotenoid based index (Figure 17b), and the SAVI which is a chlorophyll based index adjusting for soil background. All these regressions are extremely weak. Testing transformations and polynomial models did not improve any results.

The LFA infiltration index as the response variable produced weak regressions like those for the stability index, but the VIs with the strongest coefficients of determination differed (Table 21). The standard NDVI (NDVI800) had the strongest coefficient of determination (r^2 = 0.16, P < 0.01) (Figure 17c). This was closely followed by the red edge mSR705 and mNDVI705 (r^2 = 0.14, P < 0.01) (Figure 17d). All three indices are chlorophyll based vegetation indices.

Regressions between the VIs and nutrient cycling followed a similar pattern to those for the stability index. The NDLI, sensitive to lignin, had the strongest, albeit still weak, coefficient of determination (r^2 = 0.25, P < 0.01) (Figure 17e, Table 22) and the Photochemical Reflectance Index (PRI), a carotenoid based index, the second strongest (r^2 = 0.20, P < 0.01) (Figure 17f, Table 22). From the above results, I reject the hypothesis that HSRS VIs can predict LFA indices of stability, infiltration and nutrient cycling under the conditions of dry season, winter senesced vegetation.

Table 20 Regressions with the LFA stability index as the response variable and the vegetation index (VI) as the explanatory variable (n = 105, degrees of freedom = 103, * is significant at the 5 % level, and ** is significant at the 1 % level). Values in bold show the three strongest regressions.

VI	r^2	F-value	Probability
Chlorophyll based VIs:			
NDVI800	0.02	2.90	0.09
NDVI750	0.006	1.67	0.20
GNDVI	-0.004	0.56	0.46
SAVI	**0.10**	**12.41**	**0.0006** **
NDVI705	0.01	1.95	0.17
mSR705	0.002	1.22	0.27
mNDVI705	0.006	1.62	0.21
VOG2	0.01	2.38	0.13
VOG3	0.01	2.32	0.13
Mixed chlorophyll and carotenoid based VIs:			
SIPI	0.009	1.95	0.17
PSRI	0.05	6.78	0.01 *
Carotenoid based VIs:			
PRI	**0.15**	**19.21**	**< 0.0001** **
CRI1	0.01	2.23	0.14
CRI2	0.01	2.31	0.13
Anthocyanin based VIs:			
ARI1	0.01	2.33	0.13
ARI2	0.003	1.28	0.26
Plant structural based VIs:			
CAI	-0.001	0.89	0.35
NDLI	**0.24**	**33.45**	**< 0.0001** **
Plant-water based VIs:			
WBI	-0.006	0.36	0.55
NDWI	0.01	2.25	0.14
NDII	0.02	2.77	0.10
NDII5	0.02	2.98	0.09
NDII7	0.06	8.02	0.006 **

Table 21 Regressions with the LFA infiltration index as the response variable and the vegetation index (VI) as the explanatory variable (n = 105, degrees of freedom = 103, * is significant at the 5 % level, and ** is significant at the 1 % level.). Values in bold highlight the three strongest regressions amongst the VIs.

VI	r^2	F-value	Probability
Chlorophyll based VIs:			
NDVI800	**0.16**	**20.85**	**< 0.0001** **
NDVI750	0.13	16.15	0.0001 **
GNDVI	0.01	2.17	0.14
SAVI	0.09	11.67	0.0009 **
NDVI705	0.12	15.09	0.0002 **
mSR705	**0.14**	**17.42**	**< 0.0001** **
mNDVI705	**0.14**	**18.42**	**< 0.0001** **
VOG2	0.13	17.03	< 0.0001 **
VOG3	0.13	16.9	< 0.0001 **
Mixed chlorophyll and carotenoid based VIs:			
SIPI	0.07	8.31	0.005 **
PSRI	0.10	12.4	0.0006 **
Carotenoid based VIs:			
PRI	0.09	11.28	0.001 **
CRI1	0.02	3.52	0.06
CRI2	0.04	4.99	0.03 *
Anthocyanin based VIs:			
ARI1	0.04	5.82	0.02 *
ARI2	0.01	2.01	0.16
Plant structural based VIs:			
CAI	-0.004	0.56	0.46
NDLI	0.09	11.32	0.001 **
Plant-water based VIs:			
WBI	0.10	13.03	0.0005 **
NDWI	0.03	4.13	0.05 *
NDII	0.002	1.24	0.27
NDII5	0.007	1.68	0.20
NDII7	-0.0006	0.93	0.34

Table 22 Regressions with the LFA nutrient cycling index as the response variable and the vegetation index (VI) as the explanatory variable (n = 105, degrees of freedom = 103, * is significant at the 5 % level, and ** is significant at the 1 % level.). Values in bold highlight the four strongest regressions amongst the VIs.

VI	r^2	F-value	Probability
Chlorophyll based VIs:			
NDVI800	**0.15**	**19.24**	**< 0.0001** **
NDVI750	0.11	13.21	0.0004 **
GNDVI	-0.006	0.38	0.54
SAVI	0.13	16.74	< 0.0001 **
NDVI705	0.11	14.05	0.0003 **
mSR705	0.13	16.30	0.0001 **
mNDVI705	0.13	16.94	< 0.0001 **
VOG2	0.12	15.67	0.0001 **
VOG3	0.12	15.57	0.0001 **
Mixed chlorophyll and carotenoid VIs:			
SIPI	0.06	7.67	0.007 **
PSRI	**0.14**	**18.49**	**< 0.0001** **
Carotenoid based VIs:			
PRI	**0.20**	**27.04**	**< 0.0001** **
CRI1	-0.001	0.89	0.35
CRI2	0.007	1.70	0.20
Anthocyanin based VIs:			
ARI1	0.01	2.20	0.14
ARI2	-0.007	0.24	0.63
Plant structural based VIs:			
CAI	0.02	3.63	0.06
NDLI	**0.25**	**36.07**	**< 0.0001** **
Plant-water based VIs:			
WBI	0.11	13.43	0.0004 **
NDWI	0.03	4.46	0.04 *
NDII	0.003	1.35	0.25
NDII5	0.005	1.55	0.22
NDII7	0.02	3.52	0.06

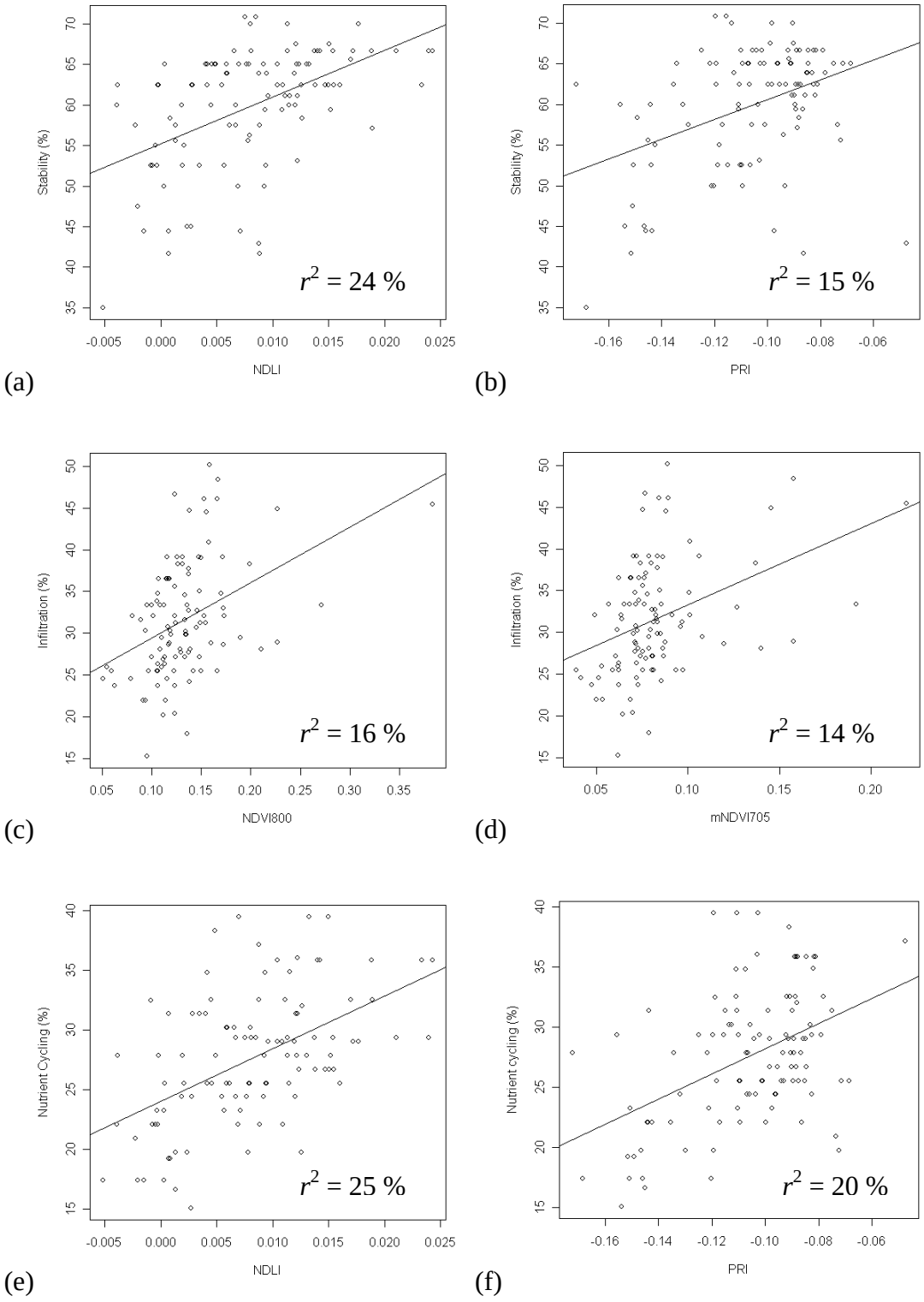

Figure 17 Regressions of VIs on LFA indices as the response and vegetation indices as the predictor variable. (a) Stability with the NDLI (lignin). (b) Stability with the PRI (carotenoids). (c) Infiltration with the standard NDVI (chlorophyll). (d) Infiltration with the modified red edge NDVI (chlorophyll). (e) Nutrient cycling with the NDLI (lignin). (f) Nutrient cycling with the PRI (carotenoids).

3.5 Partial Least Squares Regression Modelling

3.5.1 Models of Stability

Calibrating the stability models produced the lowest Root Mean Square Error of Prediction (RMSEP) of 6.241 for a 4-component model (Table 23). This model explains 98.7% of the variance in the spectral data, but only 43.8% of the variance in the stability data. Other possible models are a 2-component model (RMSEP = 6.466), 7-component model (RMSEP = 6.458), 13-component model (RMSEP = 7.991) and a 23-component model (RMSEP = 10.02) (Figure 18). Most commonly one wants a model having the lowest RMSEP (prediction error), with the lowest number of components to avoid over-fitting (Mevik and Wehrens, 2007).

The first component explains 70% of the variation in the spectral data, but only 11% of the variation in the stability data (Table 23). The second component explains a further 28% of the spectral variance, and 20% of the variance in the stability data. In other words, the first two components of the stability model explain 98% of the spectral variation, but only 32% of variation in LFA stability data. Adding components increases the variation in the stability data explained by the model, but introduces more spectral noise into the model (Figure 19). The 2-component model has a relatively smooth line plotting the regression coefficient. Noise is clearly apparent in the plot of the regression coefficient for the 7-component model. By 13 components, the plot in the SWIR region has almost disappeared in noise.

Linear regression of predictions against measured values using calibration data showed that adding components increases the coefficient of determination (Figure 20, Table 24). The coefficient of determination for a 4-component model was 44% and a 23-component model was 99%. But when applying the models to the validation data, the coefficients of determination were much lower for all models (Figure 20, Table 25). The 23-component model dropped to 34% and that of the 4-component model to 17%. The RMSEP for the validation data varied between 5.9 and 7.5 (Table 23). The 4-component model was on the high side but within this range, and the 13-component model was towards the low side. The 13-component model had a calibration coefficient of determination of 79% (Table 24) and validation coefficient of

determination with new data of 38% (Table 25; Figure 20). This was the highest validation for any of the stability models when applied to new data.

The above results imply that from a statistical modelling perspective, and avoiding over-fitting, the best model is a 4-component model, but from a predictive perspective with new data, the best model is a 13-component model of stability.

During diagnosis of the stability model, a number of outliers were detected (Table 26, Figure 21) by inspection of score plots (Mevik and Wehrens, 2007). The two very flat spectra (VR7 5-5 and VR 10 4-3) were both detected. A number of spectra showed a mirror image in portions of their spectra to the mean spectra, or large differences from the mean spectra in certain portions of their spectrum. Removing outliers and recalibrating the models suggested a 2-component, 5-component or 17-component model would be applicable. But testing these models with the validation data did not give improved coefficients of determination for prediction compared to the original values shown in Table 25 (5-component r^2 for validation = 25 %, 17-component r^2 = 29 %, data not shown).

Interpretation of the loadings was restricted to the first four components (Figure 22, Table 27), as these accounted for 98.7% (Table 23) of the modelled spectral variability. Component 1, accounting for 70 % of spectral variability, has a shallow inflection point in the loadings plot around 600 – 800 nm which is mirrored in component 2 from 600 – 700 nm, and more localised in component 3 (620, 680 – 720, 770 nm), and component 4 (600, 720 and 760 nm). Component 3 reflects an environmental feature around 450 nm. The first three components all reflect features around 920, 950 and 940 nm respectively, whereas component 4 suggests three absorption features around 900, 940 and 960 nm. Components 3 and 4 suggest two features in the 1120 – 1160 nm wavelengths. All four components identify features in the 1200 – 1260 nm and 1720 – 1760 nm wavelength range. A number of absorption features in the 2000 – 2300 nm range are identifiable in the four different component loadings but only the 2000 and 2300 nm features are present in more than one loading (Table 27).

Table 23 RMSEP values for first 25 components of the LFA stability model using LOO cross-validation, and cumulative percentage variances explained per component for spectral data (X) and LFA values (Y). Values in bold indicate local minima for RMSEP.

Number of Components	RMSEP calibration CV (n = 79)	RMSEP calibration Adj CV (n = 79)	RMSEP validation (n = 26)	Spectral Variance X (%)	Stability Variance Y (%)
Intercept	7.435	7.435	7.469		
1	7.288	7.299	7.013	69.7	11.41
2	**6.466**	**6.464**	**7.37**	**97.5**	**31.73**
3	6.515	6.505	7.234	98.07	40.61
4	**6.241**	**6.238**	**7.145**	**98.72**	**43.83**
5	6.685	6.685	7.193	99.75	44.73
6	6.756	6.744	7.178	99.8	51.79
7	**6.458**	**6.447**	**6.643**	**99.84**	**56.09**
8	6.922	6.910	6.604	99.89	57.95
9	6.976	6.964	6.349	99.93	59.64
10	7.630	7.610	6.004	99.94	64.71
11	8.113	8.087	6.252	99.96	69.12
12	8.532	8.498	5.92	99.97	73.88
13	**7.991**	**7.960**	**5.99**	**99.97**	**78.72**
14	8.141	8.106	6.239	99.97	82.86
15	8.580	8.537	6.15	99.98	86.62
16	8.140	8.100	5.942	99.98	88.88
17	8.279	8.239	5.627	99.98	90.38
18	8.672	8.631	6.114	99.99	92.41
19	9.036	8.988	5.992	99.99	94.09
20	9.203	9.149	6.086	99.99	95.88
21	10.22	10.16	6.358	99.99	96.82
22	10.05	9.988	6.272	99.99	98.04
23	**10.02**	**9.958**	**6.265**	**99.99**	**98.66**
24	10.35	10.28	6.372	100	99.2
25	10.36	10.29	6.35	99.99	99.48

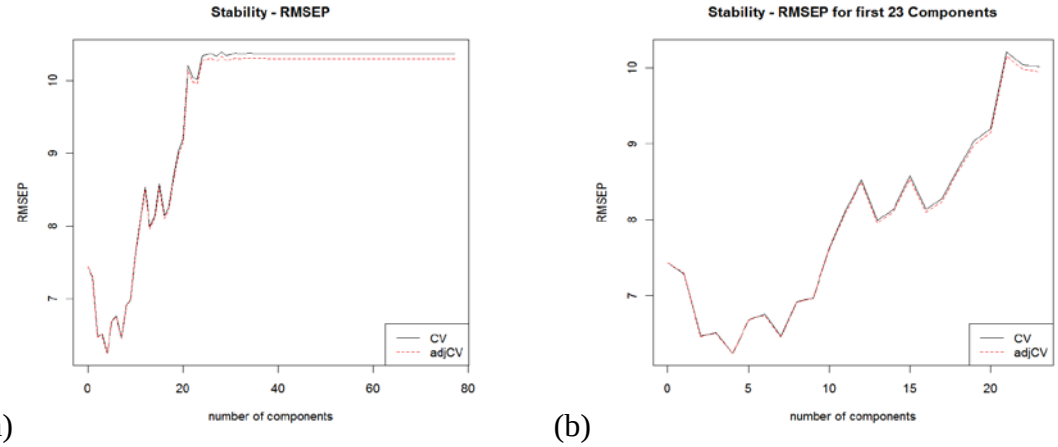

(a) (b)

Figure 18 RMSEP for stability models from calibration data (n = 79). CV is cross-validation. (a) 79 components and (b) 23 component using LOO cross-validation.

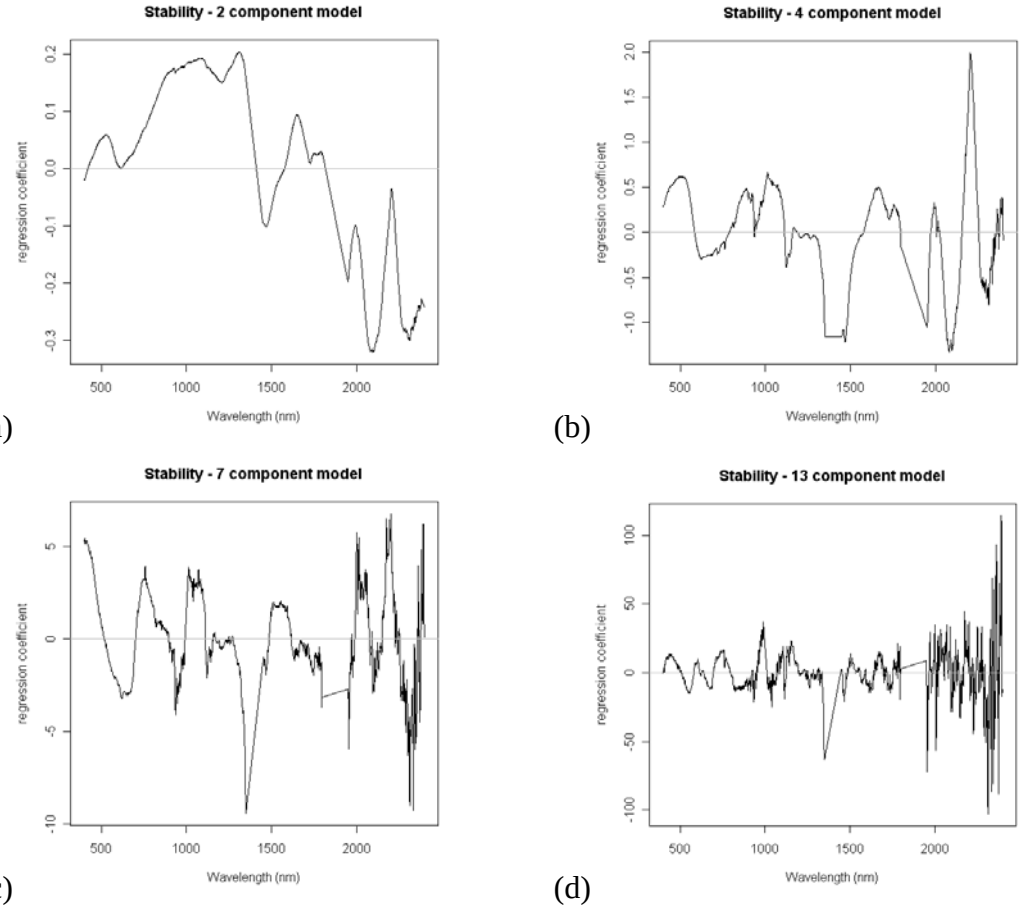

(a) (b)

(c) (d)

Figure 19 Regression coefficients for (a) 2-component, (b) 4-component, (c) 7-component and (d) 13-component models of stability.

Table 24 Coefficients of determination for predictions from the calibration of stability models (n = 79). * is significant at the 5 % level, and ** is significant at the 1 % level.

Number of Model Components	Residual Standard Error	Degrees of Freedom	Multiple r^2	F-value	Probability
4	3.69	77	0.44	60.07	< 0.0001 **
7	3.69	77	0.56	98.35	< 0.0001 **
13	3.04	77	0.79	284.9	< 0.0001 **
23	0.86	77	0.99	5659	< 0.0001 **

Table 25 Coefficients of determination for predictions from the validation of stability models (n = 26). Values in bold indicate the model with the highest r^2. * is significant at the 5 % level, and ** is significant at the 1 % level.

Number of Model Components	Residual Standard Error	Degrees of Freedom	Multiple r^2	F-value	Probability
4	4.57	24	0.18	5.04	0.03 *
7	5.01	24	0.29	9.78	0.005 **
13	**4.06**	**24**	**0.38**	**14.59**	**0.0008** **
23	4.79	24	0.37	12.20	0.002 **

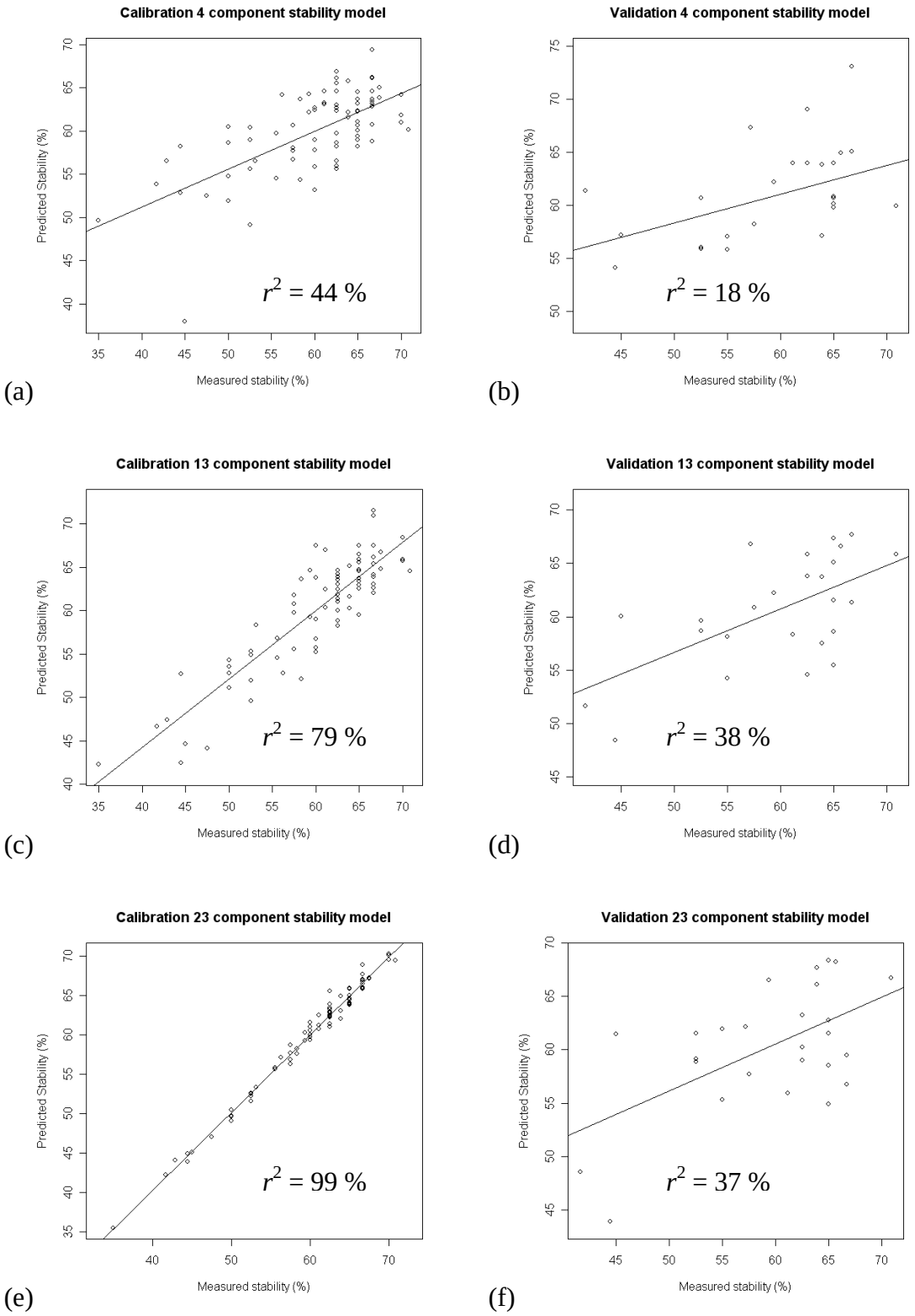

Figure 20 Calibration (n = 79) and validation (n = 26) predictions for three stability models: (a, b) 4-component, (c, d) 13-component and (e, f) 23-component models.

Table 26 Outliers identified in the development of the stability model.

Plot	Vegetation type	Disturbance	Quadrat number	Data set
VR 2	Rocky grassland	Low	1-5	Validation
VR 5	Rocky grassland	High	3-3	Calibration
VR 25	Rocky grassland	High	1-5	Calibration
VR 9	Wet grassland	Low	2-2	Calibration
VR 19	Wet grassland	Low	1-5	Calibration
VR 4	Woody shrub	High	5-1	Validation
VR 4	Woody shrub	High	4-2	Calibration
VR 7	Woody shrub	Low	1-5	Calibration
VR 7	Woody shrub	Low	5-5	Calibration
VR 10	Woody shrub	Low	4-3	Calibration
WW 4	Non-rocky grassland	Low	1-5	Calibration

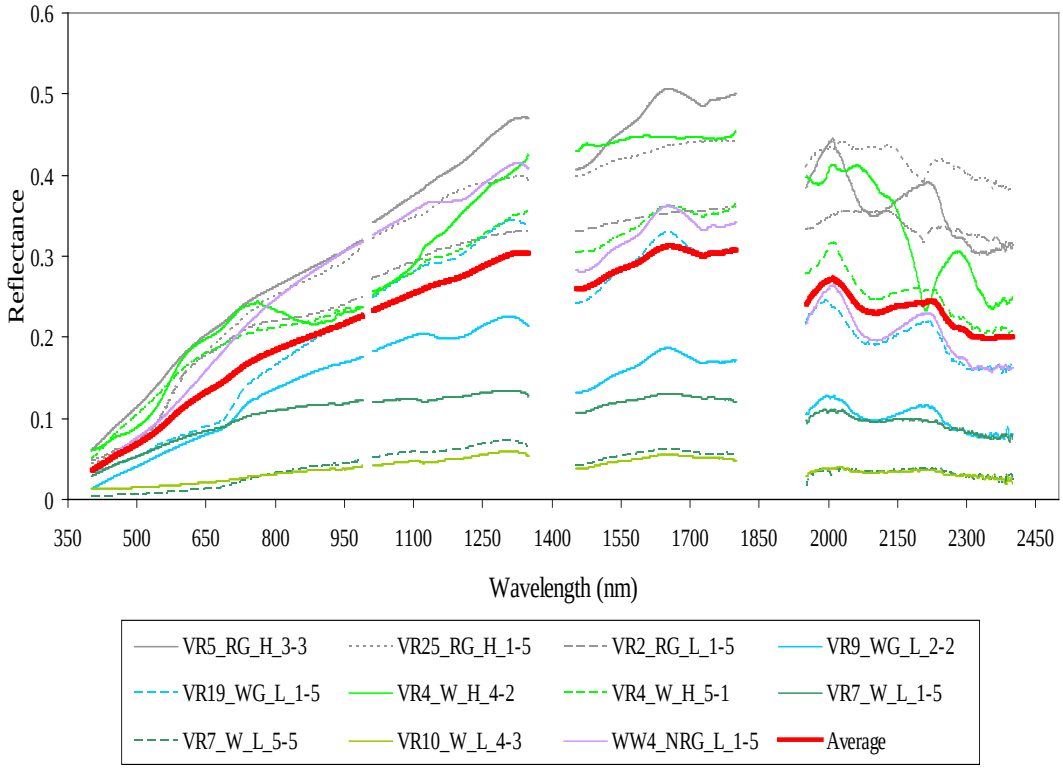

Figure 21 The spectra for the plots identified as outliers while modelling stability. Outliers were visually identified from score plots when outside the general data cloud in the plot. The mean spectrum for all spectra is also shown.

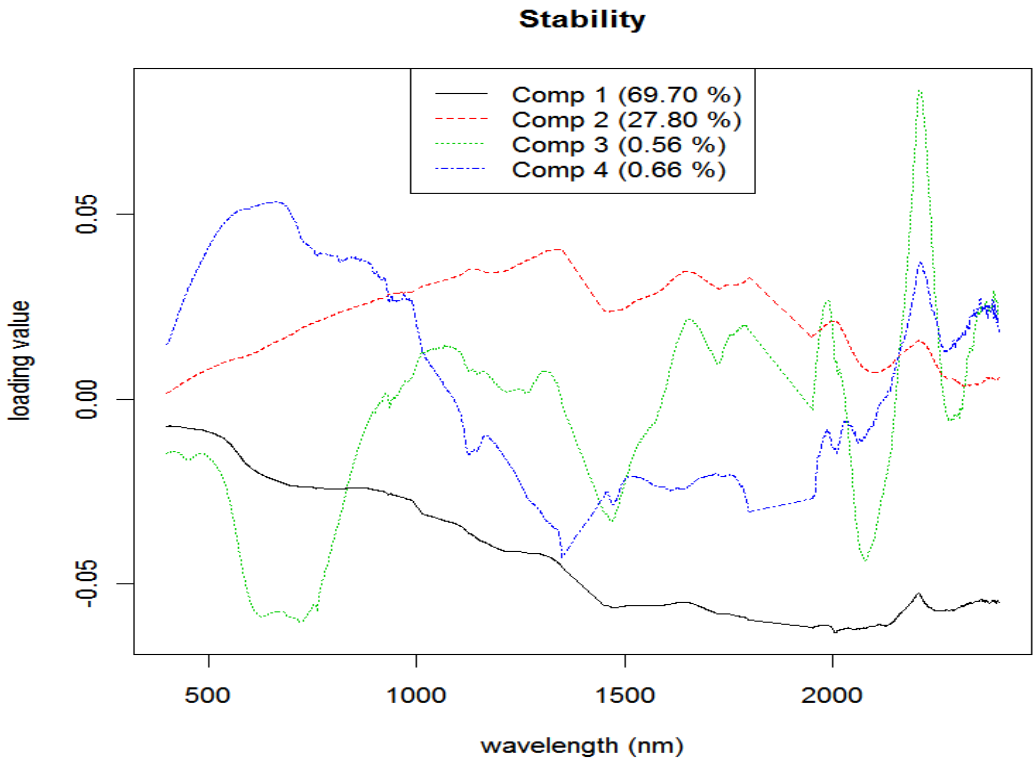

Figure 22 Loading values for the first four components of the stability model.

Table 27 Approximate wavelengths (nm) for possible absorption features identified from the loadings for the first four components of the stability model.

Component 1	Component 2	Component 3	Component 4
± 600 - 800	600 – 700	450	600
920	950	620	720
1200	1200	680 – 720	760
1260	1500	770	810
1600	1600	940	900
1720	1730	1150	940
2000	1760	1160	960
2060	2100	1220	1120
2140	2270	1260	1140
2260	2300	1590	1260
2300		1720	1580
		1750	1600
		2200	1630
		2290	1740
		2300	2000
			2080
			2280

3.5.2 **Models of Infiltration**

The infiltration model with the lowest calibration RMSEP is an 8-component model (RMSEP = 6.023), although any of the models between 4 and 8 components have very similar RMSEPs (Figure 23, Table 28). The other possible models with notable RMSEP values are a 17- or 19-component model (RMSEP = 7.619 and 7.672 respectively), and a 25-component model (RMSEP = 7.861). Like stability, the infiltration model explains most of the variation in the spectral data (88%) in the first component but only 4% of the variation in the infiltration data (Table 28). The 8-component infiltration model accounts for 99.9% of the spectral variation but only 51% of the infiltration variation, whereas the 17-component model explains 99.9 and 91% respectively. When regressing predicted against measured infiltration values for these models, a similar pattern to the stability models occurs (Figure 24). Adding components to the models using calibration data increases the resulting coefficients of determination, but this does not hold for the validation data. Coefficients of determination increase much more slowly with validation data, and then begin falling again as components are added to the model. Like the stability models, adding components increases the amount of spectral noise built into the modelling process (Data not shown, Appendix 4). The best model for predictive purposes using new validation data is the 17-component model (r^2 = 32%).

Outliers identified during the modelling process were similar to those identified for models of stability, with the exception of VR 5_5-1, a rocky grassland of high disturbance, which was not recognised as an outlier in the stability modelling (Appendix 5). Removing the outliers did not markedly improve the validation results of the recalibrated results, with the 17-component infiltration modelling improving the validation coefficient of determination from 32% to 34% (results not shown). The loadings for the first four components show a different pattern to the stability model. However, identifying the points of absorption resulted in wavelengths similar to those described in Table 27. Therefore, these loadings are not discussed further but the loadings plot is illustrated in Appendix 5.

Table 28 RMSEP values for first 30 components of the LFA infiltration model using LOO cross-validation, and cumulative percentage variances explained per component for spectral data (X) and LFA values (Y). Values in bold indicate local minima for RMSEP

Number of Components	RMSEP calibration CV (n = 79)	RMSEP calibration adjCV (n = 79)	RMSEP validation (n = 26)	Spectral variance X (%)	Infiltration variance Y (%)
(Intercept)	6.669	6.669	7.627		
1	6.630	6.635	7.893	88.47	3.69
2	6.412	6.409	7.522	97.27	17.18
3	6.064	6.061	7.281	98.66	28.14
4	**6.043**	**6.040**	**7.179**	**99.48**	**31.07**
5	6.051	6.045	7.534	99.62	39.25
6	**6.026**	**6.025**	7.564	**99.82**	**41.45**
7	6.050	6.044	7.37	99.87	46.88
8	**6.023**	**6.015**	**7.669**	**99.9**	**50.59**
9	6.159	6.151	7.689	99.92	53.49
10	6.475	6.462	6.903	99.94	57.74
11	6.696	6.683	6.796	99.96	60.49
12	7.401	7.379	7.111	99.97	65.65
13	7.912	7.871	6.483	99.97	79.06
14	8.016	7.975	6.329	99.97	83.05
15	8.049	8.011	**6.271**	99.98	85.01
16	7.982	7.944	6.642	99.98	87.89
17	**7.619**	**7.576**	**6.581**	**99.98**	**91.41**
18	8.067	8.022	6.604	99.99	92.88
19	**7.672**	**7.633**	**6.615**	**99.99**	**94.64**
20	7.755	7.711	6.589	99.99	96.25
21	8.204	8.155	6.938	100	97.7
22	8.009	7.961	7.128	99.99	98.45
23	7.992	7.943	7.278	99.99	99.04
24	7.906	7.856	7.326	99.99	99.43
25	**7.861**	**7.811**	**7.375**	**99.99**	**99.64**
26	7.880	7.830	7.395	99.99	99.75
27	7.939	7.889	7.363	99.99	99.86
28	7.981	7.930	7.366	99.99	99.91
29	8.010	7.959	7.381	99.99	99.95
30	8.032	7.982	7.379	99.99	99.97

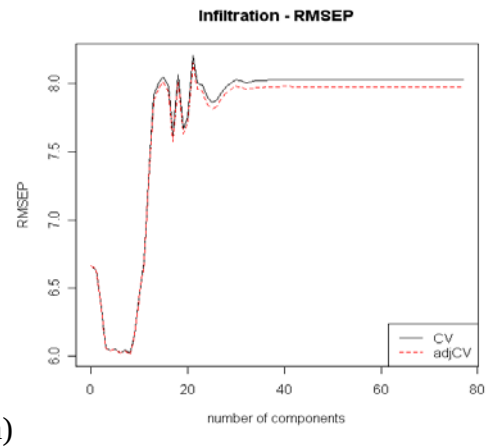

(a)

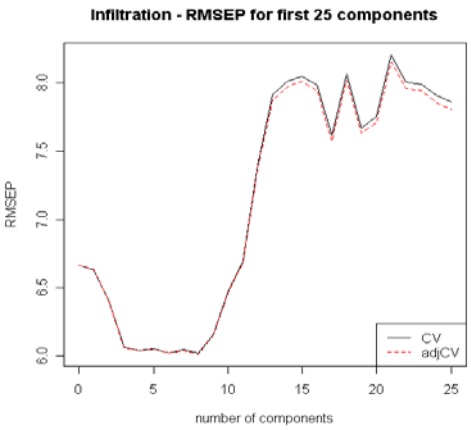

(b)

Figure 23 RMSEP for infiltration models from calibration data (n = 79), CV is cross-validation (a) 79 components and (b) 25 component, using LOO cross-validation.

Table 29 Coefficients of determination for predictions from the calibration of infiltration models (n = 79). * is significant at the 5 % level, and ** is significant at the 1 % level.

Number of Model Components	Residual Standard Error	Degrees of Freedom	Multiple r^2	F-value	Probability
4	3.09	77	0.31	34.71	< 0.0001 **
8	3.33	77	0.51	78.83	< 0.0001 **
17	1.87	77	0.91	819.2	< 0.0001 **
25	0.40	77	0.99	21400	< 0.0001 **

Table 30 Coefficients of determination for predictions from the validation of infiltration models (n = 26). Values in bold indicate the model with the highest r^2. * is significant at the 5 % level, and ** is significant at the 1 % level.

Number of Model Components	Residual Standard Error	Degrees of Freedom	Multiple r^2	F-value	Probability
4	3.59	24	0.15	4.39	0.05 *
8	5.00	24	0.13	3.72	0.07
17	**5.77**	**24**	**0.32**	**11.04**	**0.003** **
25	6.09	24	0.18	5.22	0.03 *

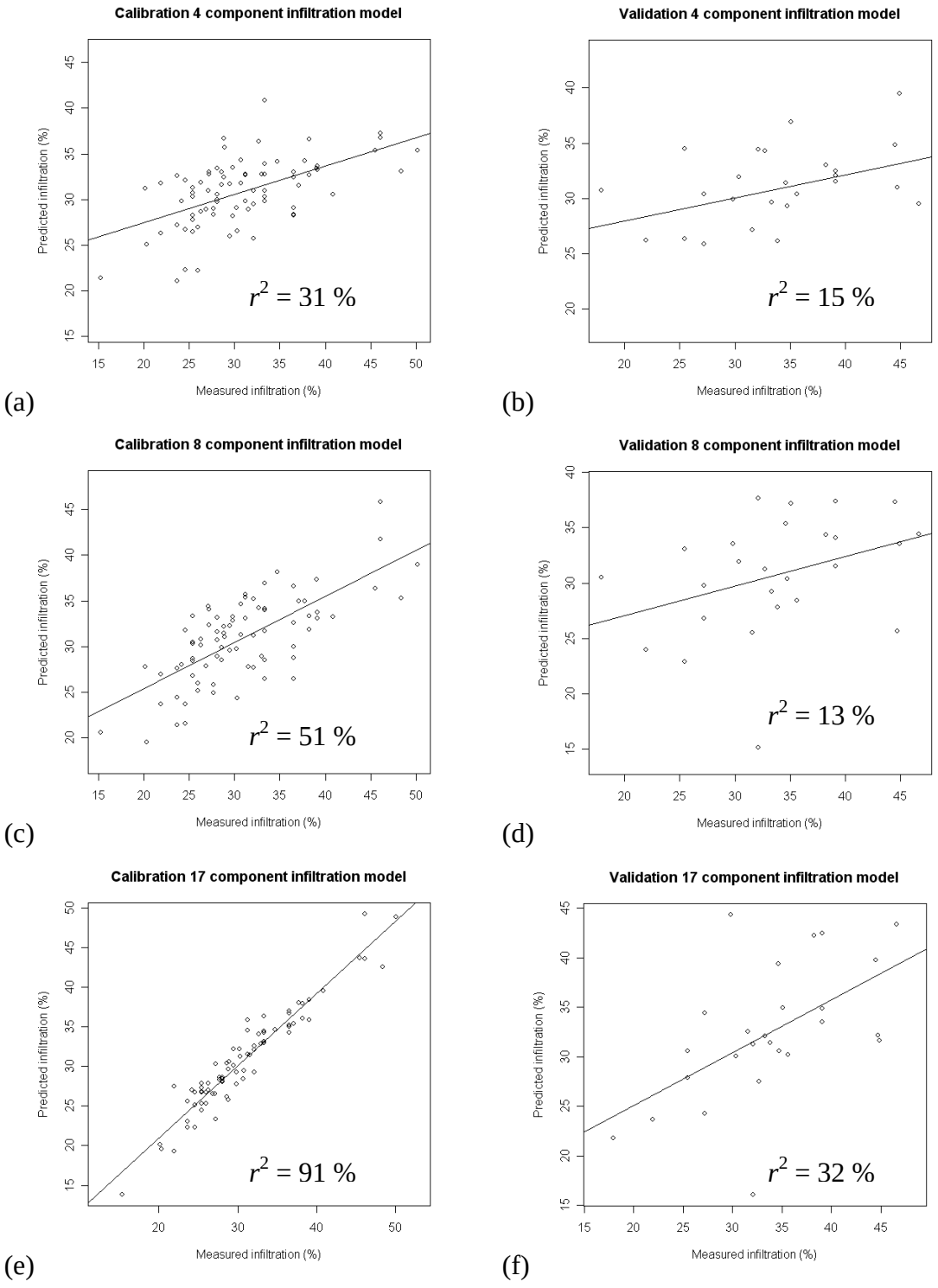

Figure 24 Calibration (n = 79) and validation (n = 26) predictions for three infiltration models: (a, b) 4-component model, (c, d) 8-component model and (e, f) 17-component model.

3.5.3 **Models of Nutrient Cycling**

Analysis of the RMSEP calculated for the calibration of the nutrient cycling models suggested four potential models (Table 31). The model with the lowest RMSEP (4.476) is the 5-component model. This is the lowest RMSEP obtained for the calibration of any stability or infiltration model. Other possible models for nutrient cycling include 9-component, 15-component and 22-component models (Table 31, Figure 25). Similar to infiltration and stability models, the nutrient cycling model with the lowest RMSEP (5-component) only explains 51% of the variation in the nutrient cycling data while explaining nearly 100% of the spectral variation. The 15-component model explains 88% of the variation in the nutrient cycling data.

When testing these four model options against a new data set (validation), the 15-component model has the highest coefficient of determination (r^2 = 54%) for nutrient cycling predictions (Figure 26, Table 33). This is considerably higher than the best models for either stability (38%) or infiltration (32%).

The outliers diagnosed in the calibration phase are similar to those for stability and infiltration models and are tabulated in Appendix 5. Removing these outliers and recalibrating the models gives a different set of optimal models, but these give poorer validation coefficients of determination (best r^2 = 45%, data not shown).

The loadings for the first four components are shown in Appendix 5. The spectral features are situated at similar wavelengths to those identified for the stability model (Table 27). However, the shape or scale of each loading in the nutrient cycling models is different to those in the stability and infiltration models.

Table 31 RMSEP values for first 30 components of the LFA nutrient cycling model using LOO cross-validation, and cumulative percentage variance explained per component for spectral data (X) and LFA nutrient cycling values (Y). Values in bold indicate local minima for RMSEP

Number of Components	RMSEP calibration CV (n = 79)	RMSEP calibration adjCV (n = 79)	RMSEP Validation (n = 26)	Spectral Variance X (%)	Nutrient cycling Variance Y (%)
(Intercept)	5.797	5.797	4.778		
1	5.605	5.619	5.068	79.976	7.913
2	5.067	5.065	4.41	97.38	31.31
3	4.674	4.672	4.485	98.65	45.69
4	4.530	4.527	4.427	99.44	48.83
5	**4.476**	**4.474**	**4.407**	**99.75**	**50.99**
6	4.689	4.685	4.545	99.84	53.46
7	4.796	4.790	4.35	99.87	57.64
8	4.827	4.819	4.527	99.9	60.44
9	**4.701**	**4.691**	**4.223**	**99.91**	**64.08**
10	5.182	5.180	3.833	99.94	67.08
11	5.943	5.911	4.59	99.94	76.3
12	6.199	6.180	4.228	99.96	78.9
13	5.980	5.954	3.797	99.97	82.7
14	5.677	5.654	3.63	99.98	84.87
15	**5.620**	**5.596**	**3.525**	**99.98**	**87.75**
16	5.642	5.615	3.641	99.98	90.62
17	5.906	5.877	3.477	99.99	92.11
18	6.067	6.037	3.568	99.99	93.63
19	6.088	6.055	3.563	99.99	95.89
20	6.199	6.164	3.609	99.99	97.04
21	6.692	6.654	3.644	99.99	97.78
22	**6.513**	**6.474**	**3.69**	**100**	**98.7**
23	6.610	6.570	3.788	99.99	99.18
24	6.564	6.522	3.792	99.99	99.62
25	6.534	6.494	3.815	99.99	99.75
26	6.531	6.490	3.822	99.99	99.82
27	6.521	6.480	3.783	100	99.9
28	6.526	6.485	3.791	99.99	99.94
29	6.524	6.483	3.802	99.99	99.96
30	6.527	6.485	3.796	99.99	99.98

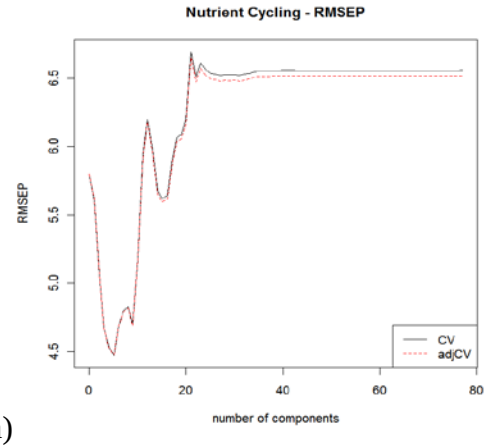

(a)

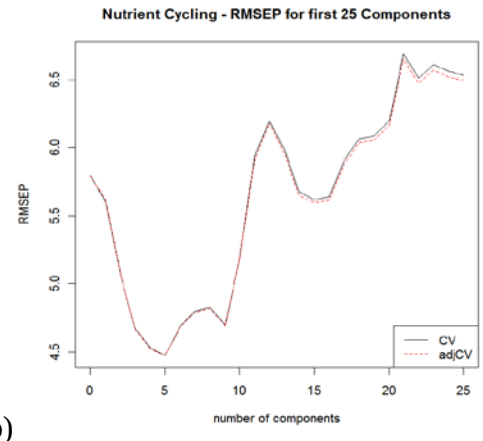

(b)

Figure 25 RMSEP for nutrient cycling models from calibration data (n = 79). CV is cross-validation (a) 79 components and (b) 25 component using LOO cross-validation.

Table 32 Coefficients of determination for predictions from the calibration of nutrient cycling models (n = 79). * is significant at the 5 % level, and ** is significant at the 1 % level.

Number of Model Components	Residual Standard Error	Degrees of Freedom	Multiple r^2	F-value	Probability
5	2.90	77	0.51	80.12	< 0.0001 **
9	2.78	77	0.64	137.3	< 0.0001 **
15	1.90	77	0.88	551.6	< 0.0001 **
22	0.66	77	0.99	5814	< 0.0001 **

Table 33 Coefficients of determination for predictions from the validation of nutrient cycling models (n = 26). Values in bold indicate the model with the highest r^2. * is significant at the 5 % level, and ** is significant at the 1 % level.

Number of Model Components	Residual Standard Error	Degrees of Freedom	Multiple r^2	F-value	Probability
5	3.54	24	0.25	8.197	0.009 **
9	3.77	24	0.36	13.79	0.001 **
15	**3.46**	**24**	**0.54**	**27.78**	**< 0.0001** **
22	3.45	24	0.44	18.82	0.0002 **

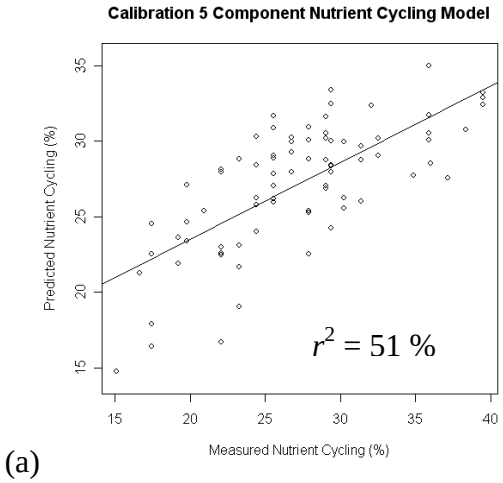

(a)

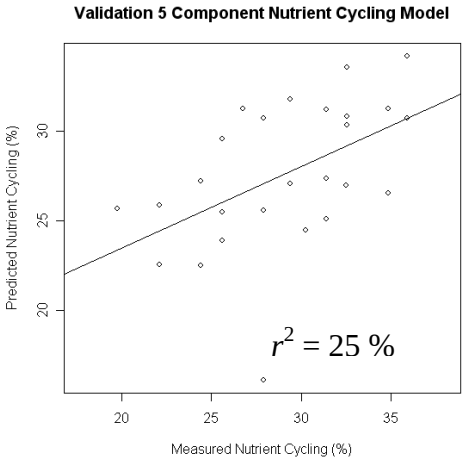

(b)

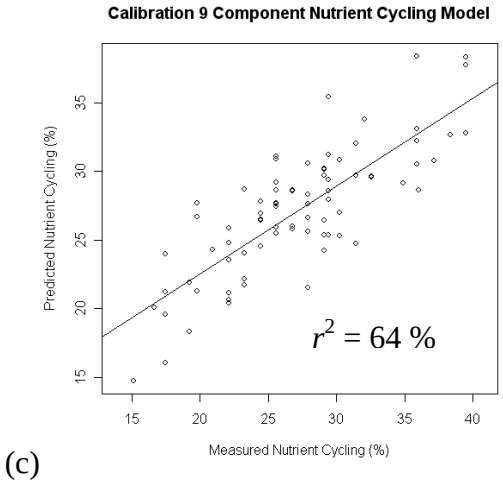

(c)

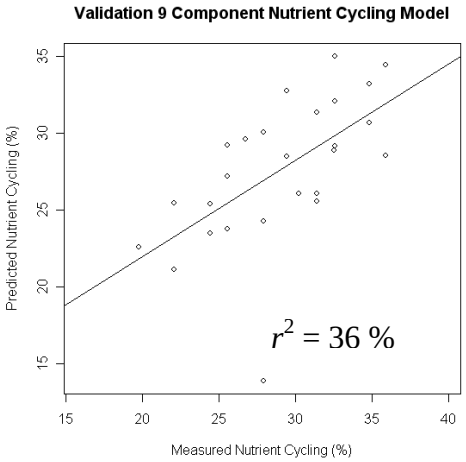

(d)

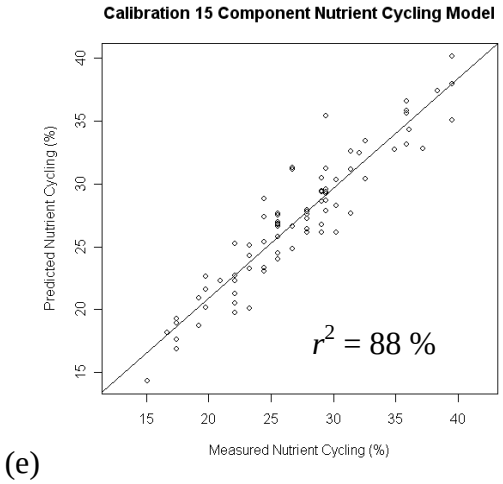

(e)

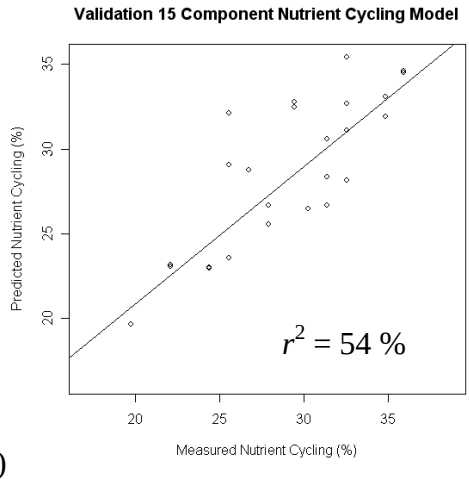

(f)

Figure 26 Calibration (n = 79) and validation (n = 26) predictions for three nutrient cycling models: (a, b) 5-component model, (c, d) 9-component model and (e, f) 15-component model.

4 Discussion

4.1 Landscape Function Analysis

McIntyre and Tongway (2005) examined grazing pressures on four grassland patches representing different grazing pressures, and found that the stability index remained high and constant, and only declined in the patches experiencing the heaviest grazing. This corresponds with my study where stability, including high disturbance sites, was generally high with 80% of quadrats above threshold (Tongway and Hindley, 2004). Infiltration indices are low relative to their threshold value, which suggests that the majority of quadrats tend to shed excess rain water, rather than infiltrate the soil (Tongway and Hindley, 2004). This, together with the high general stability of quadrats, implies that there is strong physical crust development in the soil surface. Physical soil crusts promote run-off and reduce infiltration (Mücher *et al.*, 1988; Valentin and Bresson, 1992; Parsons *et al.*, 2003). No measurements were made to determine the causes of this crusting. However, observations while collecting field data, suggest that in some quadrats it may be a function of mechanical scrapping and compaction by machinery, but this does not necessarily apply to all sites.

Nutrient cycling has an almost even distribution above (53%) and below (47%) its threshold value (Table 4, Figure 12). This suggests that a little more than half the quadrats are self-sustaining in terms of nutrient turnover (Tongway and Hindley, 2004). The higher number of quadrats above threshold for stability, with a low number above for infiltration, and an even distribution for nutrient cycling, implies that most impacts are being expressed in the biological vegetation component, rather than in the soil component of the environment (Sparrow *et al*., 2003; D. Tongway, pers. comm.). In other words, the soils in these sites are stable, and impacts on these environments are being expressed in the goods and services, supplied or performed by plants, such as litter fall and capture or promotion of infiltration (Ludwig *et al.*, 2005; Tongway and Ludwig, 2007). The ranking also illustrates the high heterogeneity within plots, with individual quadrats within a plot having both high and low LFA values.

The higher LFA infiltration and nutrient cycling indices for West Wits operations may be a result of the higher MAP at West Wits, compared to Vaal River, although this was not tested. Lauenroth and Sala (1992) showed that annual net primary production (ANPP) in North American Steppe grasslands was directly related to annual and seasonal rainfall, although there was often a lag affect between rainfall and vegetative response. Increased vegetation cover would increase infiltration by acting as a barrier to surface flow, and increased soil moisture would result in higher soil biological activity (Belnap *et al.*, 2005) and nutrient capture (Parsons *et al.*, 2003). However, observations in the field suggest that the nature of disturbance between the two mines was different. The area under study at West Wits was mainly exposed to grazing pressure with little evidence of machine induced disturbance, whereas at Vaal River, both machine induced and grazing impacts were observed, and this difference may have influenced the LFA indices.

The four vegetation types at Vaal River form a continuum in physiognomic complexity from simple wet grassland, through non-rocky grassland, rocky grassland to woody shrub, which is the most complex (Barbour *et al.*, 1987). As expected, wet grassland had higher values for all LFA indices (Figure 14). This is due to a number of factors, such as its position at the bottom of landscapes, and therefore a sink for materials and resources from higher up the landscape gradient (Moss and Walker, 1978). Wet grasslands were also generally dominated by robust sedges (*S. corymbosus*), which were observed to be minimally grazed in comparison to the grasses.

For the other three vegetation types, there was a reversal in the patterns between the three LFA indices. Stability was highest in non-rocky grassland from West Wits, while woody shrub sites were lowest for stability. The infiltration index reversed this trend, while nutrient cycling lay some where inbetween. These reversals in trend for the different LFA indices may be a function of differences in biodiversity (Ludwig *et al.*, 2004), or differences in physiognomic complexity between the vegetation types (Barbour *et al.*, 1987), but this remains untested. Ludwig *et al.* (2004) showed that in Australian conditions, low LFA indicators matched low biodiversity, and high LFA indicator values corresponded with high biodiversity. In my study sites, the biodiversity gradient went from wet grassland with lowest biodiversity, non-rocky

grasslands, woody shrub, to rocky grasslands with highest biodiversity (I. Weiersbye, pers. comm.). Rocky grasslands had slightly higher nutrient cycling indices, whereas woody shrub sites had slightly higher infiltration indices. So it remains unclear whether these LFA results are influenced by physiognomic effects, biodiversity effects or an interaction between the two. What is noticeable is that non-rocky grasslands, particularly at West Wits, have less difference between LFA indices of high and low disturbance than do either rocky grasslands or woody shrub plots. This might be a result of different levels of disturbance in the high disturbance sites of these vegetation types. Alternatively, it might indicate a decrease in resilience in response to high disturbance levels in these vegetation types with high biodiversity and/or high physiognomic complexity (Holling, 1973; Gunderson, 2000; Folke *et al.*, 2004). Unfortunately, the data is not extensive enough to clarify this issue.

The categories of high and low disturbance were adequately defined, as low disturbance sites had significantly higher LFA indices than high disturbance sites (Bastin *et al.*, 2002; Tongway *et al.*, 2003; Tongway and Hindley, 2004; McIntyre and Tongway, 2005). The low levels of depositional material (as reflected in the high stability values) suggests that erosion may have been an important factor in the past in the plots sampled, but is not currently highly active in general (Weltz *et al.*, 1998). This is supported by field observations which suggested that some of the sites, especially those showing signs of mechanical scraping in the past are in a process of natural regeneration (D. Tongway, pers. comm.). This observation needs be tested with a time series of LFA data for which this study could act as the baseline (Tongway and Hindley, 2004).

The non rocky grassland and wet grasslands at Vaal River provided exceptions to the general trends in the LFA results. This is most likely due to having only one site with five quadrats for the high disturbance category in each vegetation type. The Vaal River high disturbance non-rocky grassland plot (VR 16) is part of a very short, ephemeral, natural drainage line, and deposition of fine silt particles (Moss and Walker, 1978) may have contributed to the high LFA values for this site. High disturbance wet grassland sites with visual evidence of disturbance are difficult to find. The site in this analysis (VR 28) is located below a waste water storage dam, on the edge of a *S. corymbosus* sward. It is dominanted by *C. dactylon* with stands of *S*

corymbosus intruding around the peripheries of the site. A well used cattle path runs through the site. The location below the waste water storage dam means there is likely to be higher soil moisture through seepage from the waste water facility. These two factors probably contribute to the distortion of the LFA indices for this site.

Although the results detected differences between high and low disturbance, the structured layout of the plots caused a number of sampling problems. The patch-inter-patch structure is being missed in some plots or the woody component is falling between sampling quadrats (D. Tongway, pers. comm.). In some cases repeating the measurements but using the original LFA technique will allow comparison of the results between the two systems, and an evaluation of the two approaches. Ong *et al.* (2008) adapted their sampling between 2002 and 2006 to incorporate landscape organisation measurements. This allows the calculation of weighted means for each transect and plot, and facilitates better understanding of the landscape elements and their influence in the landscape (Tongway and Hindley, 2004). However, they still retained the circular quadrats based on the FOV of the HSRS sensor. Their adaptation allowed selection of representative patches and inter-patches (Ong *et al.*, 2008), thus reducing the problems caused by mixed pixels, as illustrated in Figure 27. This photograph clearly shows that the inter-patch area has quite different LFA values in relation to the patch. Under the current amendments, the practitioner has to decide whether to give a patch or inter-patch measurement to the quadrat.

Photographs are not suitable for deriving LFA measurements, as they provide accurate information only for the rainsplash SSI, which is essentially a measure of aerial canopy cover. All other SSIs require proper field assessment where one can examine the site from different angles and under canopies. Using photographs the researcher is often forced into “guesstimating” things that can only be partially seen.

Figure 27 A non-rocky grassland quadrat of high disturbance (VR29 1.2) illustrating the disparity between LFA values for the patch and interpatch.

4.2 **Vegetation Indices**

Most published studies have applied VIs to reflectance data sampled from green vegetation during the growing season, and therefore containing high levels of chlorophyll (e.g. Curran *et al.*, 1991; Vogelmann *et al.*, 1993; Yoder and Waring, 1994; Gitelson *et al.*, 1996, Datt, 1999). This study was carried out in winter senesced, grassland vegetation which showed very little green colour, was mainly brown in colour, and dry. Tanser and Palmer (1999) applied the NDVI to February, wet season, summer Landsat TM data. They selected four fence lines separating communal degraded areas from "good condition" rangelands in the Great Fish River Basin area of South Africa. Their averages for the NDVI ranged from 0.24 to 0.47. This is double the mean (0.13 ± 0.004) obtained for the NDVI in this study. Although the upper limit of the range in this study (0.38) falls within their range, the difference between their mean values and this study is probably due to the difference in season, and therefore chlorophyll content of vegetation. However, in agreement with my findings, Tanser and Palmer (1999) calculated higher NDVI values for "good condition" rangelands compared to degraded rangelands. Wessels *et al.*, (2004) used

a ten day maximum NDVI composite from AVHRR satellite data obtained over Limpopo Province in northern South Africa during the growing season (October to April). Like my study, they also calculated lower NDVI values for degraded areas compared to non-degraded areas.

Numata *et al.* (2003) found that NDVI values measured during the dry season in Brazilian pastures, formed after the removal of natural forest, declined as a pasture aged over a ten year chronosequence. They attributed this decline in NDVI to changes in vegetation composition and canopy structure, which showed an increase in non-photosynthetic, above-ground vegetation over time. Their NDVI values ranged between 0.15 and 0.30 (Numata *et al.*, 2003) which are within the upper limit of those found in my study. Although their study occurred over the dry season, their sites are located in tropical pasturage developed from forest removal. My sites are located in semi-arid grassland, and the winter dry season conditions are likely to be far more arid than those of Numata *et al.*, (2003). This difference in aridity might account for the slightly lower NDVI values in my study compared to their values.

van Leeuwen and Huete (1996) characterised most grasslands, savannas and shrublands into four vegetative growth stages or transitions: 1) a senescent period, 2) a transition from the dry to the wet season during which litter is decaying from yellow to grey and dark structures, 3) a growing stage depending on the distribution of precipitation, and 4) a dry-down into the senescent stage due to a lack of precipitation or extremely high or low temperatures. Throughout these vegetative stages, the soil, leaf and litter spectral properties, and leaf and litter distribution, vary due to biochemical, biophysical, and morphological changes as a response to the environment (van Leeuwen and Huete, 1996). Even during the growing stage, there may be a mixture of green vegetation, standing litter, and leaf litter on the soil surface in various stage of decomposition. Boutton and Tieszen (1983), using the RVI (not applied in this study) found that variability in the estimation of biomass in grasslands in Masai Mara Game Reserve in Kenya increased markedly when the proportion of live biomass fell below 30 % of total biomass.

Frank and Aase (1994) found that senesced grass did not adversely affect the VIs during early greening of rangeland. However, they used clipped senesced grass, laid flat in experimental plots. This would produce a different reflectance signal to that produced by natural grassland, where a large proportion of senesced vegetation is standing with the lamina in an erectophile position. Huete and Jackson (1987) showed that in arid grasslands consisting of green vegetation with senescent and weathered litter, VIs were unreliable measures of green vegetation. Yellow senescent vegetation on bare soil increased NDVI values, while senescent and weathered litter reduced NDVI values (Huete and Jackson, 1987). Furthermore, they argued that the scattering influences of vertically orientated senesced elements of the grass canopy significantly influenced the green phytomass reflectance (Huete and Jackson, 1987).

Tucker (1978) studied the spectral reflectance of blue grama (*Bouteloua gracilis* (H.B.K.) Lag.) approximately four weeks after the end of growing season. He found a direct relationship between reflectance at the 680 nm wavelength and total wet biomass or total dry biomass. This is the reverse for that of green vegetation when chlorophyll absorption causes an inverse relationship (Tucker, 1979). Furthermore, Tucker (1978) found that the direct relationship, between the two biomass variables, in the NIR 740 – 800 nm wavelengths was relatively unchanged between green vegetation and four-week, post-growth, senescent or dormant vegetation. The 680 and 800 nm wavelengths are those used in the NDVI. Therefore a switch from a direct to inverse relationship around 680 nm between dry senesced grass and green grass would have major implications for VIs using these wavelengths.

Ringrose and Matheson (1987) applied the NDVI in a Savanna woodland environment in Botswana. They found that as vegetation cover increased to about 50% the NDVI remained stable, and only began increasing at vegetation covers greater than 50%. They argued that soil reflectance masked vegetation below 50 % vegetation cover. The SAVI was developed to take into account soil influences on the NDVI. However, the SAVI, like the NDVI showed large variability when influenced by leaf angle, litter and soil colour (van Leeuwen and Huete, 1996). van Leeuwen and Huete (1996) showed that litter can cause the SAVI response to be lower or higher than that of a green canopy. Furthermore, standing litter had complex interactions with VIs as a result of the variability in litter spectral and transmission

properties. They also showed that a range of litter reflectance signatures overlapped with a range of soil reflectance signatures, which made it difficult to separate soil from litter reflectance signatures. Van Leeuwen and Huete (1996) argued that VI performance could be significantly improved with ecosystem-specific information. In my study correlations amongst the chlorophyll based VIs were very high with the exception of the SAVI and the GNDVI. In the case of the SAVI, this may have been partially a result of soil influences on the index when applied in a semi-arid environment where the majority of plots had varying degrees of soil surface exposed.

The differences in MAP between Vaal River and West Wits mining regions may have contributed to the differences between these two areas for the NDVI and other chlorophyll based indices. West Wits has a higher MAP, and had consistently high mean values for these indices compared to Vaal River. Farrar *et al.*, (1994) found that the pattern of annually integrated NDVI values more closely resembles that of rainfall, rather than soil moisture, in a semi-arid region of Botswana. They regarded the low resolution of soil moisture sampling sites as influencing this pattern. However, when comparing monthly NDVI and soil moisture, they got much better correlations ($r > 0.60$) with most soil types (Farrar *et al.*, 1994). They argued that soil type had a major influence over the NDVI as a measure of photosynthetic efficiency in semi-arid ecosystems. Factors other than soil moisture availability, such as textually determined soil moisture tension, porosity, nutrients, profile characteristics and soil chemistry, all play a role in influencing photosynthetic efficiency and therefore the NDVI (Farrar *et al*., 1994). Nicholson and Farrar (1994) claimed that the relationship between NDVI and rainfall is only linearly related between 200 – 1200 mm of annual rainfall. Both West Wits and Vaal River fall roughly in the middle of this annual rainfall range, and therefore, one could expect some relationship between rainfall and chlorophyll based VI values.

The fact that most VIs fall at the extremes, generally at the low end of their expected ranges, raises the question of whether the VIs are accurately measuring the features they are designed to measure. This is not questioning the integrity of the VI, but rather the conditions in which the VI is being applied – winter senesced vegetation with low chlorophyll and low leaf water content. Further evidence for this question is raised by the different responses of VIs that are designed to measure the same

environmental feature. For instance correlations amongst the chlorophyll based indices, with the exception of the GNDVI and SAVI are very strong. Yet when some of these VIs give a significant result, such as the standard NDVI, VOG 2 and VOG 3 in non-rocky grassland at West Wits, other chlorophyll based VIs, which are highly correlated with these three VIs, show no difference.

Another line of evidence is the relationship of the GNDVI, a chlorophyll based index, to the other chlorophyll based indices. The GNDVI is designed around the 550 nm sensitivity of chlorophyll-a, whereas the other eight chlorophyll based indices are designed around the 680 nm absorption centre of chlorophyll-a, and its associated 700 nm red-edge. We know from the winter senesced state of the vegetation, that chlorophyll is low in these environments. However, if a chlorophyll signal were being detected by the VIs, one would expect all nine indices to be highly correlated. But the GNDVI is weakly correlated with the other chlorophyll indices.

One of the characteristics of spectra is that collinearity between nearby spectra is a common feature (Martens and Næs, 1989). Any collinearity should weaken as spectral regions move further away from each other. On the other hand, if two VIs far apart are measuring the same feature, such as chlorophyll, then they should have a high correlation. The GNDVI is approximately 150 nm away from the spectral region for the other eight chlorophyll based indices. This lower correlation between the GNDVI and the other eight chlorophyll based indices, suggests that these indices are receiving a very weak chlorophyll signal, and the values calculated using these wavelengths are highly influenced by the normal collinearity of spectra. Furthermore it is well documented that senesced vegetation and soil have a very similar spectrum (van Leeuwen and Huete, 1996), and that in the visible and NIR region, this spectrum shows a rather featureless, progressively increasing reflectance as one moves to longer wavelengths. This describes most of the VIS-NIR spectra recorded in this study, and brings into question all the values for the chlorophyll VIs.

Further evidence to support this line of argument is provided by an examination of the plot of the visible/NIR spectra from wet grassland quadrats (Figure 28a). The arrow shows a sudden increase in reflectance from approximately 680 nm.

(a)

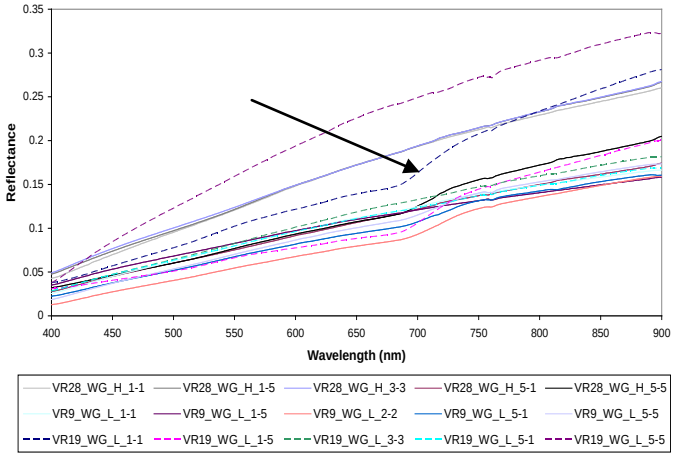

(b)

(c)

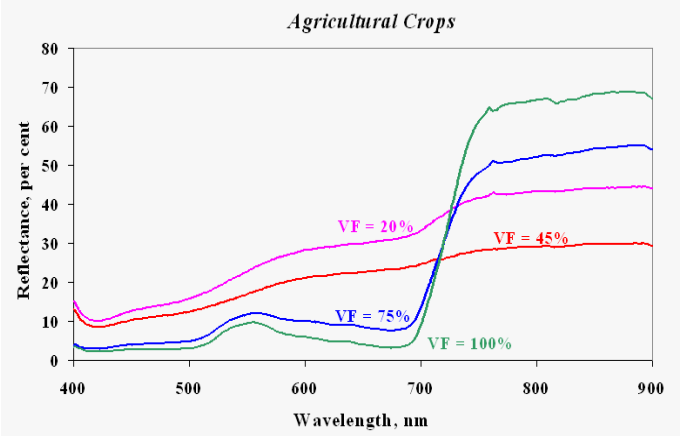

Figure 28 (a) The visible and NIR portion of the spectrum from wet grassland quadrats. The arrow points to the red-edge area of the spectrum for quadrat VR19_1-1 shown in photograph (b) with a continuous cover of sedge, *S. corymbosus*. (c) The Visible and NIR portion of the spectrum from an agricultural crop showing a well developed red edge at high vegetation fraction or cover and a corresponding weak red-edge at low vegetation fraction. (Graph courtesy of R. Stark, 2001).

This corresponds with the slight development of a weak red edge (Curran *et al.*, 1991; 1995; Datt, 1999; Vogelmann, 2008) in quadrat VR19_1.1, which has a continuous cover of mostly senesced sedge (*S. corymbosus*) with a few leaves showing some green photosynthetic tissue (Figure 28b). Conspicuous is the absence of any red-edge development in a number of these quadrats, and the weakly developed red edge in a few others. Figure 28c illustrates how the red-edge develops as vegetation cover increases in a green agricultural crop and how strongly developed the red-edge becomes at high vegetation covers (vegetation fraction > 75 %) (Stark, 2001). The graph of wet grassland quadrats (Figure 28a) corresponds with green vegetation fractions of 45% or less. All the above evidence brings the values calculated by the chlorophyll indices into serious doubt in terms of their value as a measure of plant chlorophyll or plant characteristics under the conditions of these spectral measurements.

All carotenoid and anthocyanin based VIs, like the chlorophyll indices, are using bands in the 450 to 700 nm. The lack of correlation between indices measuring the same feature (PRI vs CRI1: r = -0.09), or the very high correlations between indices for different pigments (carotenoid CRI1 vs anthocyanin ARI1), strongly suggest collinearity of the spectra, and not a response to plant pigments. Carotenoids are known to play a role in photo-inhibition, stabilisation of the light harvesting chlorophyll-protein complex, and photoprotection of the PS II reaction system (Biswal, 1995). Merzlyak *et al.* (1999) obtained values between -0.1 and 0.6 for the PSRI from leaves of maple (*Acer platanoides* L.) and coleus (*Coleus blumei* Benth.). My study had values for the PSRI ranging from 0.27 – 0.54 which is within the range described by Merzlyak *et al.* (1999). During leaf senescence in coleus, degradation of chlorophyll and carotenoids occurred simultaneously until traces of carotenoid remained in senesecent leaves. However, in maple leaves, more carotenoid is present in senesced leaves. Merzlyak (1999) described three responses of the PSRI: (1) Dark green leaves had slightly negative PSRI values; (2) Low PSRI values (ca. -0.1) which then increased, corresponding with the early stages of senescence; and (3) a rapid increase in PSRI values as senescence progressed. However, this final stage was not observed in coleus leaves during senescence (Merzlyak *et al.*, 1999). Sanger (1971) studied leaf pigments in three broad-leafed tree species and found that during autumn, carotenoids and chlorophyll began declining at about the same time. Furthermore, in

aspen (*Populus tremuloides* Michx.) and hazel (*Corylus americana* Walter), leaves abscise with virtually no pigments. However, pin-oak (*Quercus ellipsoidalis* E.J. Hill) leaves remain on the tree through winter and retain a fair amount of carotenoids and a small percentage (0.1%) of chlorophyll-*a* as pheophytin-*a* (Sanger, 1971; Biswall, 1995).

Gamon *et al.* (1997) examined the spectral properties and response to the PRI in twenty green plants grouped into three categories: annual, deciduous perennial, and evergreen perennial. Unlike the PSRI, which uses the carotenoids to follow senescent processes in plants (Merzlyak *et al.*, 1999), the PRI was designed to measure the efficiency of photosynthesis through the carotenoids (Gamon *et al.*, 1997). Amongst Gamon *et al.* (1997) annual category, they included *Zea mays* L, an agricultural monocotyledon. All sampling was from mid to late summer. They found that the annual group (including *Z. mays*) had high CO_2 uptake, high photosynthetic radiation efficiency and high, albeit negative PRI values (range: 0.00 to -0.10), compared to perennial evergreens (Gamon *et al.*, 1997). The values obtained in my study ranged from -0.048 – -0.17. Gamon *et al.* (1997) furthermore found that nutrient stress resulted in lower PRI values. In another study, Sims and Gamon (2002) tested nearly 400 green leaves from 53 plant species, including three grass species: *Avena fatua* L., *Lolium multiflorum* Lam. and *Pleuraphis rigida* Thurber. They found a significant relationship between the PRI and leaf carotenoid to chlorophyll ratio in both healthy and stressed leaves. They also tested the SIPI and PSRI and found no relationship with carotenoid to chlorophyll ratios (Sims and Gamon, 2002).

In my study, the two anthocyanin indices (ARI1 and ARI2) had a moderate correlation (r = 0.58) with each other. Sanger (1971) showed that anthocyanin appeared in both oak and hazel leaves during autumn, but by the time most leaves abscise, anthocyanin levels were almost zero. Sims and Gamon (2002) found no relationship between the red/green ratio and anthocyanin content, where red was the sum of 600 – 699 nm and green was the sum of 500 – 599 nm wavelengths. Ong *et al.* (2008) found that the ARI1, ARI2 and red/green ratio were correlated with leaf temperature. Gitelson *et al.*, (2001), for the ARI1 had a range of 0 – 0.24, whereas I had values ranging from 2.2 – 66.6, which are extremely high in comparison.

The CAI and NDLI, both plant structural indices measuring cellulose and lignin, are using widely spaced wavelengths from the SWIR portion of the spectrum. Therefore, collinearity should not be an issue, and the correlation between the two, which is very weak, supports this. In fact the CAI has very poor correlations with all other VIs, which is as expected as there is no link between cellulose and plant pigments, or plant-water content. Daughtry *et al.* (2004) found that the CAI was linearly related to crop residue, but that green vegetation at more than 30% cover tended to lower the CAI values. As there was very little green vegetation in our study, this is not expected to have influenced the CAI measurements. The range I obtained of -0.059 – 0.194 falls within the range that Daughtry *et al.* (2004) obtained for CAI values of -3 to 4. Daughtry (2001) tested the CAI on three crop residues: corn (*Z. mays*), wheat (*Triticum aestivum* L.) and soybean (*Glycine max* (L.) Merr.). They found that the CAI gave positive values for crop residue except where the crop residue was saturated. My study supports their results, as almost all values were positive for the winter senesced vegetation in our sites. However, in Daughtry's (2001) study, all CAI values calculated from soils were less than -1, even when the soil was saturated with water. As the proportion of exposed soil to ground cover was not assessed in my study, it is difficult to determine the effect of soil on my CAI values, but very few values were negative, and then only slightly negative. Roberts *et al.*, (1993), using spectral mixture analysis (SMA), found that soil and non-photosynthetic vegetation were too similar to separate. They used end members from ground-truthed and AVIRIS image data collected over Jasper Ridge Biological Preserve, California. They were only able to separate soil and non-photosynthetic vegetation using cellulose and lignin residuals from the SWIR region of the spectrum (Roberts *et al.*, 1993).

The lignin index (NDLI) had poor correlations with all VIs except the NDII7. It is unknown why the NDLI and NDII7 should show a strong correlation, as there were very weak correlations between the lignin VI and the other plant-water indices. The correlation between NDLI and NDII7 (0.75) is not related to collinearity as both wavelengths in each index come from unrelated portions of the spectrum. Serrano *et al.* (2002) found that in senescent Californian, Mediterranean (chaparral) vegetation, the relationship between lignin and the NDLI was not significant. The range for their NDLI values was between 0.005 and 0.030 which corresponds well with the range

(-0.005 – 0.024) obtained in this study. Furthermore, Grossman *et al.* (1996) found inconsistent results using multiple regression and spectral bands known to be representative of nitrogen and lignin.

The moderate correlation coefficients between the WBI and the other plant-water based indices raises the question of what the WBI is detecting in the environment. The high correlation coefficients between the NDWI, NDII, NDII5 and NDII7 suggest a commonality in response unrelated to collinearity, as apart from the NDII and NDII5, these indices are widely separated across the SWIR spectrum. The NDII and NDII5 are separated by only a few wavelengths and so collinearity would naturally lead to a high correlation. The NDWI, NDII and NDII7 are separated by distances in the order of 400 nm.

Peñualas et al. (1993) had WBI values between 0.8 and 1.05 for gerbera plants (*Gerbera jamesonii* Bolus ex Hook. f.). Values for the WBI in my study (0.89 to 0.96) show good agreement with those of Peñualas et al. (1993). These researchers found that, as relative water content decreased, the WBI increased. The WBI detected significant changes in gerbera when the RWC dropped below 85% (Peñualas *et al.*, 1993). The NDWI is based on weak absorption by water at 1240 nm and high reflectance at 860 nm (Gao, 1996). The NDWI was tested with AVIRIS data at Jasper Ridge, California and the High Plains in northern Colorado. The value for the NDWI for senescent vegetation is generally negative, whereas in general the value for green vegetation is positive. Wet and dry soils had a range of -0.4 to 0.1 for the NDWI. My study produced a range of -0.28 – -0.96 which corresponds with that obtained by Gao (1996) for senescent vegetation. Gao (1996) experienced difficulty in extracting accurate NDWI values over semi-arid regions, as soil contributions to the NDWI are mostly negative. Green vegetation is mostly positive, and soil and vegetation in the same pixel therefore tended to cancel each other out. It is unclear from Gao's (1996) study how the mix of soil and senescent vegetation would have influenced the NDWI results in my study.

Riggs and Running (1991) argued that in tree species, changes in reflectance in response to water stress were too small to be detectable using remote sensing at the landscape scale. Values obtained for the NDII by Hardisky (1983) ranged from 0.6 –

0.9 for *Spartina alterniflora* Loisel. in a salt marsh with canopy moisture content varying from 450 – 1500 $g.m^{-2}$ respectively. Values obtained for the NDII in my study were all negative (-0.08 – -0.33). This may have been a result of the senesced vegetation in my study having very low water content, but this remains unclear at this point. Ong *et al.* (2008) found poor correlations between water potential and the WBI, NDWI and MSI. Hunt and Rock (1989) working with the Moisture Stress Index (MSI) were able to calculate the minimum change in RWC detectable with this index. The MSI (not used in my study) uses very similar wavelengths to the NDII and NDII5. Their results for seven species showed that the MSI is negatively related (r^2: 0.72 – 0.80) to the equivalent water thickness (EWT). However, the minimum detectable change in RWC is 52% (Hunt and Rock, 1989). This suggests that the MSI can only detect water stress when a plant is close to senescent. They argued that the MSI is detecting something related to coniferous forest damage, which the NDVI does not detect, but that this cannot be related to the MSI detecting plant water stress. Hunt and Rock (1989) concluded that the physiological and ecological basis for various vegetation indices is poorly understood.

4.3 **Relationship Between LFA Indices and VIs**

The LFA and VI indices have weak regressions which could not be used accurately for the purpose of predicting LFA indices from VIs. Neither transformations of the data nor the application of quadratic models improved the values obtained in these regressions. Of the VIs, the lignin index gives the strongest regression values with two of the LFA indices, stability and nutrient cycling. Lignin is the second most common biopolymer after cellulose in plants (Boudet, 1998, Himmelsbach and Barton, 1980). Gebruers *et al.* (2008) studied a number of varieties of winter and spring wheat. All varieties had klason lignin with levels varying between 1.40 and 3.25% of dry matter. As these are agricultural grasses, it is likely that natural grasses would have lower nitrogen, and therefore lignin content. Lorena *et al.*, (2005) examined nitrogen and lignin content in senesced leaves of three grasses: *Poa ligularis* Nees ex Steud., *Stipa tenuis* Phil. and *Stipa speciosa* Trin. and Rupr from Patagonian Monte in Argentina. They showed that the lignin content in senesced leaves of the three grasses was significantly lower than that of three species of local

senesced shrub leaves. The lignin content of these grasses ranged between a mean of 53.60 $\pm$ 2.44 and 70 $\pm$ 4.85 $g.kg^{-1}$.

In terms of the stability index, organic matter is important for stabilising the mineral fraction of soils (Oades, 1993). Lignin is highly resistant to decomposition processes (Melillo *et al.*, 1982), so one would expect an increase in organic matter, and therefore possibly lignin, as soil stability increased. Similarly, nutrient cycling is a function of plant growth and decomposition of plant material (Burke *et al.*, 1998), so lignin would also feature strongly in decomposition residues from plant materials (Melillo *et al.*, 1982). But without some empirical evidence of lignin in the environment, it is difficult to substantiate the conclusion that the relationship between the lignin index and stability or nutrient cycling is through a relationship between soil stability, or decomposition processes, and lignin content in the environment. Furthermore, Serrano *et al*. (2002) obtained non-significant results with the NDLI and winter senesced vegetation. Grossman *et al.* (1996) found inconsistent results using multiple regression and spectral bands known to be representative of nitrogen and lignin.

The infiltration index had the strongest, albeit very weak, regression coefficients with the NDVI. In the light of the earlier discussion on the integrity of the chlorophyll VI results, it is speculative to draw any conclusions on this relationship. Infiltration is positively related to plant cover (Balliette *et al.*, 1986). Plant cover is related to leaf area index (LAI), and a positive correlation exists between LAI and the NDVI (Baret and Guyot, 1991; Asner, 1998). Numata *et al.* (2003) measured NDVI during the dry season in Brazilian pastures formed after removal of the natural forest. Linear regression between NDVI measurements from three sites, with various soil geophysical parameters (P, K, Ca, ECEC and base saturation), had a large degree of variation between sites and geophysical parameters, with coefficients of determination ranging from 0.00 – 0.72 (Numata *et al.*, 2003).

4.4 **Partial Least Squares Regression Modelling**

In my study the best model for stability is a 13-component model, for infiltration a 17-component model, and a 15-component model for nutrient cycling. My study forms an independent test of the methods used by Ong *et al.* (2004, 2008) and the number of components compares favourably with their work. They found that 13-component, 13-component and 12-component models best described stability, infiltration and nutrient cycling indices respectively. Other researchers have found optimal models with fewer components. Coops *et al.* (2003), predicting leaf nitrogen in Eucalypts, found 2- and 3-component models best. A study of winter wheat found the best performing models ranged from a 2-component model for LAI, up to 6-component models for green biomass and leaf nitrogen concentration (Hansen and Schjoerring, 2003).

In my study, the best models had coefficients of determination with validation data of r^2 = 0.38, 0.32 and 0.54 for stability, infiltration and nutrient cycling respectively. However Ong *et al.* (2008) achieved r^2 = 0.69, 0.40 and 0.62 respectively at Goldsworthy iron ore mine, and r^2 = 0.88, 0.77 and 0.88 respectively at Huntly Bauxite mine. Hansen and Schjoerring (2003) achieved results very similar to my study with their weakest model when predicting chlorophyll concentration (r^2 = 0.30). Their models for five other biophysical/biochemical parameters achieved coefficients of determination between r^2 = 0.60 for chlorophyll density, and r^2 = 0.89 for green biomass. Coops *et al.* (2003) applied PLSR to both reflectance and absorption spectra and found slightly stronger predictions for canopy nitrogen with absorption values (r^2 = 0.68) compared to reflectance (r^2 = 0.64). Finally, Kooistra *et al.* (2004) examined the influence of various metal pollutants on the spectral reflectance of grasslands in a river floodplain of Belgium and achieved prediction coefficients of determination between r^2 = 0.50 and 0.73 when predicting soil metal concentrations.

The differences between Ong *et al.* (2008) and my results may be due to a number of factors. They amended their technique to take into account landscape organisation, which we were not able to derive due to the fixed layout of quadrats along transects (Ong *et al.* 2008). They furthermore derived different models for each mining environment. Kooistra *et al.* (2004) found that spectral properties and derived models

were site and species-dependant, as herbaceous patches showed large deviations from the relations established for grass. I combined data from four different vegetation types from two mining regions to derive models. This may have contributed to the lower prediction accuracy I obtained compared to other researchers discussed above. A final factor might be related to variation in the LFA data caused by the use of photographs, and consistency between LFA practitioners. Townsend *et al.* (2003) derived models that explained 97.9% of the variation in leaf nitrogen, and only 40% of the variation in the spectra. They argued that this might be the result of selecting only portions of the spectrum with a 15 nm range either side of already known nitrogen absorption centres. They improved this with AVIRIS data, where their model was able to account for 79% of the variation in nitrogen leaf content, and 72.4% of spectral variation (Townsend *et al.*, 2003). My models required very few components to explain the spectral data but many more components to explain the variation in the LFA data.

A number of researchers applied various pre-processing techniques to spectra prior to PLSR modelling, whereas, apart from mean centering the data, I derived models directly from reflectance data. Ong *et al.* (2008) applied a wavelet smoothing algorithm to remove spectral noise in the SWIR region. Townsend *et al.* (2003) used first derivative spectral data and Huang *et al.* (2004) pre-processed their reflectance data with either first or second derivative analysis or continuum removal analysis. The continuum removal pre-treatment produced better overall results than did derivative analysis (Huang *et al.*, 2004). Coops *et al.* (2003) prepared their spectra by using reflectance, as I did, or converting reflectance to absorption values. They also applied first derivatives to the absorbance of the spectra. They obtained slightly stronger predictions of canopy nitrogen with absorption values (r^2 = 0.68) compared to reflectance (r^2 = 0.64). The first derivative of the absorbance data produced the weakest coefficient of determination (r^2 = 0.54). Kooistra *et al.* (2003) tested the potential of a number of pre-processing. They used standard normal variate or multiplicative scatter correction to scale the spectral data to zero mean and a variance of one. The two scaling techniques differ in that standard normal variate uses the individual spectra, whereas multiplicative scatter correction uses the average for all spectra as the reference spectra (Kooistra *et al.*, 2003). They further tested multiplicative scatter correction with and without a wavelet selection and found using

both reduced the number of components and increased the prediction accuracy. In retrospect, it may have been better to scale both the LFA and spectral data as these two data sets differ considerably in the magnitude between their units. The LFA data uses percentage units whereas spectral data is a ratio value between zero and one with no units (Geladi and Kowalski, 1986).

Coops *et al.* (2003) found that the wavelengths selected by multiple linear regression had good agreement with PLSR regions with high loading values. The pattern of spectral absorption amongst the various components of my models reinforced a plant signal around the 600 to 750 nm region, and weakly around 450 nm. But the resolution applied by the PLSR modelling does not distinguish which of the plant pigment spectral signatures are contributing to this plant signal. Around 900- 960 nm, all four components of the models detected absorption centres which might correspond with a water absorption band at 970 nm (Peñualas *et al.*, 1995) and amino acids or proteins at 910 nm (Townsend *et al.*, 2003). Amino acids also have corresponding absorption bands at 1200 nm and components 1 and 2 recorded an absorption centre around this wavelength. In all four components absorption centres from 1720 to 1760 nm might correspond with the lignin based VI (NDLI) around 1754 nm (Serrano *et al.*, 2002). Possible amino acid-protein absorption bands may have influenced the strong absorption around 2100 nm and 2300 nm (Townsend *et al.*, 2003). At 2220 nm, a strong spike may be related to clay minerals (Awiti *et al*., 2008) in the soil profile. Investigating the absorption centres identified above from the PLSR loading values were beyond the scope of this study.

5. Conclusions

The aim of this study was to derive LFA indices to predict rangeland condition from ground-based HSRS data on two deep-level gold mining surface environments. To this end, the first objective was to derive PLSR models to predict the three LFA indices from full spectrum HSRS. The second objective was to test the potential of twenty-three spectral VIs to predict the three LFA indices of stability, infiltration and nutrient cycling. It was concluded that VIs are generally not suitable for predicting LFA indices with winter senesced vegetation. Whereas it was shown that PLSR has potential to accurately predict LFA indices under these conditions.

The dominant pattern for all three LFA indices was that high disturbance sites have low LFA values and low disturbance sites have high LFA values as predicted. Exceptions to this general pattern were non-rocky grasslands from Vaal River for all three indices and wet grasslands from Vaal River for infiltration and nutrient cycling. These exceptions may be an artefact of a small sample size from a single high disturbance plot in both vegetation types. Stability values indicated relatively high soil crusting. This corresponded with relatively low infiltration indices, suggesting that most sites shed rain water rather than have it infiltrate the soil profile. Wet grasslands had the highest mean values for all three indices. Between the other three vegetation types there was a reversal in the pattern for stability where non-rocky grassland was highest, compared to infiltration and nutrient cycling where woody shrub sites were highest. This was a result of high biomass and litter fall in woody shrub sites compared to the two types of dry grassland sites. Overall, both mine study sites exhibited stable soil processes with erosion and deposition at low levels although evidence suggests erosion may have been higher in the past. The high stability values together with the low infiltration and median nutrient cycling values imply that disturbance is currently impacting mainly on the vegetation component rather than the soil component *per se*. Furthermore these sites are not degrading as the soil is generally stable but an increase in impacts on the vegetation component may drive these sites into a degrading state. The characterisation of high and low disturbance sites seems to be accurate, as for all three indices, high disturbance sites tended to have low LFA values, and low disturbance sites high LFA values. But, within these

high and low disturbance sites, LFA values for quadrats were well distributed across the range for all three indices, illustrating the high heterogeneity within plots.

The range obtained for VIs in this study was towards the low side of ranges obtained in other studies. However, like other studies, there were differences in VIs between high and low disturbance, but these were site and vegetation dependent. It was shown that the chlorophyll VIs were detecting a very low chlorophyll signal and this undermined any interpretation of the values calculated for these indices. The predominant cause of this was the winter senesced state of the vegetation. This raised similar doubts for the other pigment related VIs as well as the plant-water based VIs. This suggests that seasonal timing and physiological response of plants to season is important in applying a VI, especially those VIs related to plant pigments. Furthermore, without some site-truthed data for cellulose or lignin to calibrate the VI values for the CAI or NDLI, drawing conclusions for these indices is speculative.

Simple linear regressions between the VIs and LFA indices produced very weak coefficients of determination. The lignin index (NDLI) had the strongest, but still weak regression coefficients, with both the stability index and the nutrient cycling index. This weak relationship is supported by the fact that organic matter is closely correlated with soil stability and nutrient cycling. Lignin, which is resistant to decomposition, is an important component of organic matter. The infiltration index was most closely correlated with the standard NDVI. This result is a little perplexing as the NDVI is a chlorophyll based index and the evidence strongly suggests that a chlorophyll signal is weak at best. Under the results of this study, the VIs would not be a suitable surrogate measure to predict LFA indices under the conditions of winter senesced vegetation. It would be interesting to repeat this analysis with summer data when plant pigments and moisture are more prevalent in the environment. However, this would occlude most of the soil signal, and as LFA is measuring biogeophysical parameters at the soil surface, green vegetation might result in equally poor regression parameters.

The strongest PLSR model for predicting stability was a 13-component model, while for infiltration it was a 17-component model, and for nutrient cycling a 15-component model. Of these three models, predictions for the nutrient cycling index with

validation data produced the highest coefficient of determination (r^2 = 54 %). Other studies suggested that these predicted values could be improved. Most of the unexplained variance in the models was related to the LFA data. The loading values for the models suggested a plant signal around the VIS-NIR region of the spectrum and some possible amino-acid signals. One of the amino-acid signals provides some support to the lignin VI, which had highest prediction statistics for the LFA indices of stability and nutrient cycling indices. There may also be a strong response in the PLSR models to clay minerals around 2220 nm. Therefore from the results of this study, it can be concluded that PLSR models have the potential to predict the LFA indices of stability, infiltration and nutrient cycling.

5.1 **The Way Forward**

As far as the PLSR modelling is concerned, the over-riding conclusion is the need for a using standard field observation and not photographs to reduce the high variability in the LFA data. The data set should be increased to compare PLSR models between vegetation types and a model derived from all vegetation types. A set of rules to identify and characterise an outlier measurement would be useful for determining what measurements to include or exclude from the modelling process. These need to take into account the geochemistry in these pollution affected sites and the presence of pollution derived mineral salts such as sulphates and chlorides. Mine tailings are rich in pyrite minerals, which oxidise to form AMD. AMD dissolves metals contained in the tailings and spreads as pollution plumes through ground water (Tutu *et al.*, 2008). Ground water, rich in metals, is drawn to the surface through capillary action. At the surface, evaporation leaves behind a gypsum salt which forms white crusts and may be high in metal sulphates (Naicker *et al.* 2003). These salts impact on soil and plant osmotic stress which indirectly impacts plant HSRS signals. Salts may also be directly detected through HSRS. Analysis of recent data suggests that PLSR was attempting to derive a single linear model, when the HS data contains at least two possibly unrelated environmental signals. One of these signals is related to senesced vegetation, and the other related to soil in which a clay spectral feature is prominent. It may therefore be important to add a distinguishing character to the spectral data to aid calibration of PLSR model in differentiating between these signals.

The VIs were confounded by the presence of winter-senesced vegetation and it is recommended that these be tested with summer (growing season) data. Some measurement of the environmental feature for which the individual VI is designed, would be useful to contextualise the calculated values. For instance measurements of chlorophyll or plant-water content would greatly aid interpretation of the VI results. A hyperspectral index for environmental degradation in mining environments would need to be able to separate green photosynthetic vegetation from soil, and more particularly senesced vegetation from soil. Separating soil from senesced vegetation has proven to be difficult because of the heterogenous nature of soil. The composition and surface roughness of soil may vary widely over short distances, while salt and mineral crusts, and cryptogamic crusts, all influence the spectral properties of soils. In conclusion, PLSR modelling showed potential in deriving LFA indices from full spectrum hyperspectral data obtained from winter senesced grasslands on the Highveld, whereas VIs would not be suitable for predicting LFA indices from similar data under the same conditions.

6. References

1. Acocks, J.P.H., 1988. Veld types of South Africa, edn 3. *Memoirs of the Botanical Survey of South Africa* No. 57. Botanical Research Institute, Pretoria.
2. Akcil A. and Koldas, S., 2006. Acid Mine Drainage (AMD): causes, treatment and case studies. *Journal of Cleaner Production 14*: 1139 – 1145.
3. Asner, G.P., 1998. Biophysical and biochemical sources of variability in canopy reflectance. *Remote Sensing of Environment 64*: 234 – 253.
4. Awiti, A.O., Walsh, M.G., Shepherd, K.D. and Kinyamario, J., 2008. Soil condition classification using infrared spectroscopy: a proposition for assessment of soil condition along a tropical forest-cropland chronosequence. *Geoderma 143*: 73 – 84.
5. Balliette, J.F., McDaniel, K.C. and Wood, M.K., 1986. Infiltration and sediment production following chemical control of sagebrush in New Mexico. *Journal of Range Management 39*: 160 – 165.
6. Barbour, M.G., Burk, J.H. and Pitts, W.D., 1987. *Terrestrial Plant Ecology, 2nd Ed.* The Benjamin/Cummings Publishing Company, Inc. California.
7. Baret F. and Guyot, G., 1991. Potentials and limits of vegetation indices for LAI and APAR assessment. *Remote Sensing of Environment 35*: 161 – 173.
8. Basnyat, P., Teeter, L.D., Lockaby, B.G. and Flynn, K.M., 2000. The use of remote sensing and GIS in watershed level analyses of non-point source pollution problems. *Forest Ecology and Management 128*: 65 – 73.
9. Bastin, G.N., Ludwig, J.A., Eager, R.W., Chewings, V.H. and Liedloff, A.C., 2002. Indicators of landscape function: comparing patchiness metrics using remotely-sensed data from rangelands. *Ecological Indicators 1*: 247 – 260.
10. Belnap, J. and Gillette, D.A., 1998. Vulnerability of desert biological soil crusts to wind erosion: the influences of crust development, soil texture, and disturbance. *Journal of Arid Environments 39*: 133 – 142.
11. Belnap, J., Welter, J.R.., Grimm, N.B., Barger, N. and Ludwig, J.A., 2005. Linkages between microbial and hydrologic processes in arid and semiarid watersheds. *Ecology 86*: 298 – 307.

12. Ben-Dor, E., Goldshleger, N., Braun, O., Kindel, B., Goetz, A.F.H., Bonfil, D., Margalit, N., Binaymini, Y., Karnieli, A. and Agassi, A., 2004. Monitoring infiltration rates in semi-arid soils using airborne hyperspectral technology. *International Journal of Remote Sensing 25*: 2607 – 2624.
13. Ben-Dor, E., Levin, N., Singer, A, Karnieli, A., Braun, O. and Kidron, G.J., 2006. Quantitative mapping of the soil rubification process on sand dunes using an airborne hyperspectral sensor. *Geoderma 131*: 1 – 21.
14. Biswal, B., 1995. Carotenoid catabolism during leaf senescence and its control by light. *Journal of Photochemistry and Photobiology (B) 30*: 3 – 13.
15. Boudet, A.M., 1998. A new view of lignification. *Trends in Plant Science 3*: 67 - 71
16. Boutton, T.W. and Tieszen L.L., 1983. Estimation of plant biomass by spectral reflectance in an East African grassland. *Journal of Range Management 36*: 213 – 216.
17. Burke, I.C., Lauenroth, W.K., Vinton, M.A., Hook, P.B., Kelly, R.H., Epstein, H.E., Aguiar, M.R., Robles, M.D., Aguilera, M.O., Murphy, K.L. and Gill, R.A., 1998. Plant-soil interactions in temperate grasslands. *Biogeochemistry 42*: 121 – 143.
18. Carter, G.A., 1993. Responses of leaf spectral reflectance to plant stress. *American Journal of Botany 80*: 239 – 243.
19. Casenave, A. and Valentin, C., 1992. A runoff capability classification system based on surface features criteria in semi-arid areas of West Africa. *Journal of Hydrology 130*: 231 – 249.
20. Coops, N.C., Smith, M.-L., Martin, M.E. and Ollinger, S.V., 2003. Prediction of Eucalypt foliage nitrogen content from satellite-derived hyperspectral data. *IEEE Transactions of Geoscience and Remote Sensing 41*: 1338 – 1346.
21. Curran, P.J., Dungan, J.L., Macler, B.A. and Plummer, S.E., 1991. The effect of a red leaf pigment on the relationship between red edge and chlorophyll concentration. *Remote Sensing of Environment 35*: 69 – 76.
22. Curran, P.J., Windham, W.R., and Gholz, H.L., 1995. Exploring the relationship between reflectance red edge and chlorophyll concentration in slash pine leaves. *Tree Physiology 15*: 203 – 206.

23. Datt, B., 1999. A new reflectance index for remote sensing of chlorophyll content in higher plants: tests using *Eucalyptus* leaves. *Journal of Plant Physiology 154*: 30 – 36.
24. Daughtry, C.S.T., 2001. Discriminating crop residues from soil by shortwave infrared reflectance. *Agronomy Journal 93*: 125 – 131.
25. Daughtry, C.S.T., Hunt Jr., E.R. and McMurtrey III, J.E., 2004. Assessing crop residue cover using shortwave infrared reflectance. *Remote Sensing of Environment 90*: 126 – 134.
26. Davidson and Csillag, F., 2001. The influence of vegetation index and spatial resolution on a two-date remote sensing-derived relation to C4 species coverage. *Remote Sensing of Environment 75*: 138 – 151.
27. Dutartre, Ph., Bartoli, F., Andreux, F., Portal, J.M., and Ange, A., 1993. Influence of content and nature of organic matter on the structure of some sandy soils from West Africa. *Geoderma 56*: 459 – 478.
28. Edgerton, D.L., Harris, J.A., Birch, P. and Bullock, P., 1995. Linear relationship between aggregate stability and microbial biomass in three restored soils. *Soil Biology and Biochemistry 27*: 1499 – 1501.
29. Eldridge, D.J. and Leys, J.F., 2003. Exploring some relationships between biological soil crusts, soil aggregation and wind erosion. *Journal of Arid Environments 53*: 457 – 466.
30. Evans, R.D. and Belnap, J., 1999. Long-term consequences of disturbance on nitrogen dynamics in an arid ecosystem. *Ecology 80*: 150 – 160.
31. Farrar, T.J., Nicholson, S.E. and Lare, A.R., 1994. The influence of soil type on the relationships between NDVI, rainfall, and soil moisture in semiarid Botswana. II. NDVI response to soil moisture. *Remote Sensing of Environment 50*: 121 – 133.
32. Farifteh, J., Van der Meer, F., Atzberger, C. and Carranza, E.J.M., 2007. Quantitative analysis of salt-affected soil reflectance spectra: A comparison of two adaptive methods (PLSR and ANN). *Remote Sensing of Environment 110*: 59 – 78.
33. Feingersh, T., Ben-Dor, E. and Portugali, J., 2007. Construction of synthetic spectral reflectance of remotely sensed imagery for planning purposes. *Environmental Modelling & Software 22*: 335 – 348.

34. Folke, C., Carpenter, S., Walker, B., Scheffer, M., Elmqvist, T., Gunderson, L. and Holling, C.S., 2004. Regime shifts, resilience, and biodiversity in ecosystem management. *Annual Review on Ecology, Evolution, & Systematics 35*: 557 – 581.
35. Fourty, Th., Baret, F., Jacquemoud, S., Schmuck, G. and Verdebout, J., 1996. Leaf optical properties with explicit description of its biochemical composition: direct and inverse problems. *Remote Sensing of Environment 56*: 104 – 117.
36. Frank, A.B. and Aase, J.K., 1994. Residue effects on radiometric reflectance measurements of northern Great Plains rangelands. *Remote Sensing of Environment 49*: 195 – 199.
37. Frank, I.E., and Friedman, J.H., 1993. A statistical view of some chemometrics regression tools. *Technometrics 35*: 109 – 135.
38. Friedel, M.H., Sparrow, A.D., Kinloch, J.E. and Tongway, D.J., 2003. Degradation and recovery processes in arid grazing lands of central Australia. Part 2: vegetation. *Journal of Arid Environments 55*: 327 – 348.
39. Galpin, J.S., 2007. *Statistical Research Design and Analysis*. University of the Witwatersrand, Johannesburg, South Africa.
40. Gamon, J.A., Peñuelas, J. and Field, C.B., 1992. A narrow-waveband spectral index that tracks diurnal changes in photosynthetic efficiency. *Remote Sensing of Environment 41*: 35 – 44.
41. Gamon, J.A., Serrano, L. and Surfus, J.S., 1997. The photochemical reflectance index: an optical indicator of photosynthetic radiation use efficiency across species, functional types, and nutrient levels. *Oecologia 112*: 492 – 501.
42. Gao, B., 1996. NDWI – A normalized difference water index for remote sensing of vegetation liquid water from space. *Remote Sensing of Environment 58*: 257 – 266.
43. Gebruers, K., Dornez, E., Boros, D., Frás, A., Dynkowska, W., Bedo, Z., Rakszegi, M., Delcour, J.A. Courtin, C.M., 2008. Variation in content of dietary fibre and components thereof in wheats in the HEALTHGRAIN diversity screen. *Journal of Agricultural and Food Chemistry 56*: 9740 – 9749.
44. Geerken, R. and Ilaiwi, M., 2004. Assessment of rangeland degradation and development of a strategy for rehabilitation. *Remote Sensing of Environment 90*: 490 – 504.

45. Geladi P. and Kowalski, B.R., 1986. Partial Least-Squares Regression: A tutorial. *Analytica Chimica Acta 185*: 1 – 17.
46. Gitelson, A.A. and Merzlyak, M.N., 1994. Spectral reflectance changes associated with autumn senescence of *Aesculus Hippocastanum* L. and *Acer Platanoides* L. leaves. Spectral features and relation to chlorophyll estimation. *Journal of Plant Physiology 143*: 286 – 292.
47. Gitelson, A.A., Kaufman, Y.J. and Merzlyak, M.N., 1996. Use of a green channel in remote sensing of global vegetation from EOS-MODIS. *Remote Sensing of Environment 58*: 289 – 298.
48. Gitelson, A.A., Merzlyak, M.N. and Chivkunova, O.B., 2001. Optical properties and non-destructive estimation of anthocyanin content in plant leaves. *Photochemistry and Photobiology 74*: 38 – 45.
49. Gitelson, A.A., Zur, Y., Chivkunova, O.B. and Merzlyak, M.N., 2002. Assessing carotenoid content in plant leaves with reflectance spectroscopy. *Photochemistry and Photobiology 75*: 272 – 281.
50. Goodin, D.G. and Henebry, G.M., 1997. A technique for monitoring ecological disturbance in tallgrass prairie using seasonal NDVI trajectories and a discriminant function mixture model. *Remote Sensing of Environment 61*: 270 – 278.
51. Grossman, Y.L., Ustin, S.L. Jacquemoud, S., Sanderson, E.W., Schmuck, G. and Verdebout, J., 1996. Critique of stepwise multiple linear regression fro the extraction of leaf biochemistry information from leaf reflectance data. *Remote Sensing of Environment 56*: 182 – 193.
52. Gunderson, L.H., 2000. Ecological reslience – in theory and application. *Annual Review of Ecology and Systematics 31*: 425 – 439.
53. Hansen, P.M. and Schjoerring J.K., 2003. Reflectance measurements of canopy biomass and nitrogen status in wheat crops using normalized difference vegetation indices and partial least squares regression. *Remote Sensing of Environment 86*: 542 – 553.
54. Hardisky, M.A., Klemas, V. and Smart, R.M., 1983. The influence of soil salinity, growth form, and leaf moisture on the spectral reflectance of *Spartina Alterniflora* canopies. *Photogrammetric Engineering and Remote Sensing 49*: 77 – 83.

55. Himmelsbach, D.S. and Barton II, F.E., 1980. Carbon-13 nuclear magnetic resonance of grass lignins. *Journal of Agricultural and Food Chemistry 28*: 1203 – 1208.
56. Holling, C.S., 1973. Resilience and stability of ecological systems. *Annual Review of Ecology and Systematics 4*: 1 – 23.
57. Holm, A.M., Bennett, L.T., Loneragan, W.A. and Adams, M.A., 2002. Relationships between empirical and nominal indices of landscape function in the arid shrubland of Western Australia. *Journal of Arid Environments 50*: 1 – 21.
58. Holm, A.M., Cridland, S.W. and Roderick, M.L., 2003. The use of time-integrated NOAA NDVI data and rainfall to assess landscape degradation in the arid shrubland of Western Australia. *Remote Sensing of Environment 85*: 145 – 158.
59. Huang, Z., Turner, B.J., Dury, S.J., Wallis, I.R. and Foley, W.J., 2004. Estimating foliage nitrogen concentration from HYMAP data using continuum removal analysis. *Remote Sensing of Environment 93*: 18 – 29.
60. Huete, A.R., 1988. A soil-adjusted vegetation index (SAVI). *Remote Sensing of Environment 25*: 295 – 309.
61. Huete, A.R. and Escadafal, R., 1991. Assessment of biophysical soil properties through spectral decomposition techniques. *Remote Sensing of Environment 35*: 149 – 159.
62. Huete, A.R. and Jackson, R.D., 1987. Suitability of spectral indices for evaluating vegetation characteristics on arid rangelands. *Remote Sensing of Environment 23*: 213 – 232.
63. Huete, A., Justice, C. and Liu, H., 1994. Development of vegetation and soil indices for MODIS-EOS. *Remote Sensing of Environment 49*: 224 – 234.
64. Hunt, R.E. and Rock, B.N., 1989. Detection of changes in leaf water content using near- and middle-infrared reflectances. *Remote Sensing of Environment 30*: 43 – 54.
65. Jackson, R.D. and Huete, A.R., 1991. Interpreting vegetation indices. *Preventive Veterinary Medicine 11*: 185 – 200.

66. Jackson, T.J., Chen, D., Cosh, M., Li, F., Anderson, M., Walthall, C., Doriaswamy, P. and Hunt, R.E., 2004. Vegetation water mapping using Landsat data derived normalized difference water index for corn and soybeans. *Remote Sensing of Environment 92*: 475 – 482.
67. Jordaan, F.P., Biel, L.C. and du Plessis, P.I.M., 1997. A comparison of five range condition assessment techniques used in semi-arid western grassland biome of southern Africa. *Journal of Arid Environments 35*: 665 – 671.
68. Jordan, F.C., 1969. Derivation of leaf-area index from quality of light on the forest floor. *Ecology 50*: 663 – 666.
69. Kalacska, M., Bohlman, S., Sanchez-Azofeifa, G.A., Castro-Esau, K. and Caelli, T., 2007. Hyperspectral discrimination of tropical lianas and trees: comparative data reduction approaches at the leaf and canopy levels. *Remote Sensing of Environment 109*: 406 – 415.
70. Kogan, F., Stark, R., Gitelson, A., Jargalsaikhan, C., Dugrajav, C. and Tsooj, S., 2004. Derivation of pasture biomass in Mongolia from AVHRR-based vegetation health indices. *International Journal of Remote Sensing 25*: 2889 – 2896.
71. Kooistra, L., Leuven, R.S.E.W, Wehrens, R., Nienhuis, P.H. and Buydens, L.M.C., 2003. A comparison of methods to relate grass reflectance to soil metal contamination. *International Journal of Remote Sensing 24*: 4995 – 5010.
72. Kooistra, L., Salas, E.A.L., Clevers, J.G.P.W., Wehrens, R., Leuven, R.S.E.W., Neinhuis, P.H. and Buydens, L.M.C., 2004. Exploring field vegetation reflectance as an indicator of soil contamination in river floodplains. *Environmental Pollution 127*: 281 – 290.
73. Lauenroth, W.K. and Sala, O.E., 1992. Long-term forage production of North American shortgrass steppe. *Ecological Applications 2*: 397 – 403.
74. Lorena, C.A., Noe, V.D., Victoria, C.M., Beatriz, B.M., Leticia, S.C. and Julia, M.M., 2005. Soil nitrogen in relation to quality and decomposability of plant litter in the Patagonian Monte, Argentina. *Plant Ecology 181*: 139 – 151.
75. Ludwig, J.A. and Tongway, D.J., 1995. Spatial organisation of landscape and its function in semi-arid woodlands, Australia. *Landscape Ecology 10*: 51 – 63.

76. Ludwig, J.A., Tongway, D.J. and Marsden, S.G., 1999. Stripes, strands or stipples: Modelling the influence of three landscape banding patterns on resource capture and productivity in semi-arid woodlands, Australia. *Catena 37*: 257 – 273.

77. Ludwig, J.A., Tongway, D.J., Bastin, G.N. and James, C.D., 2004. Monitoring ecological indicators of rangeland functional integrity and their relation to biodiversity at local to regional scales. *Austral Ecology 29*: 108 – 120.

78. Ludwig, J.A., Wilcox, P.B., Breshears, D.D., Tongway, D.J. and Imeson, A.C. 2005. Vegetation patches and runoff-erosion as interacting ecohydrological processes in semiarid landscapes. *Austral Ecology 86*: 288 – 297.

79. Martens, H., 2001. Reliable and relevant modelling of real world data: a personal account of the development of PLS Regression. *Chemometrics and Intelligent Laboratory Systems 56*: 85 – 95.

80. Martens, H. and Næs T., 1989. *Multivariate Calibration*. John Wiley & Sons, Chichester.

81. McIntyre, S. and Tongway, D.J., 2005. Grassland structure in native pastures: links to soil surface condition. *Ecological Management & Restoration 6*: 43 – 50.

82. Melillo, J.M.; Aber, J.D. and Muratore, J.F., 1982. Nitrogen and lignin control of hardwood leaf litter decomposition dynamics. *Ecology 63*: 621 – 626.

83. Merzlyak, M.N., Gitelson, A.A., Chivkunova, O.B. and Rakitin, V.Y., 1999. Non-destructive optical detection of pigment changes during leaf senescence and fruit ripening. *Physiologia Plantarum 106*: 135 – 141.

84. Mevik, B.-H. And Cederkvist, H.R., 2004. Mean square error of prediction (MSEP) estimates for principal components regression (PCR) and partial least squares regression (PLSR). *Journal of Chemometrics 18*: 422 – 429.

85. Mevik, B.-H. and Wehrens, R., 2007. The pls package: principal component and partial least squares regression in R. *Journal of Statistical Software 18*: 1 – 24.
http://mevik.net/work/software/pls.html

86. Mineral and Petroleum Resources Development Act No 28. 2002. Government Gazette. Republic of South Africa. Vol. 448. No 23922
http://www.info.gov.za/gazette/acts/2002/a28-02.pdf

87. Moss A.J. and Walker P.H., 1978. Particle transport by continental water flows in relation to erosion, deposition, soils, and human activities. *Sedimentary Geology 20*: 81 – 139.

88. Mücher, H.J., Chartres, C.J., Tongway, D.J. and Greene, R.S.B., 1998. Micromorphology and significance of the surface crusts of soils in rangelands near Cobar, Australia. *Geoderma 42*: 227 – 244.

89. Mucina, L. and Rutherford, M.C. (Eds), 2006. The vegetation of South Africa, Lesotho and Swaziland. *Strelitzia 19*. South African National Biodiversity Institute, Pretoria.

90. Naicker, K., Cukrowska, E. and McCarthy, T.S., 2003. Acid mine drainage arising from gold mining activity in Johannesburg, South Africa and environs. *Environmental Pollution 122*: 29 – 40.

91. Nicholson, S.E. and Farrar, T.J., 1994. The influence of soil type on the relationships between NDVI, rainfall, and soil moisture in semiarid Botswana. I. NDVI response to rainfall. *Remote Sensing of Environment 50*: 107 – 120.

92. Noy-Meir, I., 1973. Desert ecosystems: Environment and producers. *Annual Review of Ecology and Systematics 4*: 25 – 51.

93. Numata, I., Roberts, D.A., Chadwick, O.A., Schimel, J., Sampaio, F.R., Leonidas, F.C. and Soares, J.V., 2007. Characterization of pasture biophysical properties and the impact of grazing intensity using remotely sensed data. *Remote Sensing of Environment 109*: 314 – 327.

94. Numata, I., Soares, J.V., Roberts, D.A., Leonidas, F.C., Chadwick, O.A. and Batista, G.T., 2003. Relationships among soil fertility dynamics and remotely sensed measures across pasture chronosequences in Rondônia, Brazil. *Remote Sensing of Environment 87*: 446 – 455.

95. Oades, J.M., 1993. The role of biology in the formation, stabilization and degradation of soil structure. *Geoderma 56*: 377 – 400.

96. O'Connor, T.G. and Bredenkamp, G.J., 1997. Grassland. In R.M. Cowling, D.M. Richardson and S.M. Pierce, *Vegetation of southern Africa*: 215 – 257. Cambridge University Press.

97. Ong, C., Lau, I., Hewson, R., Tongway, D. and Eisele, A. 2008. MERIWA Project M385: The development of a hyperspectral environmental measurement tool for monitoring mining related infrastructure and rehabilitation. CSIRO.

98. Ong, C., Tongway, D., Caccetta, M., and Hindley, N. 2004. *Phase 1: Deriving Ecosystem Function Analysis Indices from Airborne Hyperspectral Data.* Exploration and Mining Report No: P2004/388, CSIRO. Australia.

99. Parsons, A.J., Wainwright, J., Schlesinger, W.H. and Abrahams, A.D., 2003. The role of overland flow in sediment and nitrogen budgets of mesquite dunefields, southern New Mexico. *Journal of Arid Environments 53*: 61 – 71.

100. Pickup, G., Bastin, G.N. and Chewings, V.H., 1998. Identifying trends in land degradation in non-equilibrium rangelands. *Journal of Applied Ecology 35*: 365 – 377.

101. Peñuelas, J., Baret, F. and Filella, I., 1995. Semi-empirical indices to access carotenoids/chlorophyll-a ratio from leaf spectral reflectance. *Photosynthetica 31*: 221 – 230.

102. Peñuelas, J., Filella, I., Biel, C., Serrano, L. and Savé, R., 1993. The reflectance at the 950 – 970 region as an indicator of plant water status. *International Journal of Remote Sensing 14*: 1887 – 1905.

103. Price, J.C., 1998. An approach for analysis of reflectance. *Remote Sensing of Environment 64*: 316 – 330.

104. Price, J.C., 1994. How unique are spectral signatures. *Remote Sensing of Environment 49*: 181 – 186.

105. R Development Core Team (2007). R: A language and environment for statistical computing. R Foundation for Statistical Computing, Vienna, Austria. ISBN 3-900051-07-0, URL http://www.R-project.org.

106. Rees, W.G., 2001. *Physical Principles of Remote Sensing, 2nd Ed.* Cambridge University Press, United Kingdom.

107. Revivo, G. and Zur, Y., 2005. *Hyperspectral imaging aerial imaging demo: Vaal River region*. Interpretation report for CSIR, South Africa.

108. Rezaei, S.A., Arzani, H. and Tongway, D., 2006. Assessing rangeland capability in Iran using landscape function indices based on soil surface attributes. *Journal of Arid Environments 65*: 460 – 473.

109. Riggs, G.A. and Running S.W., 1991. Detection of canopy water stress in conifers using airborne imaging spectroscopy. *Remote Sensing of Environment 35*: 51 – 68.

110. Ringrose, S. and Matheson, W., 1987. Spectral assessment of indicators of range degradation in the Botswana Hardveld environment. *Remote Sensing of Environment 23*: 379 – 396.
111. Roberts, D.A., Gardner, M., Church, R. Ustin, S., Scheer, G., and Green, R.O., 1998. Mapping chaparral in the Santa Monica mountains using multiple endmember spectral mixture models. *Remote Sensing of Environment 65*: 267 – 279.
112. Roberts, D.A., Smith, O.A. and Adams, J.B., 1993. Green vegetation, nonphotosynthetic vegetation, and soils in AVIRIS data. *Remote Sensing of Environment 44*: 255 – 269.
113. Rundquist, D., Perk, R., Leavitt, B., Kayden, G. and Gitelson, A. 2004. Collecting spectral data over cropland vegetation using machine-positioning versus hand-positioning of the sensor. *Computers and Electronics in Agriculture 43*: 173 – 178.
114. Sanger, J.E., 1971. Quantitative investigations of leaf pigments from the inception in buds through autumn coloration to decomposition in falling leaves. *Ecology 52*: 1075 – 1089.
115. Schmidtlein, S. and Sassin, J., 2004. Mapping of continuous floristic gradients in grasslands using hyperspectral imagery. *Remote Sensing of Environment 92*: 126 – 138.
116. Schulze, R.E., 1997. Climate. In R.M. Cowling, D.M. Richardson and S.M. Pierce, *Vegetation of southern Africa*: 21 – 42. Cambridge University Press.
117. Serrano, L., Peñuelas, J. and Ustin, S.L., 2002. Remote sensing of nitrogen and lignin in Mediterranean vegetation from AVIRIS data: Decomposing biochemical from structural signals. *Remote Sensing of Environment 81*: 355 – 364.
118. Sharma, K.D., 1998. The hydrological indicators of desertification. *Journal of Arid Environments 39*: 121 – 132.
119. Sims, D.A. and Gamon, J.A., 2002. Relationship between leaf pigment content and spectral reflectance across a wide range of species, leaf structures and developmental stages. *Remote Sensing of Environment 81*: 337 – 354.
120. Snyman, H.A. and du Preez C.C., 2005. Rangeland degradation in a semi-arid South Africa – II: influence on soil quality. *Journal of Arid Environments 60*: 483 – 507.

121. Sparrow, A.D., Friedel, M.H. and Tongway, D.J., 2003. Degradation and recovery processes in arid grazing lands of central Australia. Part 3: implications at landscape scale. *Journal of Arid Environments 55*: 349 – 360.
122. Stark, R., 2001. *Remote sensing techniques for monitoring vegetation condition*. PhD Thesis. Ben Gurion University, Israel.
123. Stevens, A., van Wesemael, B., Bartholomeus, H., Rosillon, D., Tychon, B. and Ben-Dor, E., 2008. Laboratory, field and airborne spectroscopy for monitoring organic carbon content in agricultural soils. *Geoderma 144*: 395 – 404.
124. Sutton, M.W. and Weiersbye, I.M., 2007. South African legislation pertinent to gold mine closure and residual risk. In (Eds) A. Fourie, M. Tibbett and J. Wiertz. *Mine Closure 2007*. pp. 89 – 103.
125. Sutton, M.W., Weiersbye, I.M., Galpin, J.S. and Heller, D., 2006. A GIS-based history of gold mine residue deposits and risk assessment of post-mining land-uses on the Witwatersrand Basin, South Africa. In (Eds) Fourie, A. and Tibbett, M., *Mine Closure 2006*. Australian Centre for Geomechanics, Perth Australia.
126. Tanser, F.C. and Palmer, A.R., 1999. The application of a remotely-sensed diversity index to monitor degradation patterns in a semi-arid, heterogenous, South African landscape. *Journal of Arid Environments 43*: 477 – 484.
127. Ting, I.R., 1982. *Plant Physiology*. Addison-Wesley Publishing Company, Philippines.
128. Tongway, D.J., 2004. Landscape Function Analysis: The Rapid Assessment of Soil Health; Part 1: Introduction to the Field Procedure. Presentation. CSIRO Sustainable Ecosystems.
129. Tongway, D.J. and Hindley N.L., 2004. *Landscape Function Analysis: procedures for monitoring and assessing landscapes*. CSIRO, Australia.
130. Tongway, D.J. and Ludwig, J.A., 2007. Landscape function as a target for restoring natural capital in semiarid Australia, pp 76 – 84 *in* Aronson, J. Milton S.J. and Blignaut, J.N., editors. *Restoring Natural Capital: Science, Business and Practice*. Society for Ecological Restoration International. Washington: Island Press, Tuscon, Arizona.
131. Tongway, D.J., Sparrow, A.D. and Friedel, M.H., 2003. Degradation and recovery processes in arid grazing lands of central Australia. Part 1: soil and land resources. *Journal of Arid Environments 55*: 301 – 326.

132. Townsend, P.A., Foster, J.R., Chastain, R.A. Jr and Currie, W.S., 2003. Application of imaging spectroscopy to mapping canopy nitrogen in the forests of the Central Appalachian Mountains using Hyperion and AVIRIS. *IEEE Transactions on Geoscience and Remote Sensing 41*: 1347 – 1354.
133. Tucker, C.J., 1978. Post senescent grass canopy remote sensing. *Remote Sensing of Environment 7*: 203 – 210.
134. Tucker, C.J., 1979. Red and Photographic Infrared Linear Combinations for monitoring Vegetation. *Remote Sensing of Environment 8*: 127 – 150.
135. Tucker, C.J., Holben, B.N., Elgin, J.H. and McMurtrey, J.E. 1981. Remote sensing of total dry-matter accumulation in winter wheat. *Remote Sensing of Environment 11*: 171 – 189.
136. Tutu, H., McCarthy, T.S., and Cukrowska, E., 2008. The chemical characteristics of acid mine drainage with particular reference to sources, distribution and remediation: the Witwatersrand basin, South Africa as a case study. *Applied Geochemistry 23*: 3666 – 3684.
137. Valentin, C. and Bresson L.-M., 1992. Morphology, genesis and classification of surface crusts in loamy and sandy soils. *Geoderma 55*: 225 – 245.
138. van Gestel, M., Ladd, J.N. and Amato, M., 1991. Carbon and Nitrogen mineralization from two soils of contrasting texture and microaggregate stability: influence of sequential fumigation, drying and storage. *Soil Biology and Biochemistry 23*: 313 – 322.
139. van Leeuwen, W.J.D. and Huete, A.R. 1996. Effects of standing litter on the biophysical interpretation of plant canopies with spectral indices. *Remote Sensing of Environment 55*: 123 – 138.
140. Vogelmann, J.E., Rock, B.N. and Moss, D.M., 1993. Red Edge Spectral Measurements from sugar maple leaves. *International Journal of Remote Sensing 14*: 1563 – 1575.
141. Weiersbye, I.M. and Witkowski, E.T.F., 2003. Acid rock drainage (ARD) from gold tailings dams on the Witwatersrand Basin impacts on tree seed fate, viability, inorganic content and seedling morphology. In: Armstrong, D., de Villiers, A.B., Kleinmann, R.L.P., McCarthy, T.S. & Norton, P.J., (Eds). *Mine Water and the Environment, Proceedings of the 8th International Congress on Mine Water & the Environment*. Johannesburg, South Africa, pp. 311-328.

142. Weiersbye, I.M. and Witkowski, E.T.F., 2007. Impacts of acid mine drainage on the regeneration potential of highveld phraetophytes. In Bester, J.J., Seydack, A.H.W., Vorster, T., Van der Merwe, I.J. and Dzivhani, S. (Eds). *Multiple Use Management of Natural Forests and Woodlands: Policy Refinements and Scientific Progress IV. Department of Water Affairs and Forestry of South Africa.* www.dwaf.gov.za/forestry, pp 224 – 237.

143. Weiersbye, I.M., Margalit, N; Feingersh, T., Revivo, G., Stark, R., Zur, Y., Heller, D., Braun, O. and Cukrowska, E.M., 2006a. Use of airborne hyperspectral remote sensing (HSRS) to focus remediation and monitor vegetation processes on gold mining landscapes in South Africa. In (Eds) Fourie, A. and Tibbett, M., *Mine Closure 2006*. Australian Centre for Geomechanics, Perth Australia.

144. Weiersbye, I.M., Witkowski, E.T.F. and Reichardt, M., 2006b. Floristic composition of gold and uranium tailings dams, and adjacent polluted areas, on South Africa's deep-level mines. *Bothalia 36*: 101 – 127.

145. Wehrens, R. and Mevik, B-H., 2007. *pls: Partial Least Squares Regression (PLSR) and Principal Component Regression (PCR)*. R package version 2.1-0. http://mevik.net/work/software/pls.html

146. Weltz, M.A., Kidwell, M.R. and Fox, H.D., 1998. Influence of abiotic and biotic factors in measuring and modelling soil erosion on rabgelands: state of knowledge. *Journal of Range Management 51*: 482 – 495.

147. Wessels, K.J., Prince, S.D., Frost, P.E. and van Zyl, D., 2004. Assessing the effects of human-induced land degradation in the former homelands of northern South Africa with a 1 km AVHRR NDVI time-series. *Remote Sensing of Environment 91*: 47 – 67.

148. Wilson, M.D., Ustin, S.L. and Rocke, D.M., 2004. Classification of contamination in salt marsh plants using hyperspectral reflectance. *IEEE Transactions on Geoscience and Remote Sensing 42*: 1088 – 1095.

149. Witkowski, E.T.F. and Weiersbye, I.M., 1998. *Establishment of plants on gold slimes dams: characterization of the slimes and adjacent soils.* Plant Ecology & Conservation Series No. 6, University of the Witwatersrand report to Anglo American / Anglogold. 111 pages.

150. Wold, S., Sjöström, M. and Eriksson, L., 2001. PLS-regression: a basic tool of chemometrics. *Chemometrics and Intelligent Laboratory Systems 58*: 109 – 130.
151. Yamano, H., Chen, J. and Tamura, M., 2003. Hyperspectral identification of grassland vegetation in Xilinhot, Inner Mongolia, China. *International Journal of Remote Sensing 24*: 3171 – 3178.
152. Yoder, B.J. and Waring, R.H., 1994. The normalized difference vegetation index of small Douglas-fir canopies with varying chlorophyll concentrations. *Remote Sensing of Environment 49*: 81 – 91.
153. Zhang, G., Liu, B., Lui, G., He, X. and Nearing, M.A., 2003. Detachment rates of undisturbed soil by shallow flow. *Soil Science Society of America Journal 67*: 713 – 719.

Appendix 1

Distributions for the Three LFA Indices: Stability, Infiltration and Nutrient Cycling.

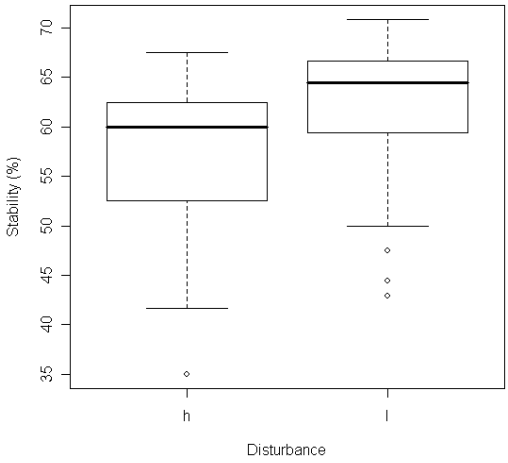

(a) Disturbance

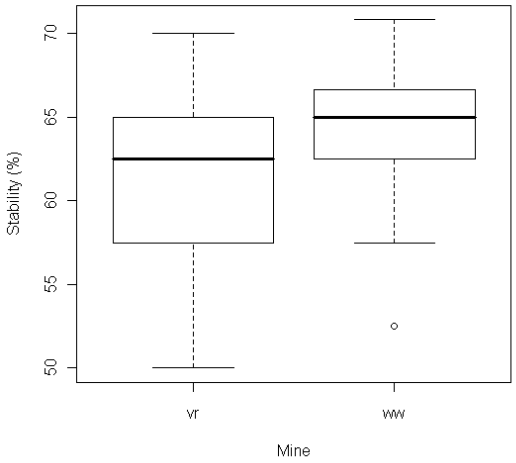

(b) Mine

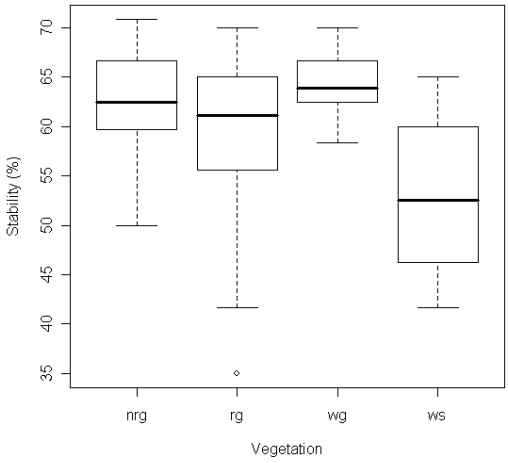

(c) Vegetation type

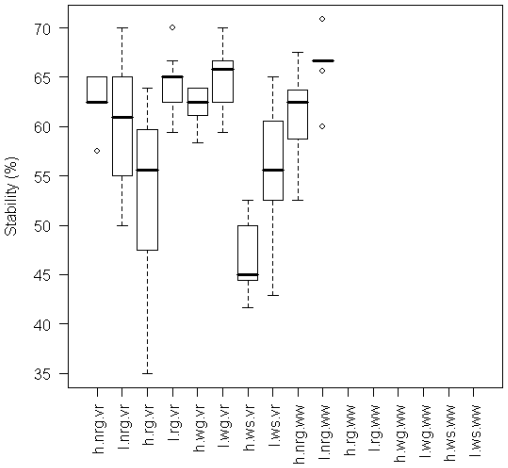

(d) Disturbance, vegetation type and mine

Four boxplots showing the distribution of stability values for different quadrat types. (a) Stability for the two disturbance levels. (b) Stability for non-rocky grasslands in the two mining environments. (c) Stability for different vegetation types. (d) Stability for disturbance, vegetation and mines. X-axis labels are h = high and l = low disturbance, nrg = non-rocky grassland, rg = rocky grassland, wg = wet grassland, ws = woody shrub, vr = Vaal River, ww = West Wits. There were no quadrats for rg, wg or ws vegetation types at West Wits.

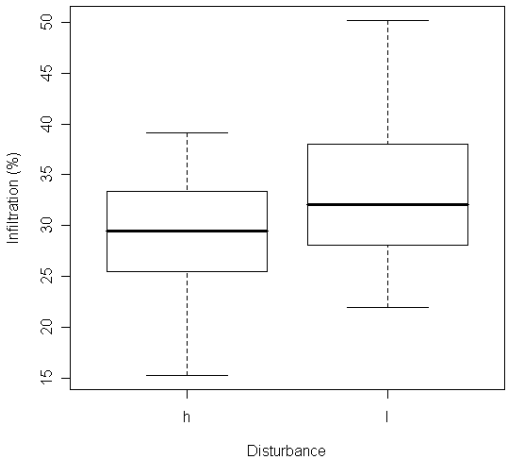

(a) Disturbance

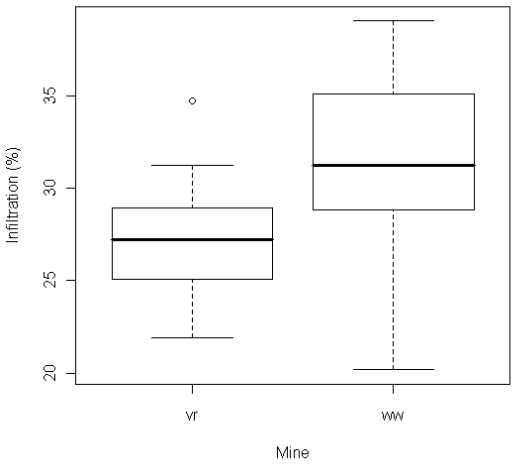

(b) Mine

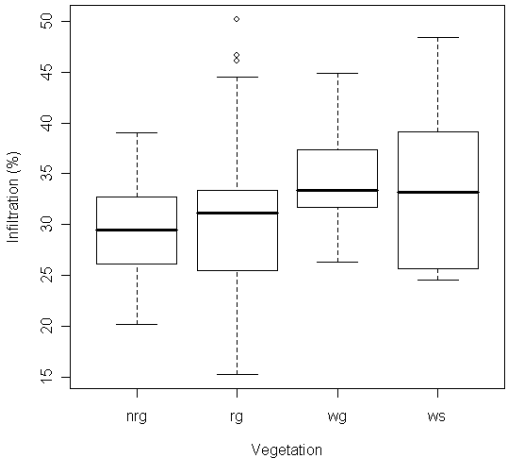

(c) Vegetation type

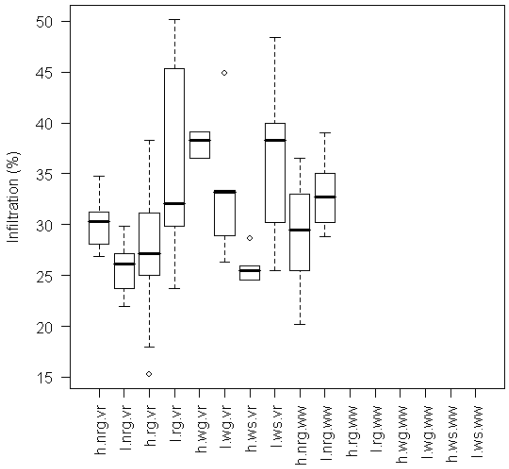

(d) Disturbance, vegetation type and mine

Four boxplots showing the distribution of infiltration for different quadrat types. (a) Infiltration values for the two disturbance levels. (b) Infiltration values for non-rocky grasslands in the two mining environments. (c) Infiltration for different vegetation types. (d) Infiltration values for disturbance, vegetation and mine levels. X-axis labels are h = high and l = low disturbance, nrg = non-rocky grassland, rg = rocky grassland, wg = wet grassland, ws = woody shrub, vr = Vaal River, ww = West Wits. There were no quadrats for rg, wg or ws vegetation types at West Wits.

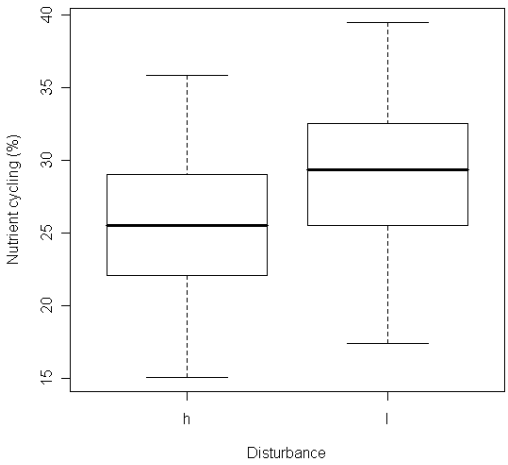

(a) Disturbance

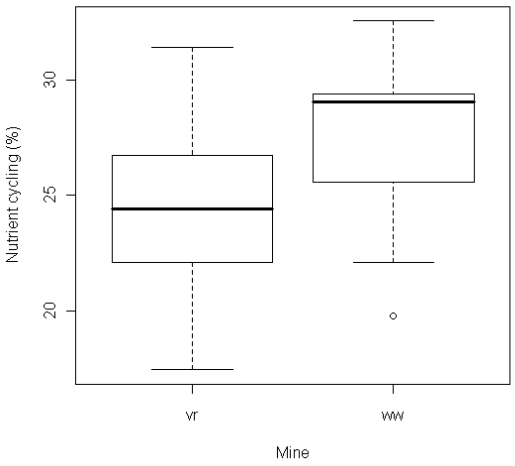

(b) Mine

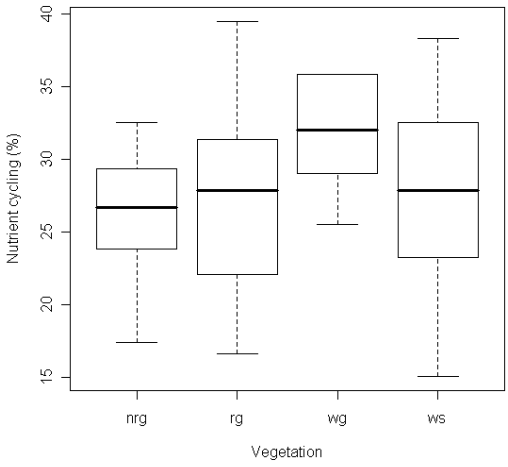

(c) Vegetation type

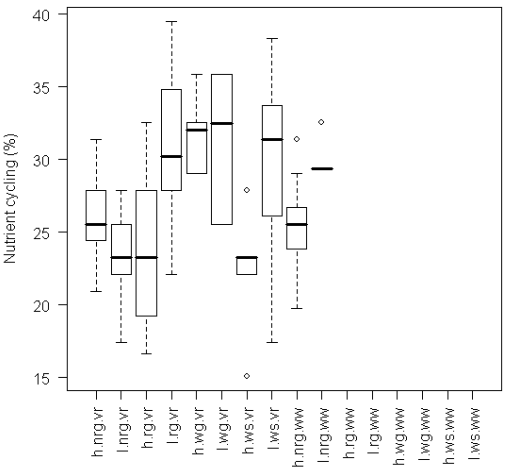

(d) Disturbance, vegetation type and mine

Four boxplots showing the distribution of nutrient cycling indices different quadrat types. (a) Nutrient cycling for the two disturbance levels. (b) Nutrient cycling for non-rocky grasslands in the two mining environments. (c) Nutrient cycling for different vegetation types. (d) Nutrient cycling for disturbance, vegetation and mine levels. X-axis labels are h = high and l = low disturbance, nrg = non-rocky grassland, rg = rocky grassland, wg = wet grassland, ws = woody shrub, vr = Vaal River, ww = West Wits. There were no quadrats for rg, wg or ws vegetation types at West Wits.

Appendix 2

Graphs of VI distributions for disturbance (h = high and l = low disturbance), vegetation type (nrg = non-rocky grassland, rg = rocky grassland, wg = wet grassland and ws = woody shrub) and mine (vr = Vaal River and ww = West Wits)

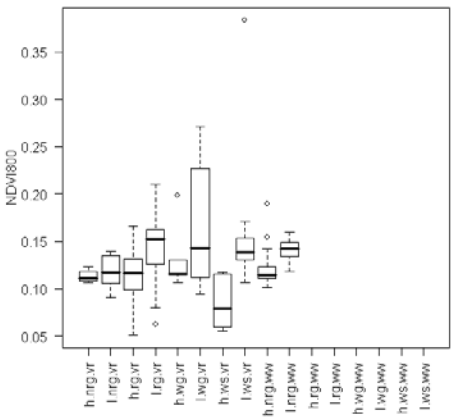

NDVI800: Chlorophyll

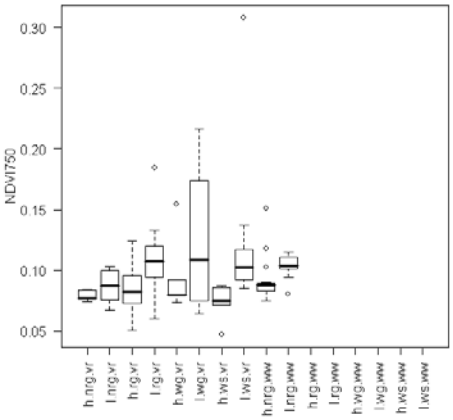

NDVI750: Chlorophyll

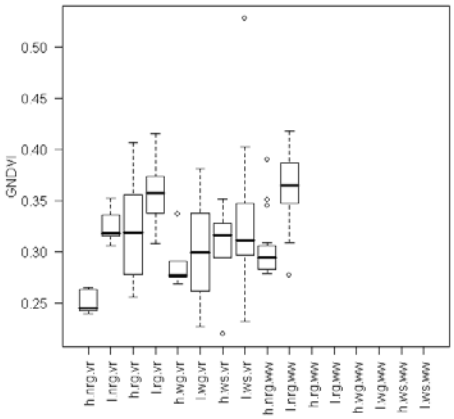

GNDVI: Chlorophyll - green absorption Centre

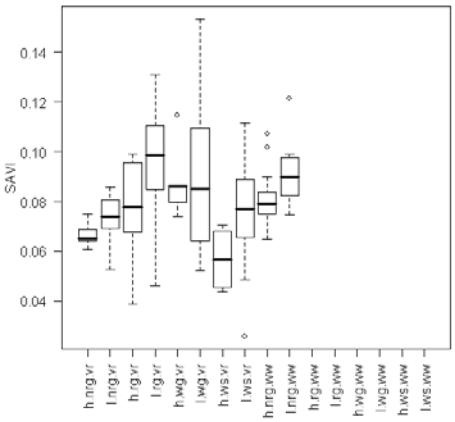

SAVI: Chlorophyll – soil adjusted

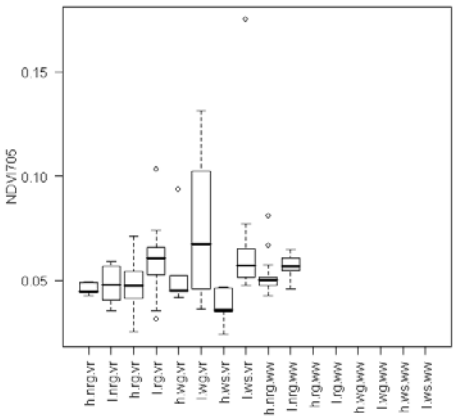

NDVI705: Chlorophyll

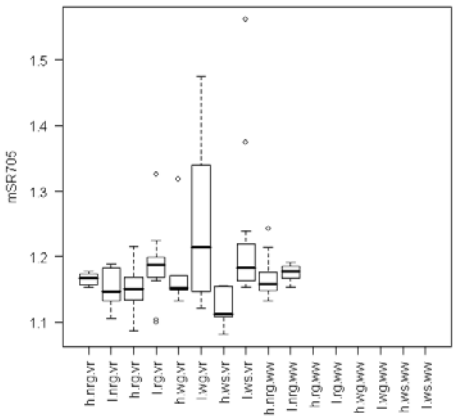

mSR705: Chlorophyll

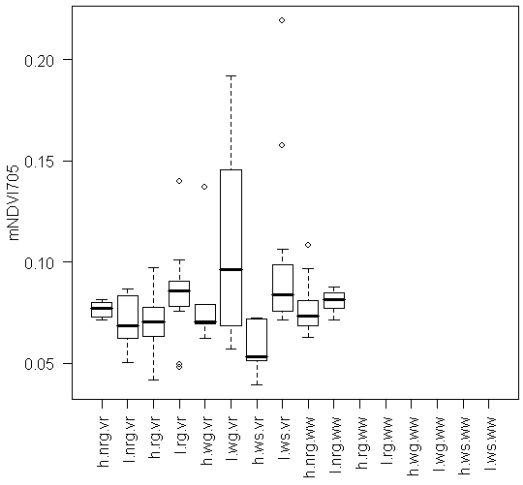

mNDVI800: Chlorophyll

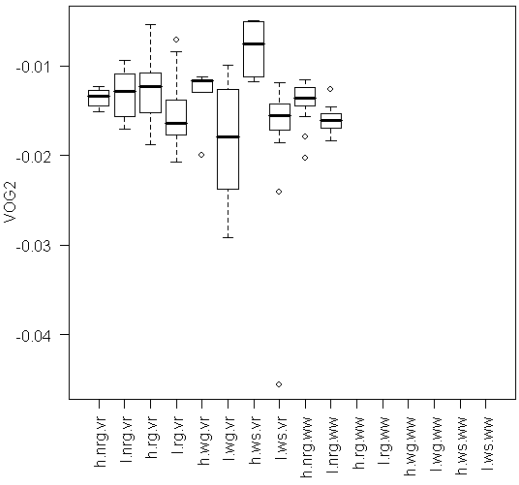

VOG2: Chlorophyll

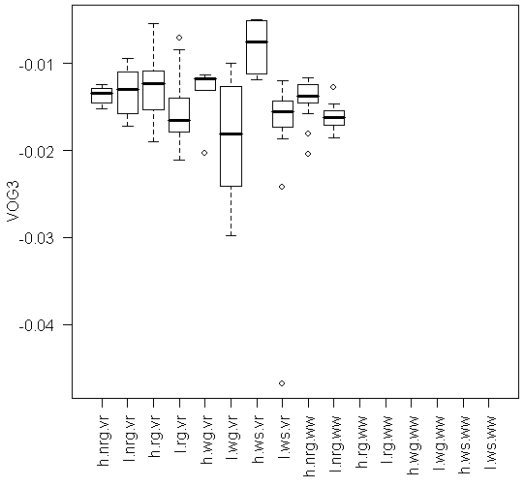

VOG3: Chlorophyll

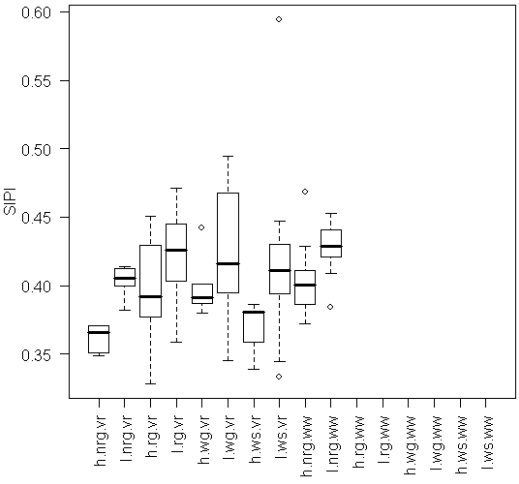

SIPI: Chlorophyll and carotenoids

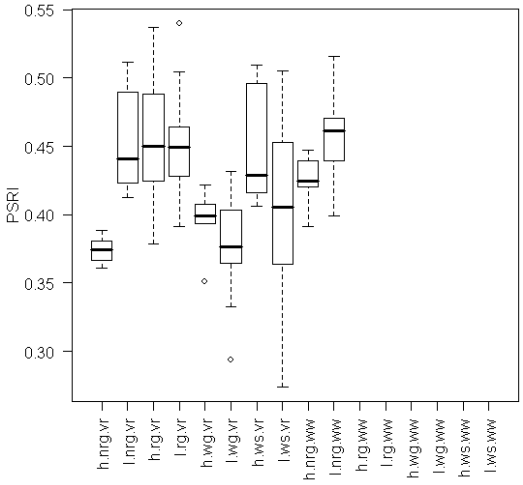

PSRI: Chlorophyll and carotenoids

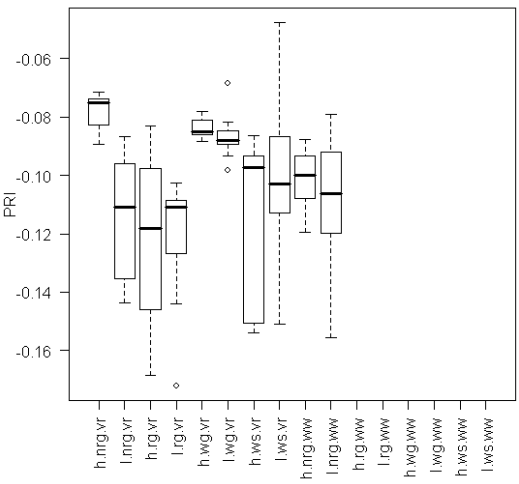

PRI: Carotenoids

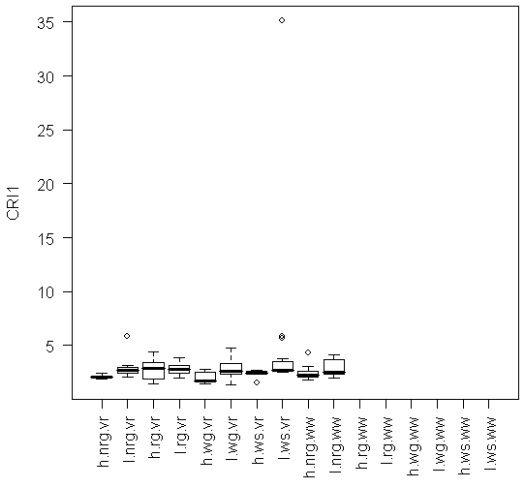

CRI1: Carotenoids

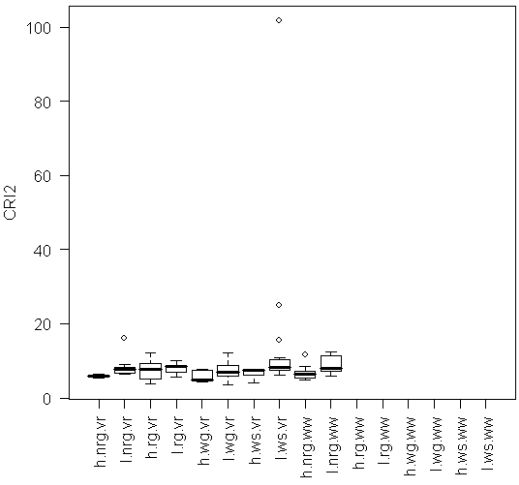

CRI2: Carotenoids

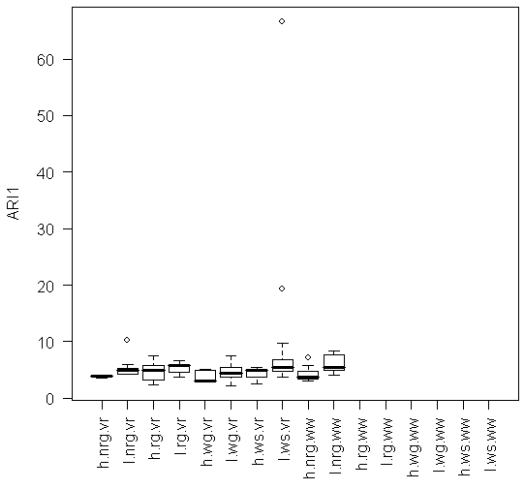

ARI1: Anthocyanins

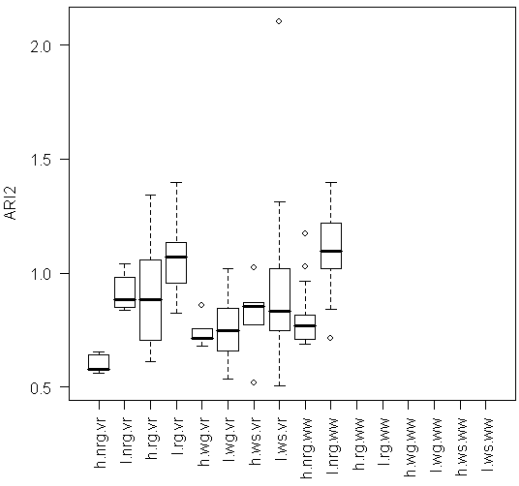

ARI2: Anthocyanins

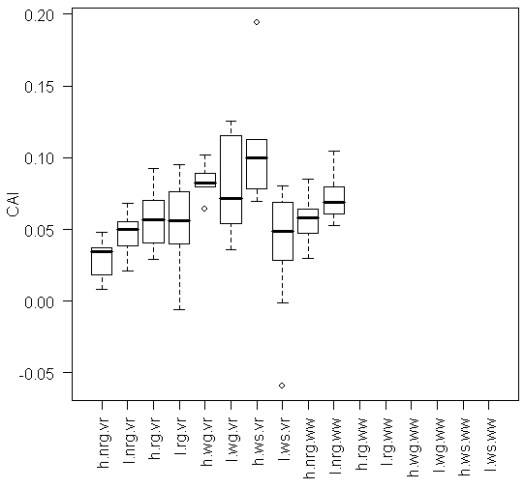

CAI: Cellulose

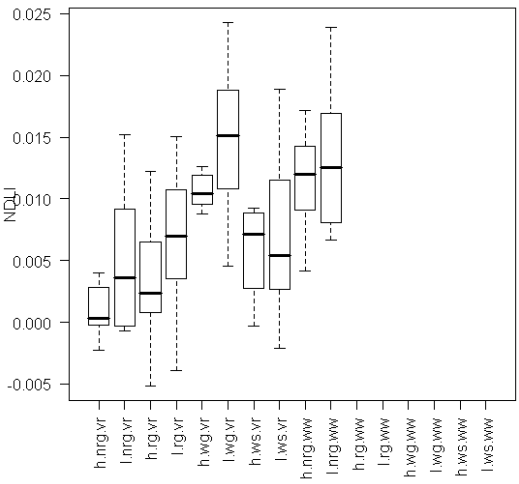

NDLI: Lignin

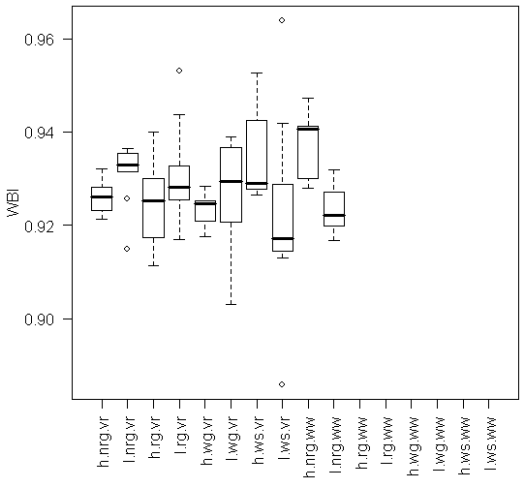

WBI: Plant-water

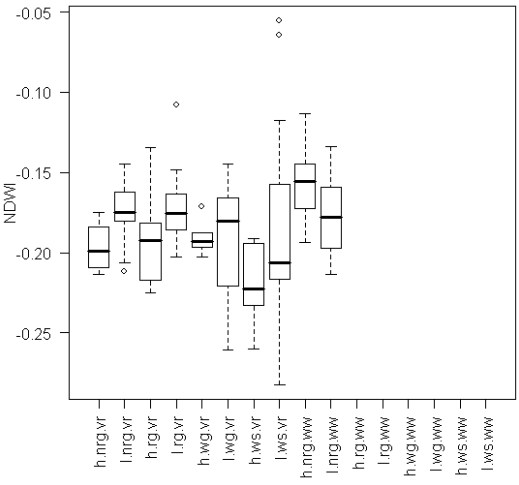

NDWI: Plant-water

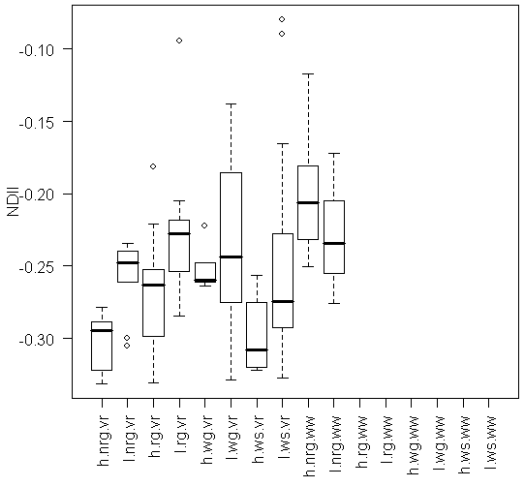

NDII: Plant-water

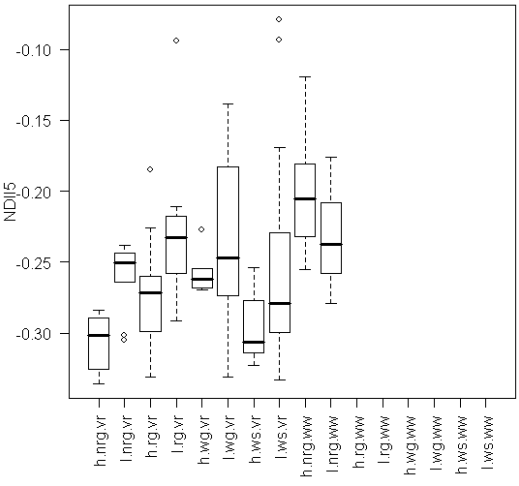

NDII5: Plant-water

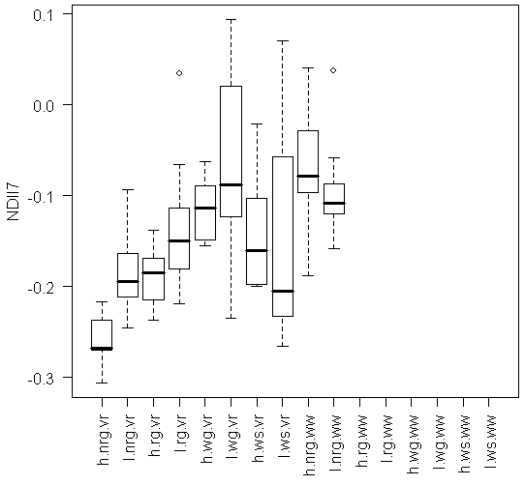

NDII7: Plant-water

Appendix 3 VI Results for Disturbance Levels in Different Vegetation Types

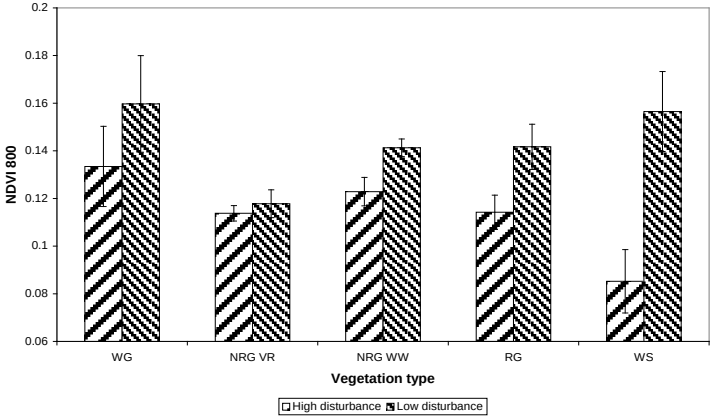

(a)

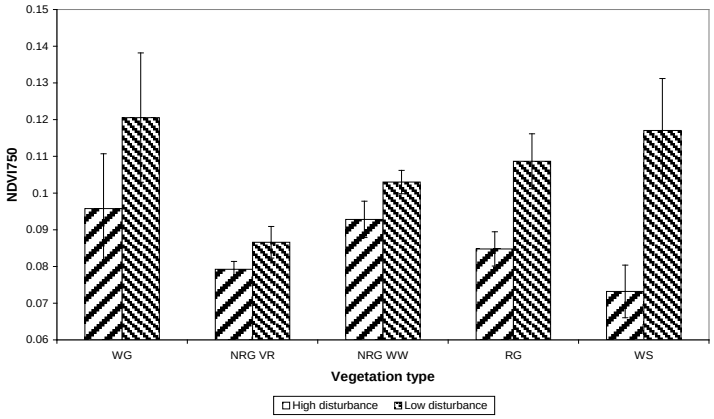

(b)

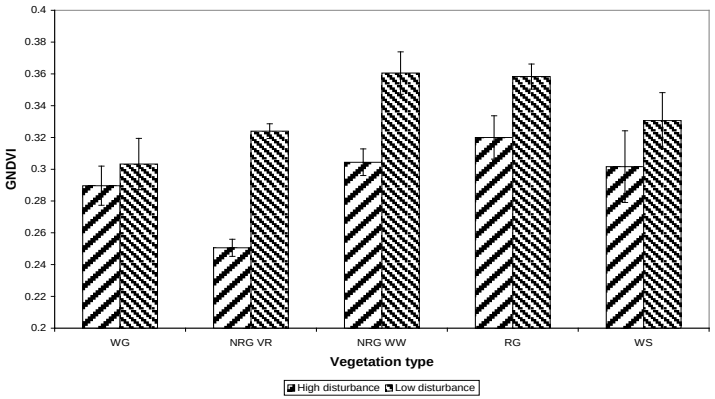

(c)

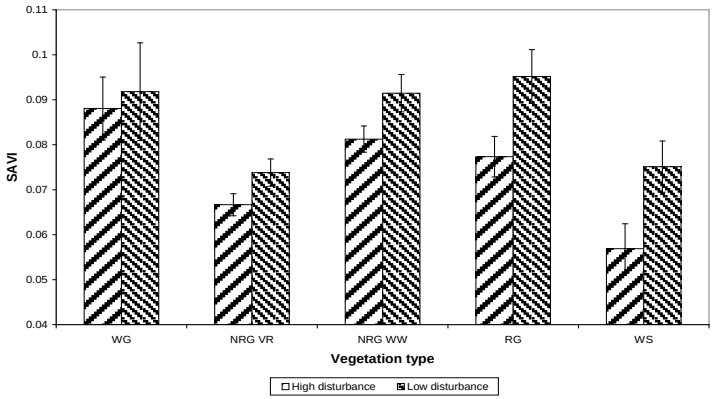

(d)

Comparing vegetation index means and standard errors for high and low disturbance quadrats in different vegetation types at Vaal River and West Wits mining regions. (a) The standard NDVI (NDVI800) measuring chlorophyll. (b) The "Anglo" NDVI (NDVI750) measuring chlorophyll. (c) The green NDVI (GNDVI) measuring chlorophyll. (d) the Soil Adjusted Vegetation Index (SAVI) measuring chlorophyll adjusted for soil background. VR = Vaal River, WW = West Wits, WG = wet grassland, NRG = non-rocky grassland, RG = rocky grassland and WS = woody shrub.

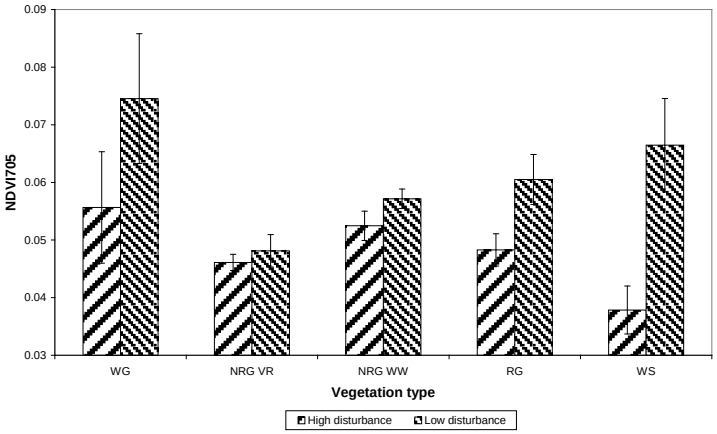

(a)

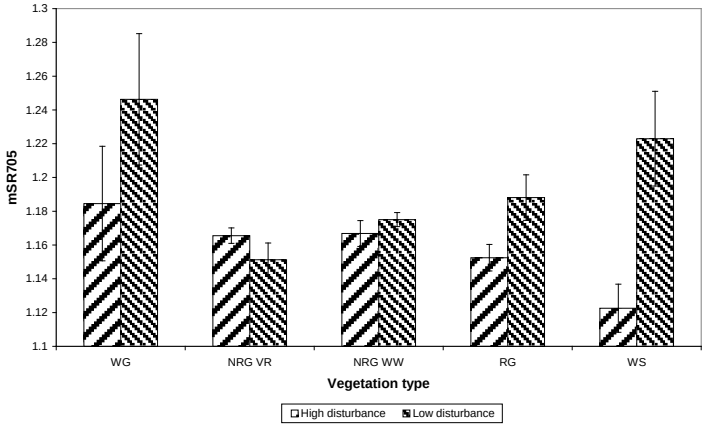

(b)

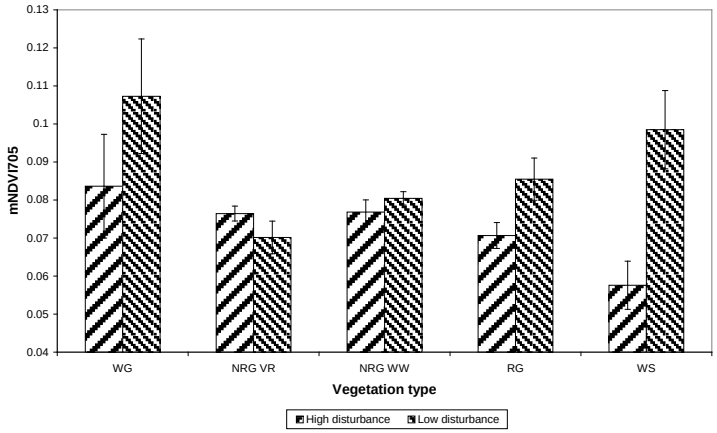

(c)

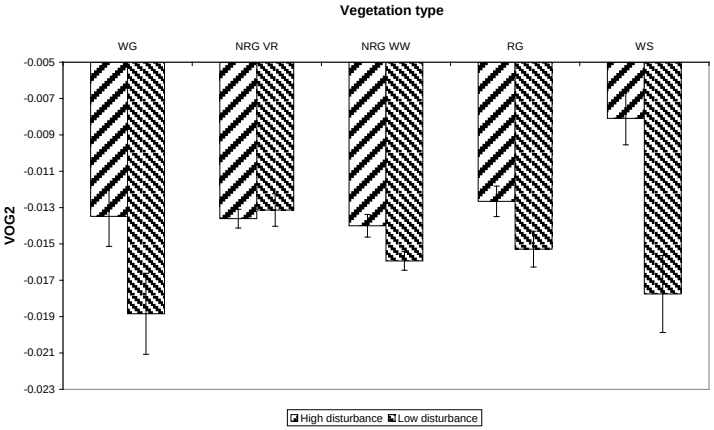

(d)

Comparing vegetation index means and standard errors for high and low disturbance quadrats in different vegetation types at Vaal River and West Wits mining regions. (a) The red edge NDVI (NDVI705) measuring chlorophyll. (b) The modified red edge Simple Ratio index (mSR705) measuring chlorophyll. (c) The modified red edge Normalised Difference Vegetation index (mNDVI705) measuring chlorophyll. (d) the Vogelmann Red Edge Index 2 (VOG2) measuring chlorophyll. VR = Vaal River, WW = West Wits, WG = wet grassland, NRG = non-rocky grassland, RG = rocky grassland and WS = woody shrub.

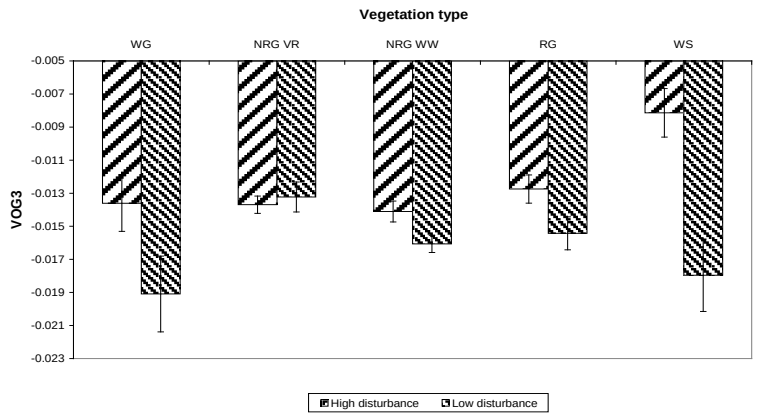

(a)

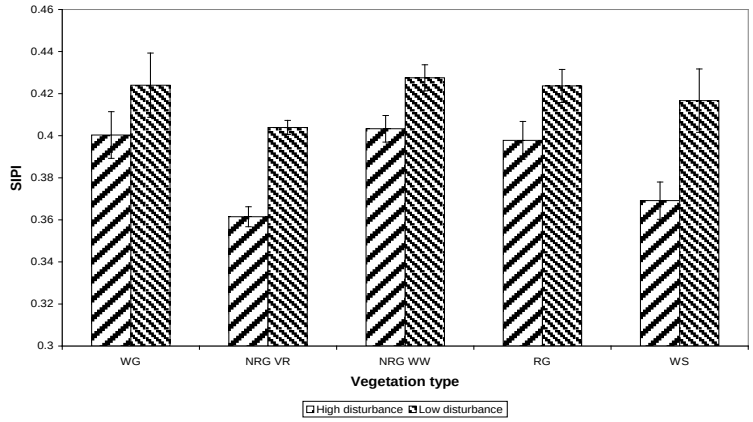

(b)

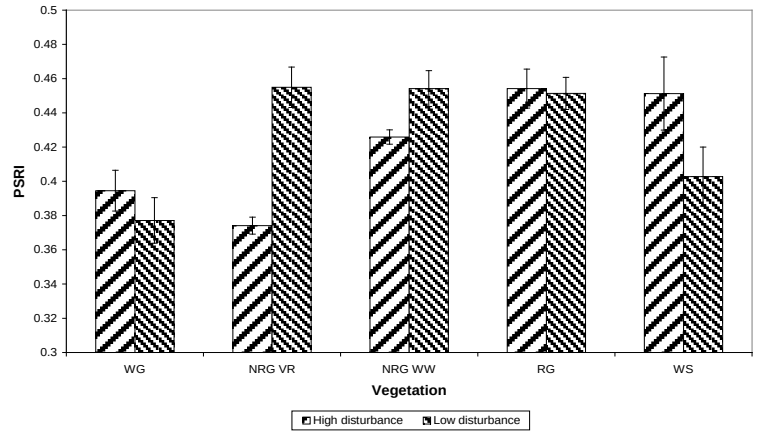

(c)

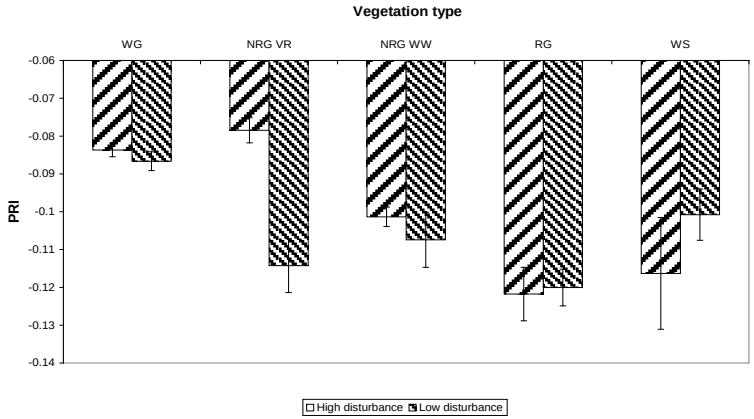

(d)

Comparing vegetation index means and standard errors for high and low disturbance quadrats in different vegetation types at Vaal River and West Wits mining regions. (a) The Vogelmann red edge index 3 (VOG3) measuring chlorophyll. (b) The Structure Insensitive Pigment Index (SIPI) measuring chlorophyll and carotenoid. (c) The Plant Senescent Reflectance Index (PSRI) measuring chlorophyll and carotenoids. (d) The Photochemical Reflectance Index (PRI) measuring carotenoids. VR = Vaal River, WW = West Wits, WG = wet grassland, NRG = non-rocky grassland, RG = rocky grassland and WS = woody shrub.

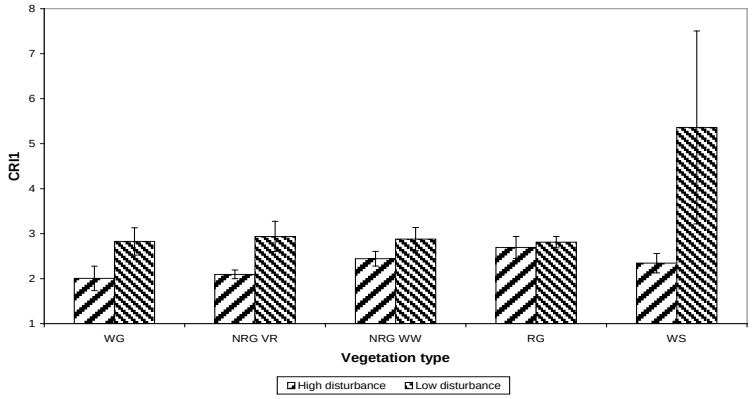

(a)

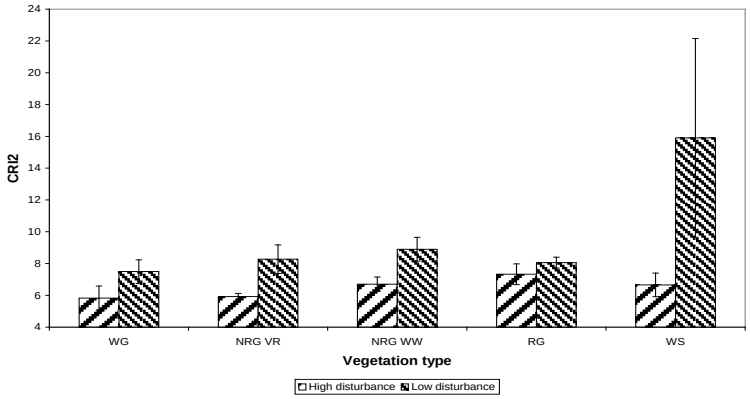

(b)

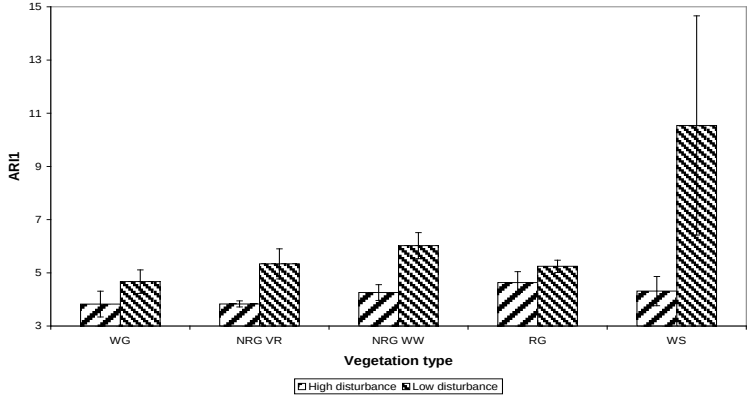

(c)

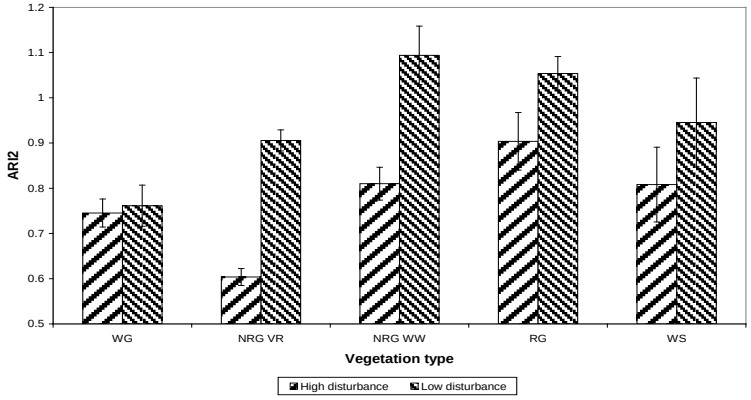

(d)

Comparing vegetation index means and standard errors for high and low disturbance quadrats in different vegetation types at Vaal River and West Wits mining regions. (a) The Carotenoid Reflectance Index 1 (CRI1) measuring carotenoids. (b) The Carotenoid Reflectance Index 2 (CRI2) measuring carotenoids. (c) The Anthocyanin Reflectance Index 1 (ARI1) measuring anthocyanins. (d) The Anthocyanin Reflectance Index 2 (ARI2) measuring anthocyanins. VR = Vaal River, WW = West Wits, WG = wet grassland, NRG = non-rocky grassland, RG = rocky grassland and WS = woody shrub.

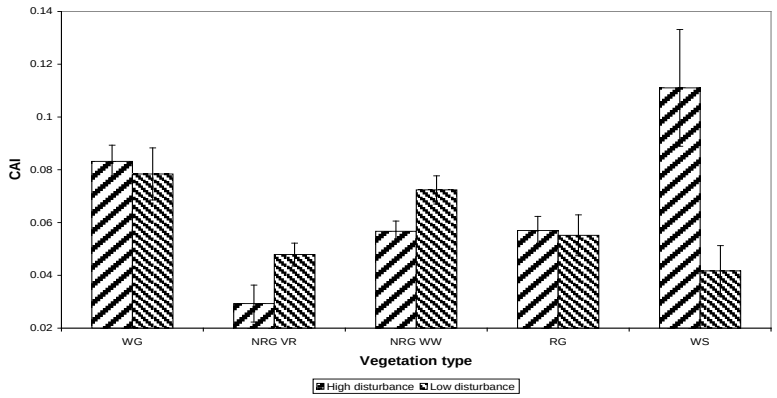

(a)

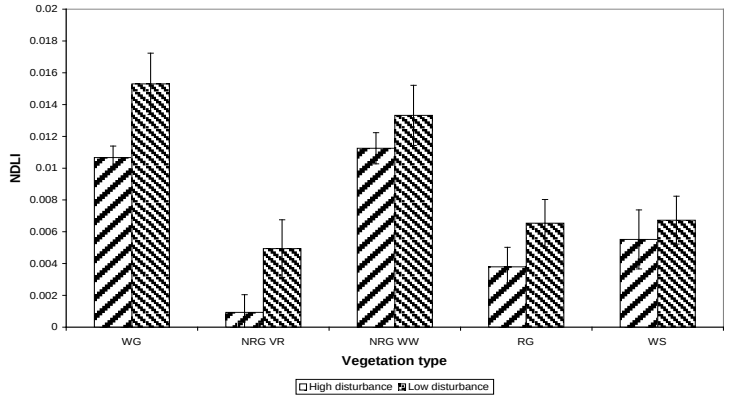

(b)

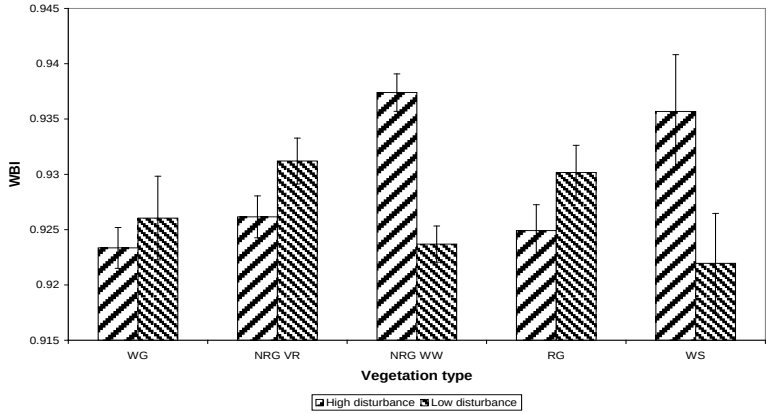

(a)

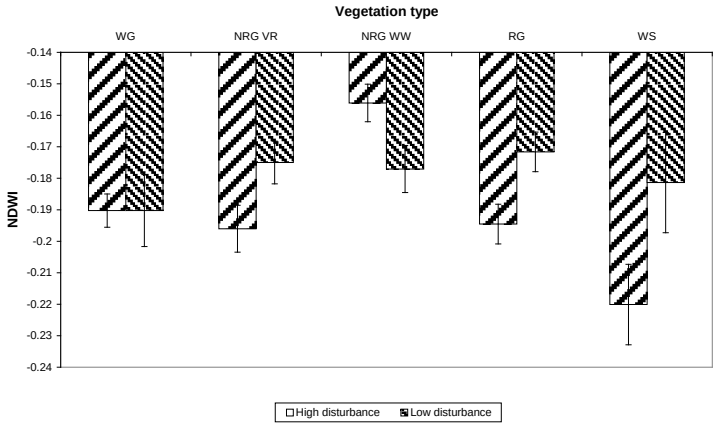

(d)

Comparing vegetation index means and standard errors for high and low disturbance quadrats in different vegetation types at Vaal River and West Wits mining regions. (a) The Cellulose Absorption Index (CAI) measuring cellulose. (b) The Normalised Difference Lignin Index (NDLI) measuring lignin. (c) The Water Band Index (WBI) measuring plant water. (d) The Normalised Difference Water Index (NDWI) measuring plant water. VR = Vaal River, WW = West Wits, WG = wet grassland, NRG = non-rocky grassland, RG = rocky grassland and WS = woody shrub.

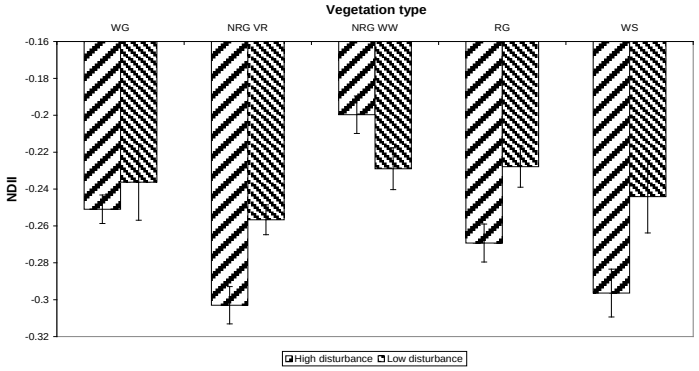

(a)

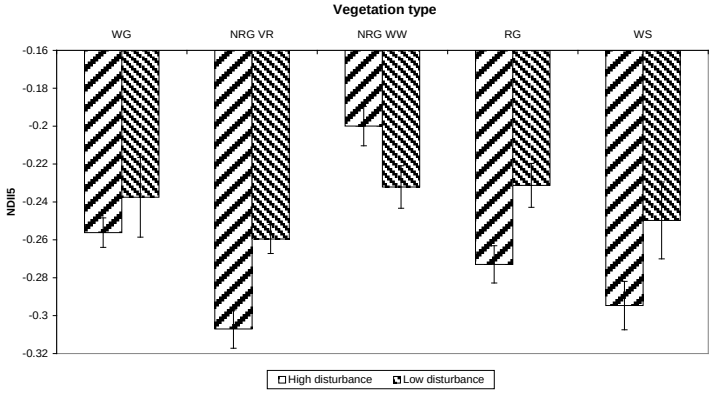

(b)

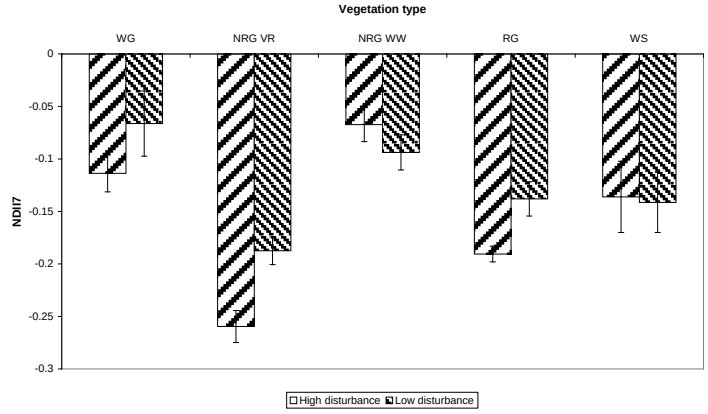

(c)

Comparing vegetation index means and standard errors for high and low disturbance quadrats in different vegetation types at Vaal River and West Wits mining regions. (a) The Normalised Difference Infrared Index (NDII) measuring plant water. (b) The Normalised Difference Infrared Index 5 (NDII5) measuring plant water. (c) The Normalised Difference Infrared Index 7 (NDII7) measuring plant water. VR = Vaal River, WW = West Wits, WG = wet grassland, NRG = non-rocky grassland, RG = rocky grassland and WS = woody shrub.

Appendix 4 Graphs of the Visible NIR Portion of the Spectra

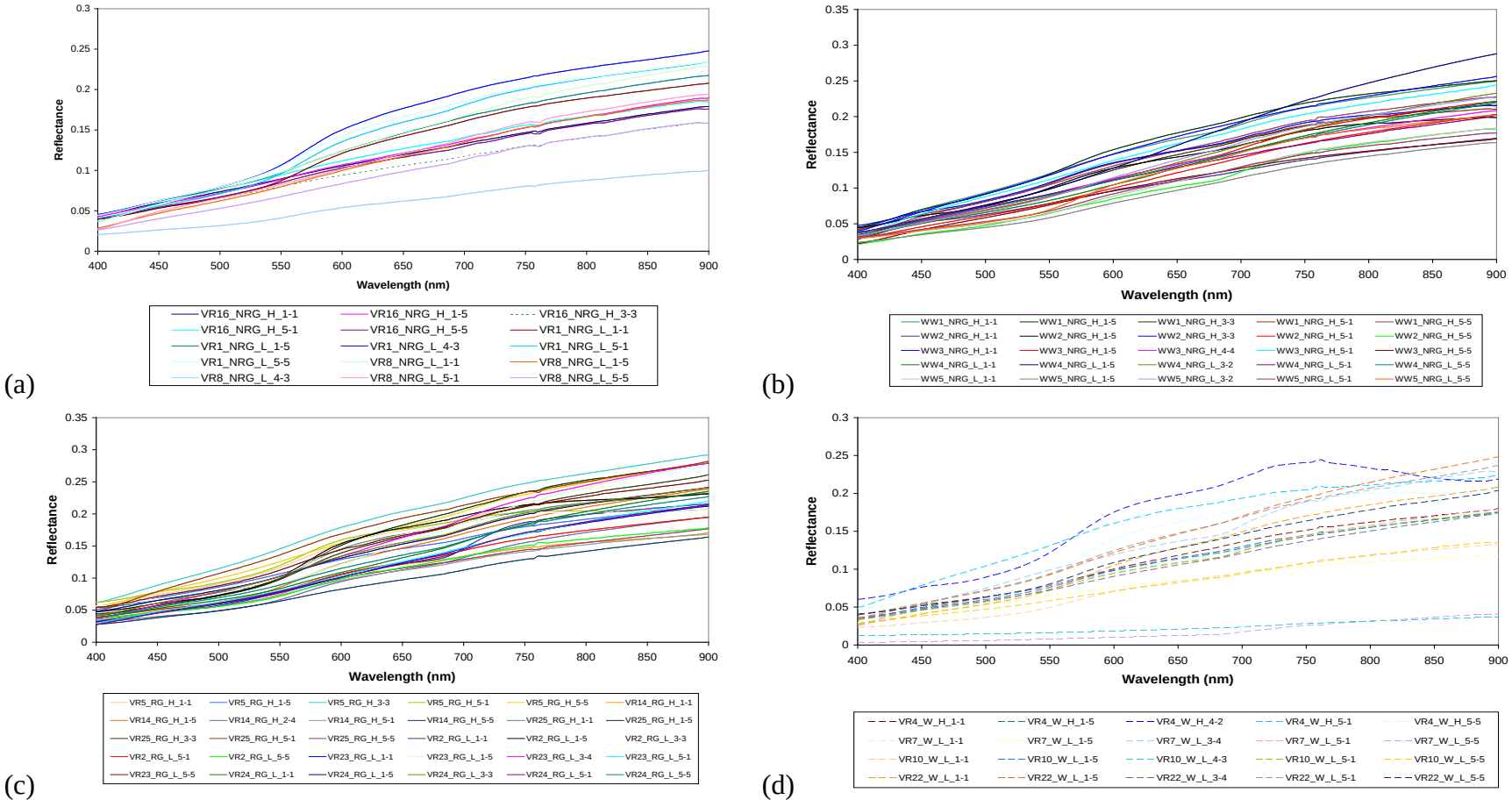

The visible and NIR portion of the spectrum for (a) non-rocky grasslands from Vaal River, (b) non-rocky grasslands from West Wits, (b) rocky grasslands from Vaal River and (d) woody shrub quadrats from Vaal River with a very weak red-edge signal indicating very little chlorophyll in these quadrat.

Appendix 5

PLSR Tables and Graphs

Outliers identified during the development of infiltration models

Plot	Vegetation type	Disturbance	Quadrat number	Data set
VR 2	Rocky grassland	Low	1-5	Validation
VR 5	Rocky grassland	High	3-3	Calibration
VR 5	Rocky grassland	High	5-1	Calibration
VR 25	Rocky grassland	High	1-5	Calibration
VR 4	Woody shrub	High	5-1	Validation
VR 4	Woody shrub	High	4-2	Calibration
VR 7	Woody shrub	Low	5-5	Calibration
VR 10	Woody shrub	Low	4-3	Calibration
WW 4	Non-rocky grassland	Low	1-5	Calibration

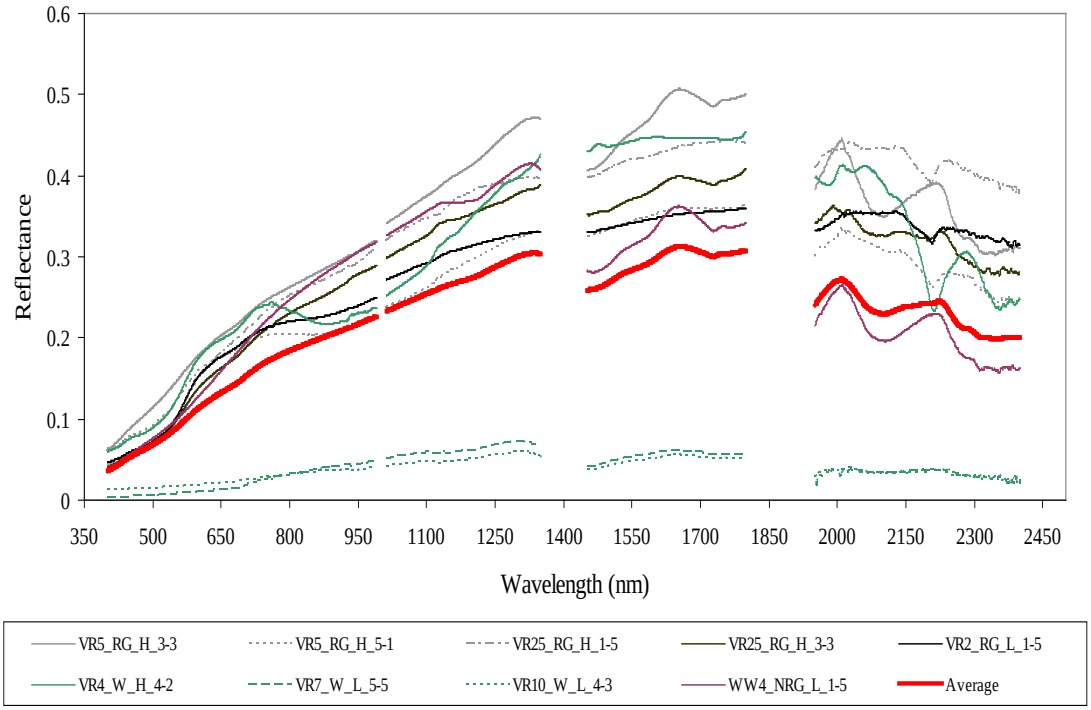

The spectra for the plots identified as outliers while modelling infiltration. The mean spectrum for all spectra is also shown.

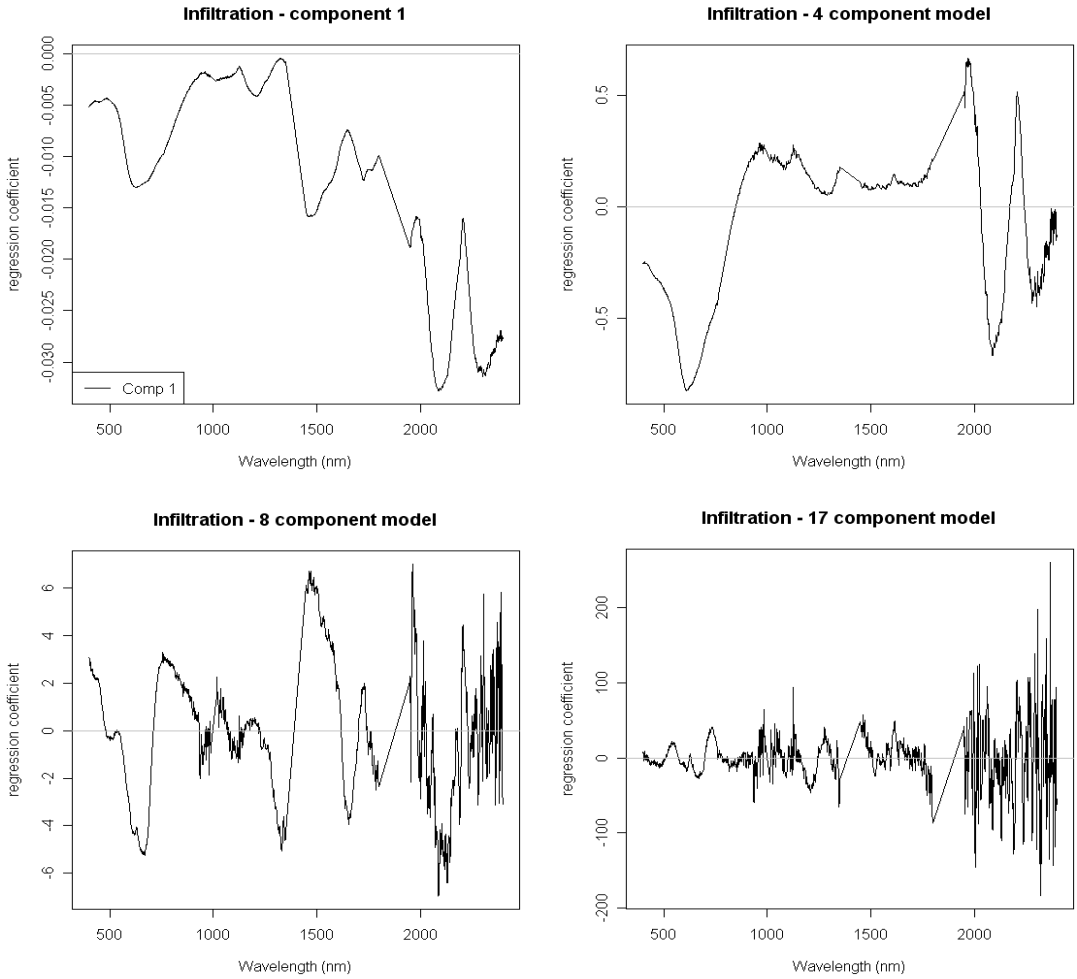

Regression coefficients for 1-component, 4-component, 8-component and 17-component models of infiltration.

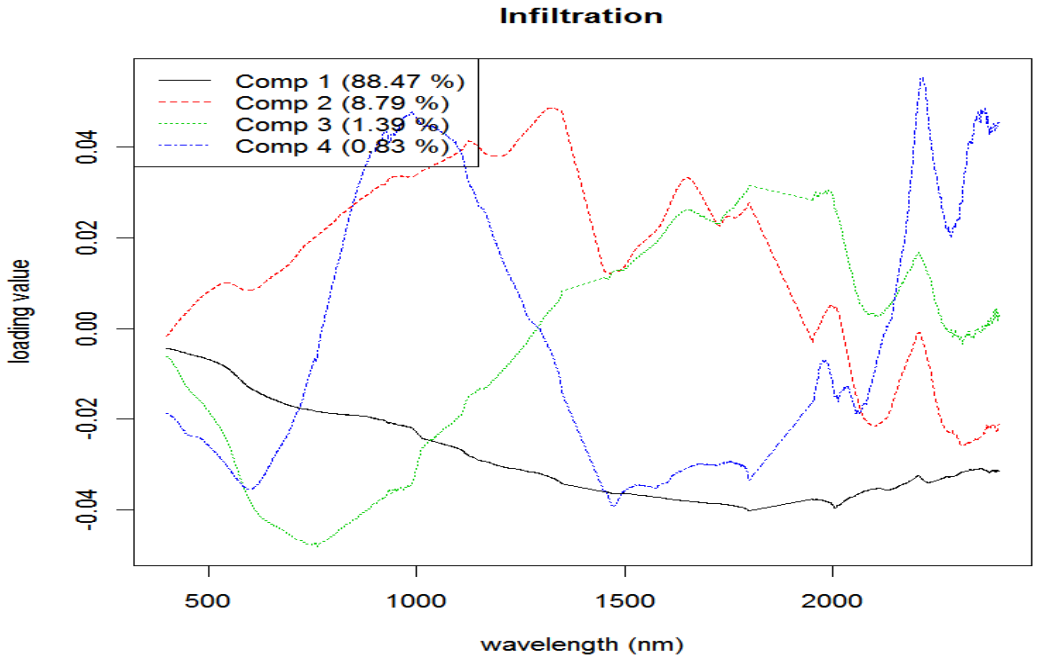

Loadings for the first four components of the infiltration model.

Outliers identified during the development of nutrient cycling models.

Plot	Vegetation type	Disturbance	Quadrat number	Data set
VR 2	Rocky grassland	Low	1-5	Validation
VR 5	Rocky grassland	High	1-5	Calibration
VR 25	Rocky grassland	High	5-1	Calibration
VR 25	Rocky grassland	High	1-5	Calibration
VR 19	Wet grassland	Low	1-5	Calibration
VR 4	Woody shrub	High	4-2	Validation
VR 4	Woody shrub	High	5-5	Calibration
VR 7	Woody shrub	Low	5-5	Calibration
VR 10	Woody shrub	Low	4-3	Calibration
WW 4	Non-rocky grassland	Low	1-5	Calibration

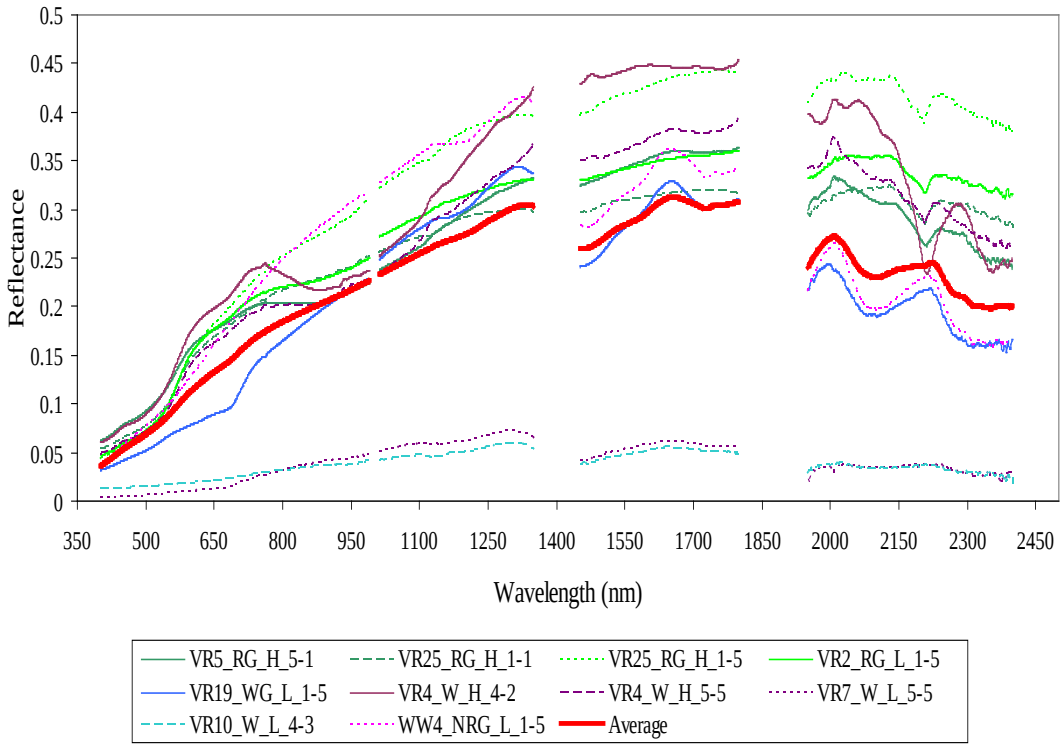

The spectra for the plots identified as outliers while modelling nutrient cycling. The mean spectrum for all spectra is also shown.

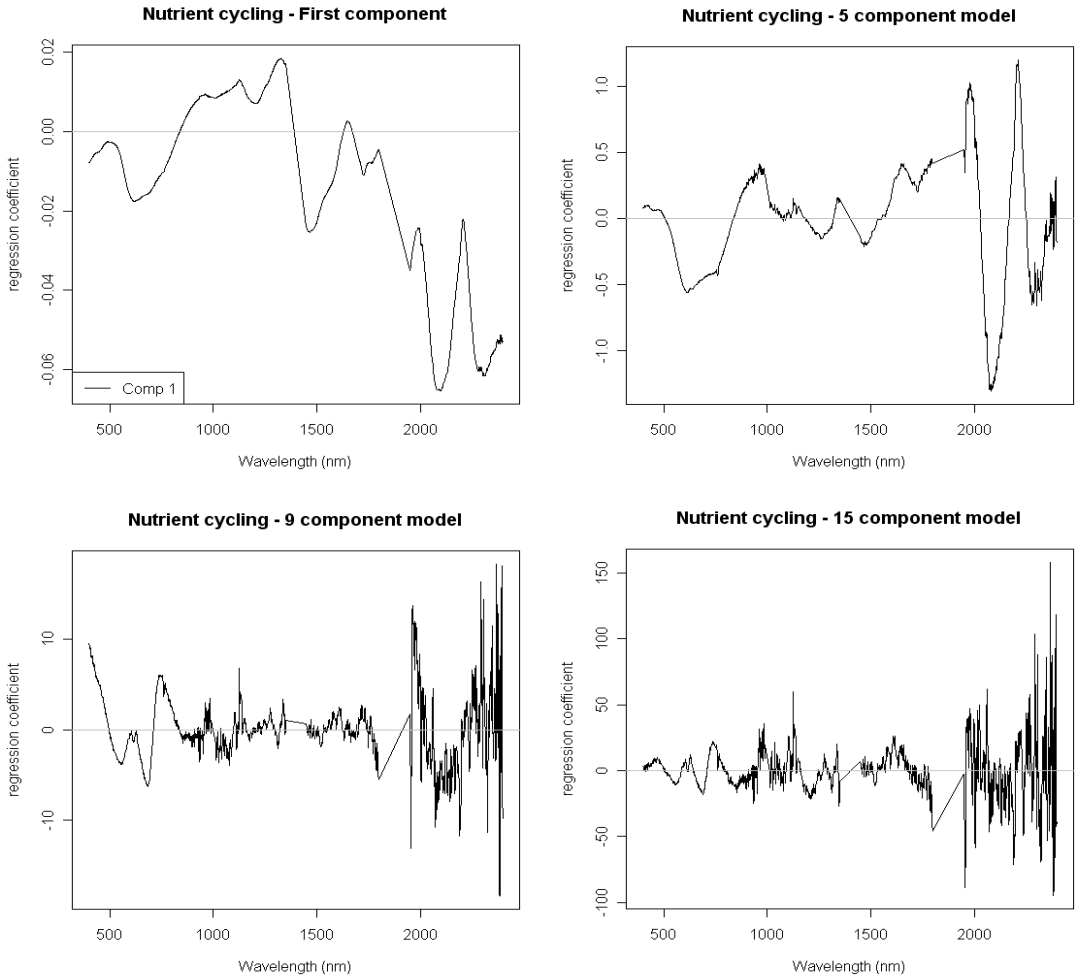

Regression coefficients for 1-component, 5-component, 9-component and 15-component models of nutrient cycling.

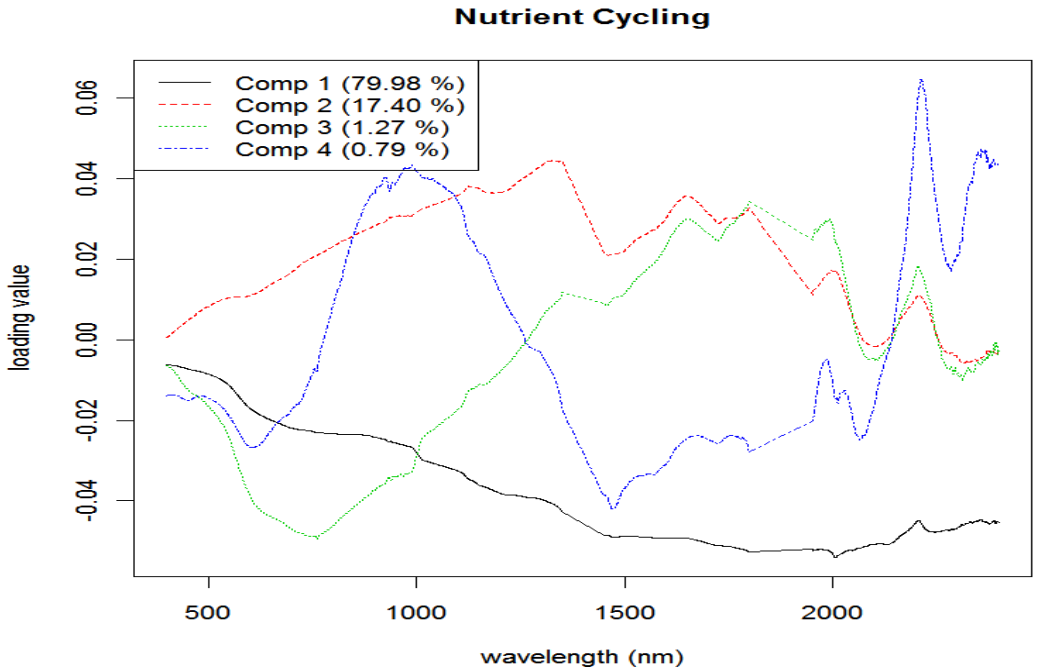

Loadings for the first four components of the nutrient cycling model.